Brief Communications

Stable *Drosophila buzzatii-Drosophila koepferae* Hybrids

I. Marín and A. Fontdevila

Previous experiments discovered high rates of chromosomal rearrangements in the progeny of males containing a telomeric segment of *Drosophila koepferae* in a *D. buzzatii* genetic background (segmental males). We have performed similar experiments, designed to test whether this chromosomal instability could be explained by a phenomenon similar to P-M hybrid dysgenesis or, alternatively, by a generalized telomeric effect. However, the results obtained have not allowed us to fully characterize this process, because we have not observed chromosomal rearrangements in the progeny of the putative unstable males. Our results suggest that chromosomal instability is independent of the introgressed fragment. A reasonable hypothesis to explain these results is that mutator factors are occasionally introduced by the hybridization. The effect of sampling, caused by the fact that only a small region is introgressed in a particular line, may explain why only some hybridizations lead to instability.

The impact of repetitive sequences, and especially mobile elements, on evolutionary processes is still poorly understood. The discovery of hybrid dysgenesis attracted the attention of evolutionary biologists because of the effects of high rates of transposition on the "hybrid" organisms obtained in crosses between stocks containing and those lacking certain mobile elements (see reviews in Berg and Howe 1989). The most interesting of these effects is sterility, caused by chromosomal breakage in the germ line of the hybrids (Engels 1989). These results lead to the hypothesis that similar processes might happen in interspecific hybrids, resulting in a "genomic disease" (Rose and Doolittle 1983). There are suggestive evidences indicating that interspecific hybrids are suffering, at least occasionally, these type of processes (reviewed in Fontdevila 1987, 1992). Among them, one of the most compelling was described by Naveira and Fontdevila (1985) in interspecific hybrids obtained between the pair of species *Drosophila buzzatii* and *D. koepferae* (this last species was then known as *D. serido* "from Argentina," see Fontdevila et al. 1988). In that work, a very high rate of chromosomal rearrangements (with an average of 2% aberrations per gamete and generation) was observed in the offspring of males carrying in heterozygosis a telomeric fragment of chromosome 5 of *D. koepferae* in an otherwise *D. buzzatii* background. These results, highly suggestive of a dysgenic phenomenon, stimulated our work on the repetitive component of these two species (Marín and Fontdevila 1996; Marín et al. 1992). So far, our group has characterized five different transposable elements, at least three of them active in one or both of these species (Francino et al. 1994; Labrador and Fontdevila 1994; Marín and Fontdevila 1995, 1996). In one case we have directly demonstrated substantial rates of transposition of a newly described retrotransposon, *Osvaldo*, in *D. buzzatii-D. koepferae* hybrids (Labrador and Fontdevila 1994).

To further study the phenomena that occur in these hybrids, a testable hypothesis of why instability occurs is required. The simplest explanation for Naveira and Fontdevila's (1985) results would be a phenomenon similar to P-M hybrid dysgenesis (reviewed in Engels 1989). Their experimental protocol began with the production of a hybrid F_1 by crossing *D. buzzatii* males with *D. koepferae* females. F_1 females are fertile. Individuals with small chromosome fragments of *D. koepferae* in a *D. buzzatii* background (called "segmental" flies) can then be obtained by performing successive backcrosses of hybrid females against *D. buzzatii* males. The parallelism with the P-M system would be as follows. *D. koepferae* elements present in the introgressed fragments would remain stable while the cytoplasm of the cross is of *koepferae* type. Because the crosses are established always in the direction *D. buzzatii* males $\times$ *D. buzzatii-D. koepferae* hybrid females, the instability would remain suppressed. However, the production of fertile hybrid males allows the crosses to be performed in the reciprocal direction (hybrid males $\times$ *D. buzzatii* females). This situation would be equivalent to a cross of males P $\times$ females M, with the consequent production of offspring with a dysgenic germ line. The main difference with the P-M system is that only male *buzzatii-koepferae* hybrids are unstable, while in P-M dysgenesis both sexes are affected.

However, Naveira and Fontdevila's (1985) experiments did not completely characterize the phenomenon. First, as suggested by the authors themselves, their results could be explained alternatively by mechanisms related with the introgressed fragment itself and independent of mobile element transpositions. Particularly, the experiments were performed with males introgressed for the telomeric tip of chromosome 5 (region 5A-B1d). The inclusion of a foreign telomere could be significant. In *Nicotiana* hybrids a chromosome breakage syndrome has been found that seems to be caused by differences in telomeric heterochromatin (Burns and Gerstel 1969; Gerstel and Burns 1967). A second important difficulty concerns the experimental design used. All the unstable lines came from a single introgressed segment that was kept intact, being transmitted from father to son for no less than five generations before testing for instability. If, as suggested before, the hybrid males suffer from a P-M-like dysgenic syndrome, transposition would

Table 1. Number of larvae examined and rearrangements observed in the offspring of second generation flies (sons and daughters of first generation segmental males)

Line	Introgressed segment	Parental individuals: Segmental males (N = 33)	Segmental females (N = 14)	No segmental males (N = 17)	No segmental females (N = 13)	New rearrangements
6.3	5A-C1	70	42	29	20	0
53.39	5A-B4	33	9	0	10	9[a]
11.8	5A-B1	86	30	26	17	0
51.4	5A-A5	103	16	33	5	0
51.5	5A-A5	81	20	18	16	0
Total		373	117	106	68	9[a]

N = number of second generation parental flies tested in each class.

[a] This nine exceptional larvae descended from a segmental male. They all carried the same inversion in chromosome 2. As explained in the text, the parental male himself was mutant.

be happening at high rates in these individuals. This situation creates the possibility of accumulation of active factors during the generations of maintenance previous to the experiment, especially in the chromosome that contains the hybrid segment, which—because of the lack of recombination in males and the fact that individuals that carry this chromosome are selected as progenitors—is transmitted intact along all these generations. The effect would be an artificial increase of the mutation rate in the experimental hybrids, unrelated with the mutator power of the original introgression.

In this work we have designed experiments to test directly whether these hybrids are suffering from a syndrome similar to P-M dysgenesis. We have followed procedures to avoid the potential problem of accumulation of mutator activity. By testing for rearrangements in the first putative dysgenic generation, we have ruled out the possibility of accumulation of mutator factors. However, the results obtained have been negative: we have not found the high rates of chromosomal rearrangements observed by Naveira and Fontdevila (1985). The production of a single new inversion has allowed us to test directly for possible cumulative effects. Again, we have not observed new rearrangements in the progeny of individuals where the inversion was segregating. Therefore our results (1) establish that not all the *buzzatii-koepferae* hybrid lines show instability, and (2) do not support an accumulation of mutator power in the progeny of males carrying the introgressed fragments. Moreover, because we also tested telomeric fragments of chromosome 5, they argue against the possibility of a generalized telomeric effect on chromosomal instability. The implications of these results are discussed.

Materials and Methods

The stocks used are called BSL (*D. buzzatii*) and KO2 (*D. koepferae*). Both stocks originated from San Luis, Argentina, where these two species live sympatrically. Flies from these two stocks interbreed easily in the laboratory, producing abundant F_1. Hybrid F_1 females are partially fertile and can be backcrossed against *D. buzzatii* males. In this experiment, 60 virgin KO2 females were crossed with about the same number of BSL males. To avoid genetic heterogeneity, out of the offspring of the F_1 females, a single female was chosen as a starting point for the experiments. It was determined that this female carried a fragment of chromosome 5 of *D. koepferae*, including its telomere (5A-C1; cytology refers to the maps by Ruíz et al. 1982). This fragment includes the region introgressed by Naveira and Fontdevila (1985), allowing direct comparisons with their experiments. All the cytological characterizations were performed according to Naveira et al. (1986). Larvae, offspring of the individuals to be characterized, were examined for the presence of asynaptic, and hence hybrid, fragments in the polytene chromosomes of their salivary glands. At least five larvae are examined per cross, establishing a proper characterization of the parent as carrier or not of a hybrid segment in at least 96.9% of the cases (assuming Mendelian segregation; probability of error = $1 - (0.5)^n$, where n is the number of larvae examined).

So far the protocol is identical to that used by Naveira and Fontdevila (1985). From now on, however, they diverge. In our experiments, successive backcrosses of hybrid females with *D. buzzatii* males were established. In these backcrosses we used females that carried introgressed telomeric segments (containing either the intact 5A-C1 fragment, as the founder female, or smaller fragments produced by recombination, never smaller than 5A-A5). Because hybrid females are not unstable (Naveira and Fontdevila 1985), the successive female backcrosses should not release the mutator activity of these strains. If we call the founder female B_1 (backcross 1), the successive experiments were performed with the progeny of B_2 to B_4 females. From these females, a limited number of fertile males were obtained that carried the introgressed fragments. We will call them "first generation" males (first generation refers to the fact that it is the first time fertile hybrid males are obtained in the crosses). As we explained in the introduction to this work, supposing a P-M dysgenic system, these males would be equivalent to P males. They should not be unstable (they still carry *koepferae* cytoplasm). Once these first generation males were obtained, we did not establish maintenance lines for several generations, as in Naveira and Fontdevila's experiments. Instead, we crossed them with BSL females to obtain what we have called "second generation" males and females. If the analogy with the P-M system holds, the second generation hybrid males are expected to be unstable. Second generation males and females were then crossed individually with BSL females and their progeny analyzed by scoring their chromosomal complement. Only those larvae where all the chromosomes were analyzed for rearrangements have been included in this study.

The rescue of a single segregating chromosomal inversion in chromosome 2 (see Results) allowed us to look for cumulative effects. Males carrying both a 5A-B4 introgressed segment [that includes the region studied by Naveira and Fontdevila (1985)] and this chromosome 2 inversion were crossed with either sister females or BSL flies for up to eight generations. These crosses allow the possibility of accumulation of mutator transposable elements in the two marked chromosomes, 2 and 5. Again, dissections of the progeny of these males were performed to test for increased chromosomal instability, and only those larvae where all the chromosomes were analyzed have been included.

Results

Table 1 summarizes the results obtained when the progeny of second generation individuals from five different introgressed lines were checked for new chromosomal

Table 2. Test for rearrangements in the lines (derived from 53.39) where flies carrying both the second chromosome inversion and the introgressed fragment 5A-B4 were selected as progenitors through several generations

Maintenance regime	Number of generations	Number of larvae examined	Number of rearrangements
Exo	3	30	0
Exo	4	9	0
Exo	8	181	0
Endo	5	47	0
Total		267	0

Exo: maintenance by crossing segmental-inversion carrier males with BSL females. Endo: maintenance by crosses of these males with non-hybrid sisters. Number of generations: the number of maintenance generations before the test.

rearrangements. Two hundred ninety-one of the examined larvae were obtained from nonhybrid males or from hybrid and nonhybrid females. According to Naveira and Fontdevila (1985), all these individuals do not show chromosomal instability and can be considered controls. As expected, none of these larvae presented new rearrangements. From the progeny of second generation hybrid males, 373 larvae were obtained. All except nine of them were normal. The nine exceptional larvae carried the same mutation (a paracentric inversion in chromosome 2) and they were all descendant from a single hybrid male of the line known as 53.39. To determine whether in fact this male was mutant himself or whether a cluster of mutant gametes were produced in his germ line, the male was crossed with other *D. buzzatii* females. In the new offspring, the rearrangement was also observed. We conclude that the male carried the mutation. This segregating rearrangement was used to test for accumulation of mutator potential (see Materials and Methods). Results are detailed in Table 2. None of the 267 larvae examined carried new chromosomal mutations.

Discussion

The interpretation of our results depends on two expectations: (1) the basal rate of chromosomal rearrangements in these crosses, and (2) the expected rate under dysgenic conditions. The available literature on basal rates of chromosomal mutation in natural populations of *Drosophila* species is very fragmentary and it is complicated by the occurrence of hybrid dysgenesis (Yamaguchi 1976; Yamaguchi et al. 1976; Yamaguchi and Mukai 1974; see Woodruff et al. 1983). Apparently even closely related species may have substantial differences in this basal rate. Inoue (1988) found that the number of rearrangements found only a single time in populations of *D. melanogaster* was about 8×10^{-3} (all rates from now on refer to rearrangements per genome and generation), while in its sibling *D. simulans* it was about 4×10^{-3}. It is therefore fortunate that we have direct data concerning one of our species: the extensive survey of the chromosomal variability present in *D. buzzatii* populations by Ruíz et al. (1984). In this work six exceptional rearrangements were found out of 5,103 genomes examined. Assuming that these larvae correspond to new mutations, the basal rate in this species would be 1.2×10^{-3}. We can suppose this is also the basal rate in our hybrids because 95% of their genomes originate from *D. buzzatii*. Contrasting with this low basal rate, Naveira and Fontdevila (1985) found rates in the offspring of segmental hybrid males ranging from 8.2×10^{-3} to 9×10^{-2} (average 2.1×10^{-2}), that is 7 to 75 (average 18) times larger than the basal rate. With this data in mind, we can easily conclude that our experiments did not show any sign of instability. A total of 640 larvae descendant of putative unstable segmental males (373 in the first set of experiments and 267 in the second set) were examined without finding (once the segregating inversion is excluded, see below) any chromosomal rearrangement. With this sample size and according to a Poisson distribution, there is a probability higher than 95% of obtaining at least one rearrangement if the rate is higher than 4.4×10^{-3}. This demonstrates that the rate of production of new rearrangement in our lines is much lower than the minimum rate obtained by Naveira and Fontdevila (1985). In fact, the possibility of accumulation of segregating rearrangements through the generations means that we are underestimating the number of genomes characterized, further strengthening the conclusion of lack of instability. The single rearrangement found in the first generation male carrier of a new inversion is irrelevant to the conclusion of lack of instability in our lines. This mutation was produced in the father (BSL) or in the mother (hybrid segmental female), neither of which are expected to be unstable. With our total sample size (931 individuals; see Tables 1 and 2), and according to the results described in Ruíz et al. (1984), about one spontaneous rearrangement is expected.

Thus, we have been unable to replicate Naveira and Fontdevila's results. The lack of instability has made it impossible to check the hypothesis that a P-M hybrid dysgenesis syndrome was acting in these hybrids. However, our experiments contribute to a better understanding of those previous results. First, we have determined that a generalized mutator effect associated to the introgression of the distal end of chromosome 5 does not occur. Our results show that the introgression of telomeric fragments very similar to that obtained by Naveira and Fontdevila (1985) may not cause instability. The process is therefore restricted to particular lines in a way that seems to be independent of the introgressed fragment. A second interesting aspect is that our results do not support an accumulation of mutator factors during the maintenance generations as a likely explanation of Naveira and Fontdevila's results. Even when two chromosomes (instead of one as in Naveira and Fontdevila 1985) were selected in each generation, no rearrangements were found. However, because of the limited number of larvae examined, it is still possible for a low degree of instability (lower than 1.1×10^{-2} rearrangements/gamete/generation) to be present in our maintenance lines.

The conditions that determine chromosomal instability in these hybrids remain unexplained. Two different problems complicate substantially experiments in dysgenic conditions. First, transpositions and rearrangements are visualized in the offspring of dysgenic individuals. If male fertility is severely affected by these processes, as it happens in P-M dysgenic individuals, it may preclude the production of the appropriate material to test our hypothesis. In Naveira and Fontdevila (1985) and this study, this problem was avoided by analyzing the progeny of segmental males. Some of these males have an apparently normal fertility. However, this procedure introduces a second problem. If, in fact, a limited number of mutator factors are involved, the effect of the introgression of small segments is expected to be much less severe than the introgression of larger portions of the genome (up to 50% in the F_1), because of the lower number of factors introduced. All the available information suggests that the number of active families of transposable elements—the best candidates to act as mutator factors—in these species is low (see Marín and Fontdevila 1996 for a discussion). This fact, together with likely differences in activity of different introgressed elements may contribute to an important effect of

sampling. On the other hand, if in fact transposable elements are involved, their distribution in the genome will be different among strains. Therefore fragments able to cause instability in some cases will not produce it in others. In what certainly is an a posteriori recapitulation, we conclude that negative results are not altogether unexpected [see also Coyne (1989) and Hey (1989) for similar negative results in other *Drosophila* species]. Only new experiments, designed to test in parallel different chromosomal fragments in inbred stocks, can shed light on the important question of whether instability is produced often or only exceptionally in these hybrids.

From the Departamento de Genética, Facultad de Biología, Universidad de Valencia, 46100 Burjassot (Valencia), Spain, (Marín) and the Departamento de Genética y Microbiología, Facultad de Ciencias, Universidad Autónoma de Barcelona, 08193 Bellaterra (Barcelona), Spain (Fontdevila). This work was supported by grant PB93/0843 from DGICYT (Spain) to A.F.

References

Berg DE and Howe MM, 1989. Mobile DNA. Washington, D.C.: American Society for Microbiology.

Burns JA and Gerstel DU, 1969. Consequences of spontaneous breakage of heterochromatic segments in *Nicotiana* hybrids. Genetics 63:427–439.

Coyne JA, 1989. Mutation rates in hybrids between sibling species of *Drosophila*. Heredity 63:155–162.

Engels WR, 1989. P elements in *Drosophila melanogaster*. In: Mobile DNA (Berg DE and Howe MM, eds). Washington, D.C.: American Society for Microbiology; 437–484.

Fontdevila A, 1987. The unstable genome: an evolutionary approach. Genet Iber 39:315–349.

Fontdevila A, 1992. Genetic instability and rapid speciation: are they coupled? Genetica, 86:247–258.

Fontdevila A, Pla C, Hasson E, Wasserman M, Sánchez A, Naveira H, and Ruíz A, 1988. *Drosophila koepferae*: a new member of the *Drosophila serido* (Diptera: Drosophilidae) superspecies taxon. Ann Entomol Soc Am 81: 380–385.

Francino O, Cabré O, and Fontdevila A, 1994. Distribution of the *copia* transposable element in the *repleta* group of *Drosophila*. Genet Sel Evol 25:501–516.

Gerstel DU and Burns JA, 1967. Phenotypic and chromosomal abnormalities associated with the introduction of heterochromatin from *Nicotiana otophora* into *N. tabacum*. Genetics 56:483–502.

Hey J, 1989. Speciation via hybrid dysgenesis: negative evidence from the *Drosophila affinis* subgroup. Genetica 78:97–104.

Inoue Y, 1988. Chromosomal mutation in *Drosophila melanogaster* and *Drosophila simulans*. Mut Res 197:85–92.

Labrador M and Fontdevila A. 1994. High transposition rates of *Osvaldo*, a new *Drosophila buzzatii* retrotransposon. Mol Gen Genet 245:661–674.

Marín I and Fontdevila A, 1995. Characterization of *Gandalf*, a new inverted-repeat transposable element of *Drosophila koepferae*. Mol Gen Genet 248:423–433.

Marín I and Fontdevila A, 1996. Evolutionary conservation and molecular characteristics of repetitive sequences of *Drosophila koepferae*. Heredity 76:355–366.

Marín I, Labrador M, and Fontdevila A, 1992. The evolutionary history of *Drosophila buzzatii*. XXIII. High content of nonsatellite repetitive DNA in *D. buzzatii* and in its sibling *D. koepferae*. Genome 35:957–964.

Naveira H and Fontdevila A, 1985. The evolutionary history of *Drosophila buzzatii*. IX. High frequencies of new chromosome rearrangements induced by introgressive hybridization. Chromosoma 91:87–94.

Naveira H, Pla C, and Fontdevila A, 1986. The evolutionary history of *Drosophila buzzatii*. XI. A new method for cytogenetic localization based on asynapsis of polytene chromosomes in interspecific hybrids of *Drosophila*. Genetica 71:199–212.

Rose MR and Doolittle WF, 1983. Molecular biological mechanisms of speciation. Science 220:157–162.

Ruíz A, Fontdevila A, and Wasserman M, 1982. The evolutionary history of *Drosophila buzzatii*. III. Cytogenetic relationships between two sibling species of the *buzzatii* cluster. Genetics 101:503–518.

Ruíz A, Naveira H, and Fontdevila A, 1984. La historia evolutiva de "Drosophila buzzatii". IV. Aspectos citogenéticos de su polimorfismo cromosómico. Genet Iber 26:13–35.

Woodruff RC, Slatko BE, and Thompson JN Jr, 1983. Factors affecting mutation rates in natural populations. In: The genetics and biology of *Drosophila* (Ashburner M, Carson HL, Thompson JN Jr, eds). London: Academic Press; 37–124.

Yamaguchi O, 1976. Spontaneous chromosome mutation and screening of mutator factors in *Drosophila melanogaster*. Mut Res 34:389–406.

Yamaguchi O and Mukai T, 1974. Variation of spontaneous occurrence rates of chromosomal aberrations in the second chromosomes of *Drosophila melanogaster*. Genetics 78:1209–1221.

Yamaguchi O, Cardellino RA, and Mukai T, 1976. High rates of occurrence of spontaneous chromosome aberrations in *Drosophila melanogaster*. Genetics 83:409–422.

Received January 7, 1997
Accepted July 8, 1997

Corresponding Editor: Ross MacIntyre

The Molecular Basis of a Microsatellite Null Allele From the White Sands Pupfish

A. G. Jones, C. A. Stockwell, D. Walker, and J. C. Avise

Microsatellite loci were cloned and characterized from the White Sands pupfish (*Cyprinodon tularosa*), a New Mexico state-listed endangered species. One locus exhibited a high-frequency nonamplifying allele localized to a single population. This null allele was PCR amplified by redesign of one of the original primers and multiple individuals homozygous for null as well as for nonnull alleles were sequenced using the new primer. These molecular dissections revealed that the original failure to amplify some alleles from this microsatellite locus was due to a 4 bp deletion in one of the original PCR priming sites. Furthermore, the reamplifications revealed five distinct size classes of alleles that had been masquerading as the original null. These null alleles did not overlap in length with the nonnull alleles, and they also differed consistently by a linked nucleotide substitution. Results suggest that the original null allele (as well as the nonnull class) has diversified considerably since its origin and has not recombined frequently with the nonnull class of alleles.

Microsatellite markers have become valuable tools for studies involving population genetics, kinship, and parentage assessment (Bruford and Wayne 1993; Queller et al. 1993), but a potential complication arises from the presence of nonamplifying or null alleles (Pemberton et al. 1995). Null alleles can produce serious problems for population-level studies by creating an apparent excess of homozygotes, resulting in incorrect allele frequency estimates and overestimates of inbreeding. In parentage studies they can result in false exclusions. Null alleles have been encountered in studies of numerous organisms, including mammals (Hulme et al. 1994; Phillips et al. 1993), birds (Primmer et al. 1995), fish (Jones and Avise 1997), insects (Cooper et al. 1996; Oldroyd et al. 1996), and crustaceans (Tam and Kornfield 1996). Despite the pervasiveness of microsatellite null alleles and the difficulties associated with their assay, little is known about their molecular basis (but see below), and even less is known about the evolutionary histories of the null alleles relative to their nonnull allele counterparts.

The state-listed endangered White Sands pupfish (*Cyprinodon tularosa*) is known from only four locations (Salt Creek, Lost River, Malpais Spring, and Mound Spring), all of which are in New Mexico. During the cloning and characterization of microsatellites from this species we encountered a null allele at high frequency in the Malpais Spring population. Here we investigate the molecular basis of this null allele and assess its evolutionary relationships to the nonnull alleles by redesigning PCR primers and sequencing multiple alleles at the region surrounding the microsatellite locus.

Materials and Methods

Microsatellite Cloning

Total genomic DNA was extracted from a single *C. tularosa* specimen (from the Salt

Creek population) by a standard phenol/chloroform procedure. The DNA was digested with *Nde*II and size selected by excising the 300–700 bp fragments from a 2% agarose gel after electrophoresis. Fragments were purified using the Prep-A-Gene DNA Purification System (BioRad) and ligated into *Bam*HI-digested, dephosphorylated pBluescript phagemid (Stratagene). Ligations were heat-shock transformed into competent XL1-Blue *E. coli* (Stratagene). The transformation was spread on LB plates containing ampicillin and X-gal. Approximately 1000 white colonies were picked to four patch plates for screening. Colonies were transferred to Hybond-N nylon membranes (Amersham International) following the manufacturer's recommendations and probed twice at 42°C (in 6× SSC, 0.1% SDS, 5× Denhardt's reagent) with two different cocktails of end-labeled oligonucleotides. Each hybridization was followed by two 30 min washes at 42°C in 6× SSC, 0.1% SDS. First, the oligonucleotides $(GT)_{10}$, $(GGAT)_4$, $(GACA)_4$, and $(TAG)_6$ were used, followed by stripping and reprobing with $(GA)_{10}$, $(GATA)_4$, $(TTAGGG)_3$, and $(TTC)_5$. Phagemid DNA was prepared from the 12 colonies that hybridized to the probes (Qiagen QIAprep spin plasmid miniprep kit). The inserts were sequenced using the *fmol* DNA sequencing system (Promega) and primers were designed for microsatellite-containing loci.

The PCR was performed in 10 μl reaction volumes containing 1× Promega *Taq* buffer, 1.5 mM $MgCl_2$, 0.15 μM of each primer, 0.1 mM of each dNTP, and 0.5 units of Promega *Taq* polymerase. The thermal cycling consisted of 30 cycles of denaturation at 94°C for 1 min, annealing at 55°C for 1 min, and extension at 72°C for 1 min, preceded by 2 min of denaturation at 94°C and followed by an additional 4 min extension at 72°C. Microsatellite polymorphisms were detected by labeling one primer with 1 μCi γ-^{32}P ATP per 5 pmol of primer and electrophoretically resolving fragments on standard 6% polyacrylamide denaturing sequencing gels.

Null Allele Analysis

A high-frequency null allele was suspected for locus WSP11 in the Malpais Spring population of pupfish because many individuals failed to amplify from the original PCR primer pair (WSP11UP, 5′-AACAAATCCAATAATGTATTAGAA-3′; and WSP11LO, 5′-GATGAACGAGGAGAAAGAATAG-3′), despite the fact that they amplified successfully for other loci. To solve this problem a new PCR primer (WSP11LO-A; 5′-CCCCTGCTGCCTCAAAG-3′) external to WSP11LO was designed from the original cloned sequence. When used in conjunction with WSP11UP, the new flanking primer (WSP11LO-A) produced excellent amplification of the WSP11 locus from all assayed individuals from all four populations.

To determine the molecular basis of the original null allele, several individuals (N = 5) that yielded no PCR product from the original primers, and that were homozygous when assayed with the new primer set (WSP11UP and WSP11LO-A), were sequenced using the *fmol* kit (Promega). We also sequenced 10 individuals that were recorded as homozygotes with both the original and new primer pairs, and thus did not contain the null allele.

Results

The Null Alleles

Amplification of a sample of 30 individuals from the Malpais Spring population with the original WSP11 PCR primers resulted in eight apparent homozygotes for a fragment 177 bp in length. The other 22 individuals yielded no product whatsoever. Other populations (Salt Creek, Lost River, and Mound Spring) assayed displayed apparently normal genotypes: all individuals amplified and the samples did not deviate significantly from Hardy-Weinberg expectations (Stockwell et al., in preparation). Thus the null allele appears to occur only in the Malpais Spring population.

The redesigned primer WSP11LO-A, external to the original primer, permitted amplification of all individuals from the Malpais Spring sample (Figure 1). For the three additional populations, amplification by the new primer pair left the microsatellite genotypes unchanged with the following exception: the resulting fragments were larger than the original products since they were being amplified using a primer external to one of the original primers (e.g., amplification of the original 177 bp allele, for example, now yielded a product of 202 bp). The nonnull alleles corresponded to 194, 196, 198, 200, and 202 bp with the new primer pair. The null class of alleles, endemic to the Malpais Spring population, included fragments of size 173, 179, 181, 187, and 189 bp. So an entire class of previously undetected alleles, distinct and nonoverlapping in size compared to the nonnull alleles, had been hidden within the single null allele in the original assays (Figure 1).

Sequence data were generated for 38 nucleotides flanking the microsatellite, including the original lower priming site. A total of 15 sequences were analyzed, including null alleles of size 179 (N = 1), 181 (N = 2), and 187 (N = 2), as well as nonnull alleles of size 194 (N = 4), 200 (N = 4), and 202 (N = 2). All nonnull alleles were identical in flanking sequence to one another and to the original sequence cloned from the *C. tularosa* library (Figure 2). The five sequenced null alleles were also identical to one another and differed from the cloned sequence by a 4 bp deletion within one of the original priming sites. Thus this deletion was the cause of the original null condition. The null alleles also differed consistently from the nonnull alleles by a single G to A transition at a nucleotide position 1 bp removed from the start of the microsatellite array (Figure 2).

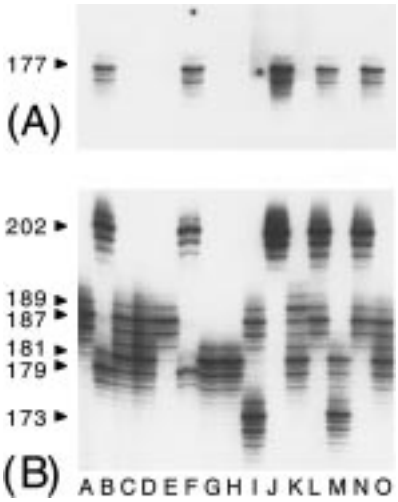

Figure 1. Autoradiographs of sequencing gels resolving the amplified products from 15 pupfish from the Malpais Spring population. **(A)** Amplification using the original WSP11 primers (WSP11UP and WSP11LO). **(B)** Amplification of the same templates using the alternative primers (WSP11UP and WSP11LO-A). Note in **(B)** that the alternative primers revealed a host of different alleles that had appeared as a null in the original assays **(A)**. The allele 177 amplified with the original primers in **(A)** corresponds to the 202 bp fragment produced by the new primers in **(B)**.

Discussion

Null alleles have been reported in a number of studies employing microsatellite loci. In our case the null allele was readily apparent because it occurred with sufficiently high frequency as to be present in homozygotes. Null alleles usually are more difficult to document. For example, had the null allele been infrequent in our population, it would have occurred primarily in heterozygotes and likely would have remained undetected. Null heterozygotes

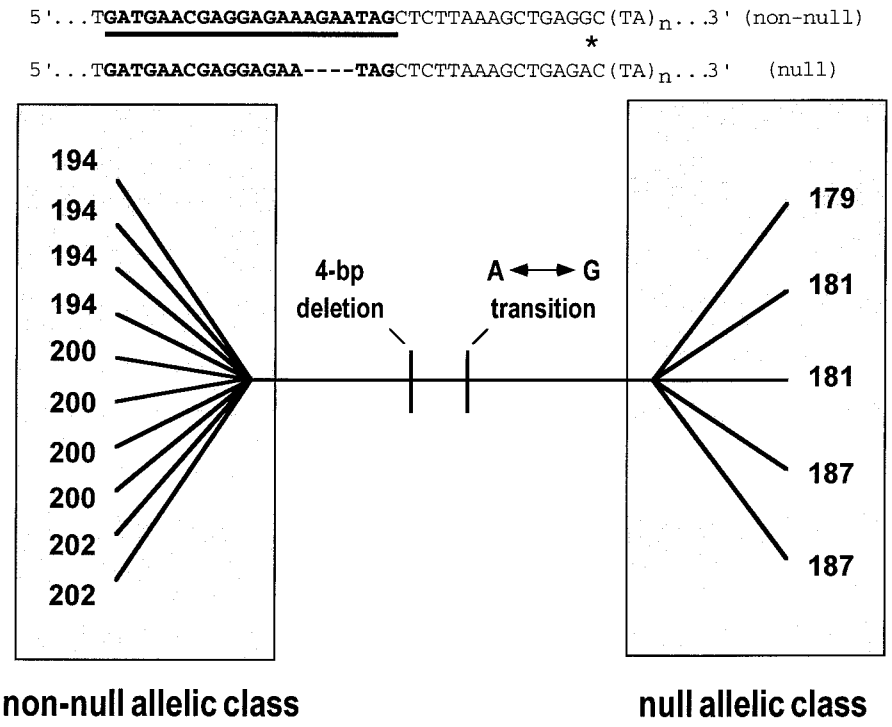

Figure 2. (Above) The sequence of the microsatellite WSP11 nonnull allele compared to the sequence retrieved from null alleles amplified from the Malpais Spring population of pupfish. The original primer WSP11LO is underlined. The second AGAA motif is shown as the site of the deletion (relative to the nonnull allele), but in reality any 4 bp segment of the AGAAAGAA sequence could have been the cause of the lesion. The asterisk denotes a point mutation that was perfectly linked to the 4 bp deletion. (Below) A graphical representation of the mutational distinctions in the 38 bp flanking sequence among the total of 15 haplotypes sequenced from the null and nonnull allelic classes. Numbers indicate the sizes (in bp) of the alleles sequenced.

would appear as nonnull homozygotes, and the blank gel profiles in the few true null homozygotes might have been attributed to sample degradation or failed PCR. Furthermore, rare null alleles would be unlikely to cause statistically significant deviations from Hardy-Weinberg equilibrium with the sample sizes employed in most population genetic surveys. Given these detection difficulties, null alleles probably are even more commonplace than indicated by reports in the literature.

In our case the high frequency of the pupfish null allele offered the advantage that null alleles often occurred in homozygous form such that direct sequencing of alternative alleles could be accomplished without the added difficulty of physically isolating haplotypes from heterozygous diploid tissues (e.g., Ortí et al. 1997). Although the microsatellite haplotypes in each such homozygote are not necessarily identical by descent, and hence might in principle retain some sequence variety whose phase (*cis* or *trans*) would remain unspecified, such complications did not arise in our assays. Thus sequences for three different size classes of null alleles (as well as three size classes of nonnull alleles) were obtained without ambiguity.

Few studies have examined the molecular basis of null alleles at microsatellite loci. Three studies conducted previously have documented point mutations that disrupt the problematic priming site (Ishibashi et al. 1996; Lehmann et al. 1996; Paetkau and Strobeck 1995). Two other studies identified short deletions in the priming site with similar effects: Callen et al. (1993) found an 8 bp deletion of one *GGTG* and one of the *TCTG* motifs from the sequence CCTC *TCTG GGTG TCTG* TGTC, and Ede and Crawford (1995) found the lesion to be a 12 bp deletion of a TAAGTTGCGTCC sequence that was preceded directly by an almost perfect tandem repeat, TCAGTTGCGTCC.

In our study a deletion was also found, in this case involving one of a pair of tandemly repeated AGAA sequence motifs (Figure 2) (of course, the evolutionary event could have been an insertion that converted an ancestral null allele into a non-null as assayed by the original primers). Interestingly, in both this study and that by Ede and Crawford (1995), the indels producing null alleles involved repetitive DNA. Though it is difficult to generalize from these few observations, it seems reasonable that tandem repeats should be avoided as PCR priming sites when possible.

In this study the original null allele actually concealed a class of five different microsatellite alleles distinct in size from the various nonnull alleles. This suggests that the 4 bp indel responsible for the null allele arose long enough ago to have accumulated a number of microsatellite length mutations. This suspicion is supported further by the nucleotide substitution that also cleanly distinguished all of the null alleles from the nonnulls.

Another conceivable way that the null alleles could have acquired microsatellite variation would be through recombination with the nonnull alleles. If this were the case the null alleles might be expected to mirror the variation of the original nonnull alleles, but to be shifted downward in length by 4 bp. This scenario is not consistent with our observations: The nonnull alleles were of size 194, 196, 198, 200, and 202 bp, whereas the null alleles were 173, 179, 181, 187, and 189 bp in length.

The two prior reports of null-producing deletions at microsatellite loci (Callen et al. 1993; Ede and Crawford 1995) entailed a situation similar to the present in which null alleles represented distinct size classes relative to the nonnulls. Conversely, for microsatellite nulls caused by point mutations, the allelic size variants appeared to be similar to those of the nonnull alleles (Lehmann et al. 1996; Paetkau and Strobeck 1995).

From the Department of Genetics, University of Georgia, Athens, GA 30602 (Jones, Walker, and Avise) and the Savannah River Ecology Laboratory, Aiken, South Carolina (Stockwell). C. A. Stockwell is currently at the Department of Zoology, North Dakota State University, Fargo, North Dakota. This work was supported by an NIH training grant to A.G.J. and D.W., by an NSF grant and University of Georgia funds to J.C.A., by contract DE-FC09–96SR18546 between the U.S. Department of Energy and the University of Georgia's Savannah River Ecology Laboratory, and by Department of Defense Legacy Funds from USAF, Holloman Air Force Base, New Mexico, to C.A.S. Mike Goodisman, Hsiu-Ping Liu, Margaret Mulvey, Bill Nelson, Hildy Reiser, Guillermo Ortí, Devon Pearse, Kurt Wollenberg, and Lorenzo Zane offered valuable comments on the manuscript. Fish were collected under New Mexico state permit 2887 issued to C.A.S. Thanks to Hildy Reiser and John Pittenger for assistance in collecting fish. Address correspondence to Dr. Avise at the address above.

References

Bruford M and Wayne R, 1993. Microsatellites and their application to population genetic studies. Curr Opin Genet Dev 3:939–943.

Callen DF, Thompson AD, Shen Y, Phillips HA, Richards

RI, Mulley JC, and Sutherland GR, 1993. Incidence and origin of "null" alleles in the (AC)n microsatellite markers. Am J Hum Genet 52:922–927.

Cooper G, Miller PL, and Holland PWH, 1996. Molecular genetic analysis of sperm competition in the damselfly *Ischnura elegans* (Vander Linden). Proc R Soc Lond B 263:1343–1349.

Ede AJ and Crawford AM, 1995. Mutations in the sequence flanking the microsatellite at the *KAP8* locus prevent the amplification of some alleles. Anim Genet 26:43–44.

Hulme DJ, Silk JP, Redwin JM, Barendse W, and Beh KJ, 1994. Ten polymorphic ovine microsatellites. Anim Genet 25:434–435.

Ishibashi Y, Saitoh T, Abe S, and Yoshida MC, 1996. Null microsatellite alleles due to nucleotide sequence variation in the grey-sided vole *Clethrionomys rufocanus.* Mol Ecol 5:589–590.

Jones AG and Avise JC, 1997. Microsatellite analysis of maternity and the mating system in the Gulf pipefish *Syngnathus scovelli,* a species with male pregnancy and sex-role reversal. Mol Ecol 6:203–213.

Lehmann T, Hawley WA, and Collins FH, 1996. An evaluation of evolutionary constraints on microsatellite loci using null alleles. Genetics 144:1155–1163.

Oldroyd BP, Smolenski AJ, Cornuet JM, Wongsiri S, Estoup A, Rinderer TE, and Crozier RH, 1996. Levels of polyandry and intracolonial genetic relationships in *Apis dorsata* (Hymenoptera: Apidae). Ann Entomol Soc Am 89:276–283.

Ortí G, Hare MP, and Avise JC, 1997. Detection and isolation of nuclear haplotypes by PCR-SSCP. Mol Ecol 6: 575–580.

Paetkau D and Strobeck C, 1995. The molecular basis and evolutionary history of a microsatellite null allele in bears. Mol Ecol 4:519–520.

Pemberton JM, Slate J, Bancroft DR, and Barrett JA, 1995. Nonamplifying alleles at microsatellite loci: a caution for parentage and population studies. Mol Ecol 4: 249–252.

Phillips HA, Thompson AD, Kozman HM, Sutherland GR, and Mulley JC, 1993. A microsatellite marker within the duplicated D16S79 locus has a null allele: significance for linkage mapping. Cytogenet Cell Genet 64: 131–132.

Primmer CR, Møller AP, and Ellegren H, 1995. Resolving genetic relationships with microsatellite markers: a parentage testing system for the swallow *Hirundo rustica.* Mol Ecol 4:493–498.

Queller DC, Strassmann JE, and Hughes CR, 1993. Microsatellites and kinship. Trends Ecol Evol 8:66–75.

Tam KT and Kornfield I, 1996. Characterization of molecular markers in *Homarus* (Crustacea, Decapoda). Mol Mar Biol Biotechnol 5:230–238.

Received June 17, 1997
Accepted December 13, 1997

Corresponding Editor: William S. Modi

Cream Fur: A New Mouse Mutation That May Cause Unusual Lipid Metabolism

J. Hayakawa, H. Nikaido, T. Ohkawa, and J. Kitoh

In 1986 an albino mouse with cream yellow coat color was discovered in a breeding colony of strain CAL20, which is an *IgH-C* congenic strain of BALB/c mice, supported by the Institute for Experimental Animals, Faculty of Medicine, Kanazawa University. Genetic analysis revealed that the cream yellow coat color phenotype was controlled by a single recessive mutant gene on chromosome 13. A preliminary study with biochemical and histologic examinations showed that cream yellow hair contained more fatty acid than unaffected normal hair and a large number of lipid droplets accumulated in parenchyma cells of the liver in mutant mice, as early as the age of 32 days old, suggesting that the cream yellow coat color was due to unusual lipid metabolism. The locus was designated cream fur locus and was given the gene symbol *crf*. In addition, it was found that recombination frequencies in the vicinity of the region of the *crf* locus were markedly different between male and female meiosis.

Metabolite deposit due to abnormal metabolism, such as excess of bilirubin in jaundice, is easily recognized in albino mice because of the lack of pigment in skin and fur. Several mutations have been discovered which tint unpigmented coat of albino mice (Hetherington 1977; Oba et al., personal communication; Tusk et al., personal communication). However, few describe the origin of the substance causing the tint in the coat of albino mice.

In this article we describe a cream yellow coat color that was found in a colony of albino mice maintained at the animal facility of our institute. The mutant is inherited in an autosomal recessive fashion. Homozygotes are recognizable at 10 days after birth by cream yellow coat color. The cream fur contains a larger quantity of medium size fatty acids compared with the fur from unaffected siblings. Although the mutation does not affect the viability and fertility of either male or female mice, a large number of lipid droplets is found in the hepatic cells as early as 32 days of age. We designate this new mutant locus cream fur (*crf*).

Materials and Methods

Mice

Mice were maintained under standard conditions in the Institute for Experimental Animals, Faculty of Medicine, Kanazawa University. The original mutant mouse was discovered in a colony of mice originally obtained from the National Institutes of Health (Bethesda, Maryland) in November 1986. It was propagated by mating, followed by submitting, and two lines have been established: one line has been maintained as a segregating inbred strain (CRH) and the other as fixed homozygous for cream yellow fur mutation (CRF). In further biochemical and histopathological experiments CRH strain mice were used and unaffected littermates were used as normal controls. Hereafter the affected cream yellow mice are designated CRF mice. C57BL/6-c^{2J}/c^{2J} mice used for genetic analysis were kindly supplied by Dr. Yonekawa from the Tokyo Metropolitan Institute of Medical Science. Dr. Oba (School of Medicine, Tohoku University) kindly supplied ICR-*ly* (ICR-light yellow) mice that have phenotypically similar coat color to CRF mice found in an ICR colony of Tohoku University. Other inbred mice used in this study were maintained in our animal facility.

Test for Allelism of the Albino Locus and Complementation of Known Loci

To test whether the cream yellow color derives from a mutant allele at the albino locus of CRF mice, CRF mice were mated to C57BL/6 and the backcross progeny between CRF and F_1 mice were produced. The resulting backcross progeny with albino phenotype and nonalbino phenotype were examined for coat color. Complementation between light yellow phenotype and CRF phenotype was examined in F_1 hybrid mice between ICR-*ly* and CRF mice.

Biochemical Analysis of Clipped Hair

Approximately 0.5 g of clipped hair was suspended in 1 N NaOH (50 ml) and heated at 100°C for 4–5 h. The completely resolved hair solution was neutralized with 1 N HCl. After cooling at room temperature the solution was evaporated at 50°C. The lipid component of the residue was extracted with chloroform and methanol mixture (3:1) and then extracted with ether. The extraction procedures were repeated twice and the extracts were combined. The combined extract was dried by evaporation and analyzed by gas chromatography and mass spectrometry. The precipitate remaining after lipid extraction was subjected to phenylthio hydration reaction (PTH). The resultant PTH amino acid derivatives were analyzed by high-performance liquid chromatography.

Histopathology

Males and females of either CRF and control mice at 32, 52, 100, 360, 480, and 540 days of age were used for light and electron microscopic examination. Under deep ether anesthesia, mice were perfused

through the left ventricle with 10% buffered formalin or glutar- and paraformaldehyde/phosphate buffer containing 0.05% picric acid fixative. Tissue blocks of liver and skin were processed with routine paraffin embedding or epoxy resin embedding procedures. Some tissue sections fixed with phosphate-buffered formalin were cut on a freezing microtome and stained by Sudan black B to confirm lipid accumulation. Paraffin sections were cut and stained by hematoxylin and eosin. About 0.5 μm epon sections were cut and stained by 0.1% toluidine blue for light microscopic observation. Ultrathin sections were stained with uranyl acetate and lead citrate, then observed on a JEOL-100CX electron microscope.

Linkage Analysis

CRF mice were mated with C57BL/6-c^{2J}/c^{2J} albino mice. The F_1 hybrids were reciprocally backcrossed to CRF mice. DNA was extracted using ordinary phenol and the chloroform method from liver. Polymerase chain reactions for microsatellite markers (*SSLP* loci) were carried out and size differences of the products were detected as previously described (Nikaido et al. 1995). The sequences of primer pairs for microsatellite amplification and simple sequence length polymorphism between strains were sought using the database provided by the Whitehead Institute/MIT Center for Genome Research. The primer pairs of *SSLP* loci *D13Mit3* and *D13Mit13* were kindly prepared by Dr. S. Murakami at the Laboratory of Molecular Biology, Cancer Research Institute, Kanazawa University. The primer pairs for other *SSLP* loci were purchased from Funakoshi Co. (Tokyo, Japan). Gene order and recombination frequencies were calculated with the Map Manager computer program (Manly 1993).

Results

Gross Appearance and Histological Findings

Mutant mice with cream yellow fur could be easily recognized at 8 to 10 days old when their hair had completely grown (Figure 1). They were healthy and grew normally like the unaffected control mice. After weaning no growth retardation was noted and both males and females were completely fertile. In adulthood CRF mice became neither obese nor slender. At autopsy no gross morphological abnormality in viscera was found. Although in naked eye observations the liver of CRF mice showed no remarkable differences of color, size, or solidity compared with the normal control mice, in light and electron microscopic observations histopathologic changes were found at 32 days of age as a kind of fatty change in both male and female CRF (Figure 2). Many small lipid droplets appeared in the cytoplasm of the liver parenchyma cells, especially in and/or around the glycogen areas, but no droplets were found in the Kupffer cells. Accumulation of the lipid droplets showed no tendency to begin from a central site nor from the periphery of lobules. As age advanced the lipid droplets increased markedly in number but little in size. Lipid droplets accumulated in the glycogen areas, then an increase of the lipid droplets appeared to be accompanied by a decrease of glycogen content. Eccentricity of nuclei and transformation of mitochondria and other cell organellae under pressure of lipid accumulation were not shown. Degenerating cells or cells with necrotic changes were not found in liver. At over 100 days of age, very big lipid droplets appeared in the Kupffer cells. However, the accumulation of big lipid droplets in the Kupffer cells was also observed in the normal control mice of advanced age. It seemed that the above-mentioned lipid accumulation in the liver parenchyma cells differed from the pathological changes observed in the fatty degeneration or the fatty liver.

Figure 1. A mutant mouse with cream yellow fur and her normal and mutant pups.

Accumulation of the adipose cells or of cells that engulfed fat was not found in the dermis, although the surface of the epidermis and fur and the sebaceous glands were stained strongly with Sudan black B in the CRF mice. However, the morphological changes of skin and hair were not distinct.

Biochemical Analysis of the Clipped Hair

Biochemical analysis revealed that the concentration of lipid in hair from the CRF mice was significantly higher than that from the normal control mice. Mass spectrometer analysis indicated that the extract with organic solvent from the CRF hair contained three to four times more fatty acids with carbon numbers 12, 14, 16, and 18 than those from normal control hair. HPLC analysis of PTH derivatives of amino acids showed that the amino acid composition and its quantity in hair did not differ between the CRF mice and normal controls.

Genetics and Linkage Analysis

Complementation with previously known light-yellow phenotype. No F_1 mice between cream yellow and light-yellow mice showed cream or light-yellow coat color, suggesting two similar phenotypes are caused by genes at different loci.

Among backcross progeny of CRF mated to F_1 mice between CRF and C57BL/6 mice, only one-half of albino progeny showed cream yellow fur, unless all albino progeny carry albino alleles from CRF mice, while the coat color of nonalbino mice carrying nonalbino allele from C57BL/6 could not be classified. This indicates that cream

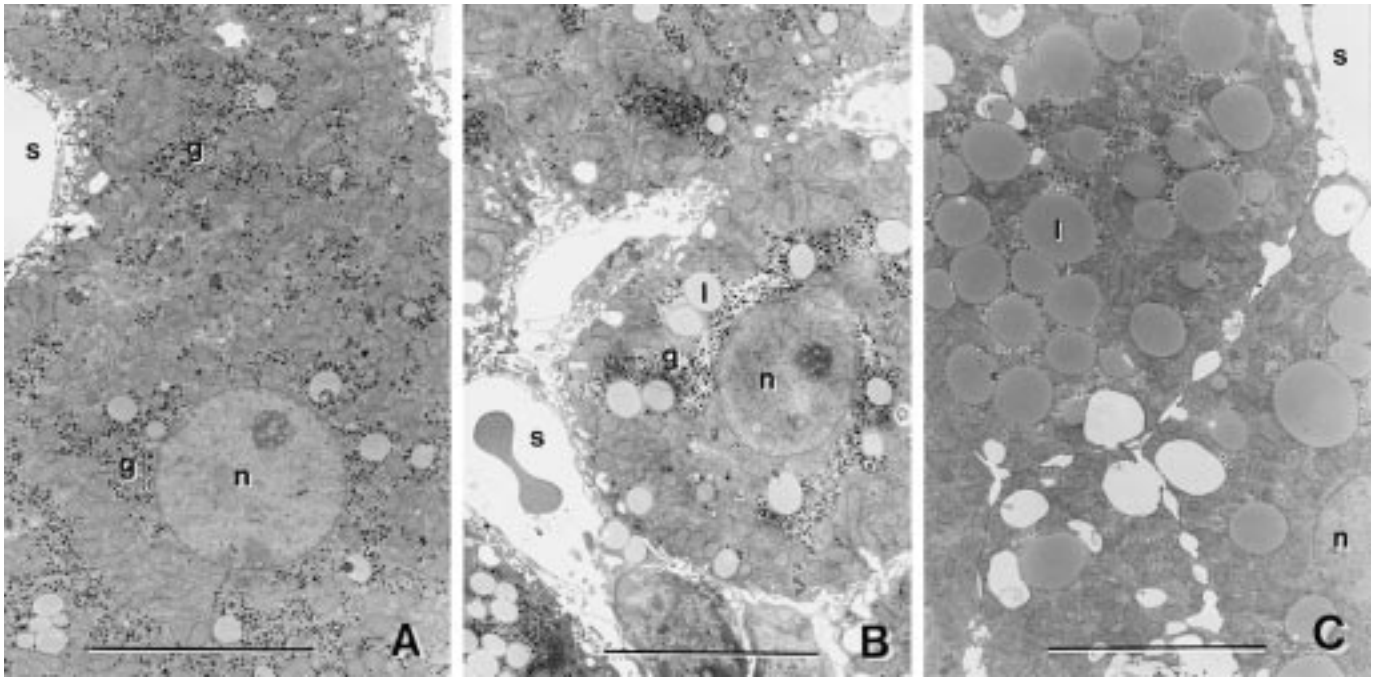

Figure 2. Electron micrographs of the hepatic cell in **(A)** a normal control 100-day-old male; **(B)** the CRF 32-day-old male; and **(C)** the CRF 300-day-old male. Scale bars indicate 10 μm. g = glycogen area, l = lipid droplet, n = nucleus of the hepatic cell, s = sinusoidal cavity.

yellow coat color is genetically independent of albino locus and it can be phenotypically distinguished only in albino mice.

Mode of inheritance and linkage analysis. Breeding records and early mating experiments with albino strains of AKR/J and A/J mice indicated that the CRF phenotype was inherited in a single recessive manner. However, we could not detect a close linkage between several biochemical markers and the *crf* locus. As a result of the recent development of microsatellite markers, we could attempt to detect linkage between *SSLP* loci on all autosomes. In this experiment CRF mice were mated to coisogenic albino mice of C57BL/6 mice. A total of 223 backcross progeny of F_1 mice crossed with CRF mice were screened for cosegregation with *SSLP* loci on each autosome. Finally, close linkage between CRF phenotype and *SSLP* loci on chromosome 13 was found. The genetic distances estimated from combined recombination frequencies of male and female meiosis among *SSLP* loci and the *crf* locus are depicted in Figure 3. The nearest distal or proximal *SSLP* locus to *crf* locus was *D13Mit231* and *D13Mit142,* respectively. The observed gene order *SSLP* loci and the *crf* locus were *D13Mit3*—18.8 cM—*D13Mit13*—4.0 cM—*D13Mit142*—7.6 cM—*crf*—4.0 cM—*D13Mit231*—12.6 cM—*D13Mit107*—21.5 cM—*D13Mit151.* The gene order and the distance intervals of these *SSLP* loci were consistent with those previously compiled in the Mouse Genome Database except the distance interval between *D13Mit142* and *D13Mit231.* However, there were significant sex-specific differences in recombination frequencies in the proximal region to *D13Mit231,* for example, the recombination frequency between *D13Mit13* and the *crf* locus in male meiosis was 0.065 (7/107), whereas that in female meiosis was 0.161 (19/118). The recombination frequency between *crf* and the *D13Mit151* locus that is mapped to the distal region of the chromosome was rather greater in male meiosis than in female meiosis (Figure 4).

Discussion

In this study we mapped a mutation that tints the coat color of albino mice cream yellow. The map distance of the mutant locus *crf* was estimated to be approximately 7.6 cM distal to *D13Mit142* and 4.0 cM proximal to *D13Mit231.* The *SSLP* loci *D13Mit142* and *D13Mit231* were mapped 37 cM and 39 cM from the top of chromosome 13, respectively (Mouse Genome Database).

The mutation is different from previously found mutations that produce similar coat color; for example, the *Crm* (cream) mutation discovered by Hetherington (1977) is X-linked (Beechey and Searle 1979) and causes fluorescence of the coat in long-wave UV light (Peters and Searle 1979). A similar pale yellow coat color in albino IVCS mouse is controlled by a gene on the X chromosome (Tsuji et al., personal communication). Another light yellow coat color discovered by Oba et al. (personal communication) in ICR mice is inherited as autosomal recessive. The present complementation test showed that the light-yellow coat color and cream fur in CRF mice were not allelic. Thus the cream yellow coat color described in this study is caused by a mutation which has not been described previously. The substance causing the cream yellow hair has not been identified. It is speculated that the color is probably due to abnormal metabolite, since biochemical analysis and histopathologic examination indicated increased fatty acid in clipped hair and accumulation of lipid droplets in the liver parenchyma cells, while no morphological changes were found in dermis or hair texture. The metabolic system disrupted by this mutation is unknown at present. It is interesting that unlike the degenerated liver cells, lipid droplets localize in the glycogen area of the cells. This lipid droplet accumulation in CRF mice occurs as early as 32 days of age.

Recently, genetic factors responsible for lipoprotein and cholesterol metabolism have been extensively mapped in mice. The region in chromosome 13 at which the *crf* locus mapped includes a rate-limiting enzyme in cholesterol synthesis, HMG-

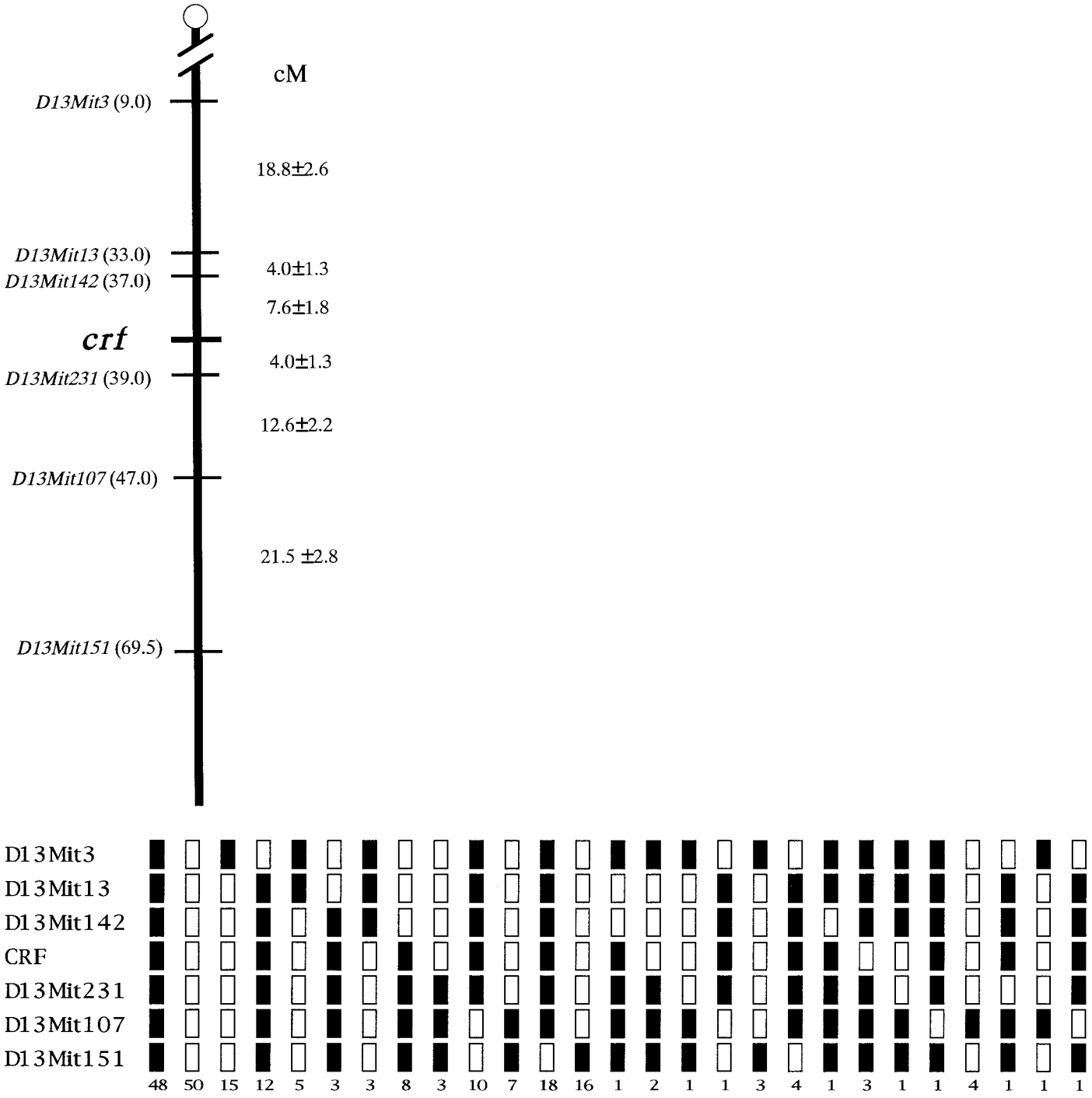

Figure 3. Linkage map of *crf* locus. (Top) Distances between loci are shown as centiMorgans ± standard error to the right of the map (recombinants/total progeny). The distances are calculated from combined recombination frequencies in a total of 223 backcross progeny derived from 118 female meiosis and 105 male meiosis. The centiMorgan position of each *SSLP* locus retrieved from the Mouse Genome Database at The Jackson Laboratory is indicated in parentheses. (Bottom) Haplotype figure from the backcross. Black and white boxes represent loci typed as homozygous and heterozygous, respectively. The number of animals with each haplotype is given at the bottom of each column of boxes.

CoA (3-hydroxy-3-methylglutaryl coenzyme A) reductase, HMG-CoA synthase, and some quantitative trait loci for plasma low density lipoprotein/very low-density lipoprotein (Welch et al. 1996). However, preliminary biochemical examination of the plasma indicated that there was no significant difference between the CRF mice and normal controls in plasma cholesterol and triglyceride levels as well as plasma glucose level. In this region on chromosome 13 several enzyme-related loci such as steroid 5 alpha-reductase 1, arylsulfatase complex, etc. are mapped, but we have no rational reason to predict that one of these loci may be identical to the *crf* locus. It is necessary to clarify the factors related to the cream yellow coat color and also to generate a high-resolution map in the region of chromosome 13.

Concerning a fine mapping, it is noteworthy that there is a marked difference in recombination frequencies in the vicinity of the *crf* locus between male and fe-

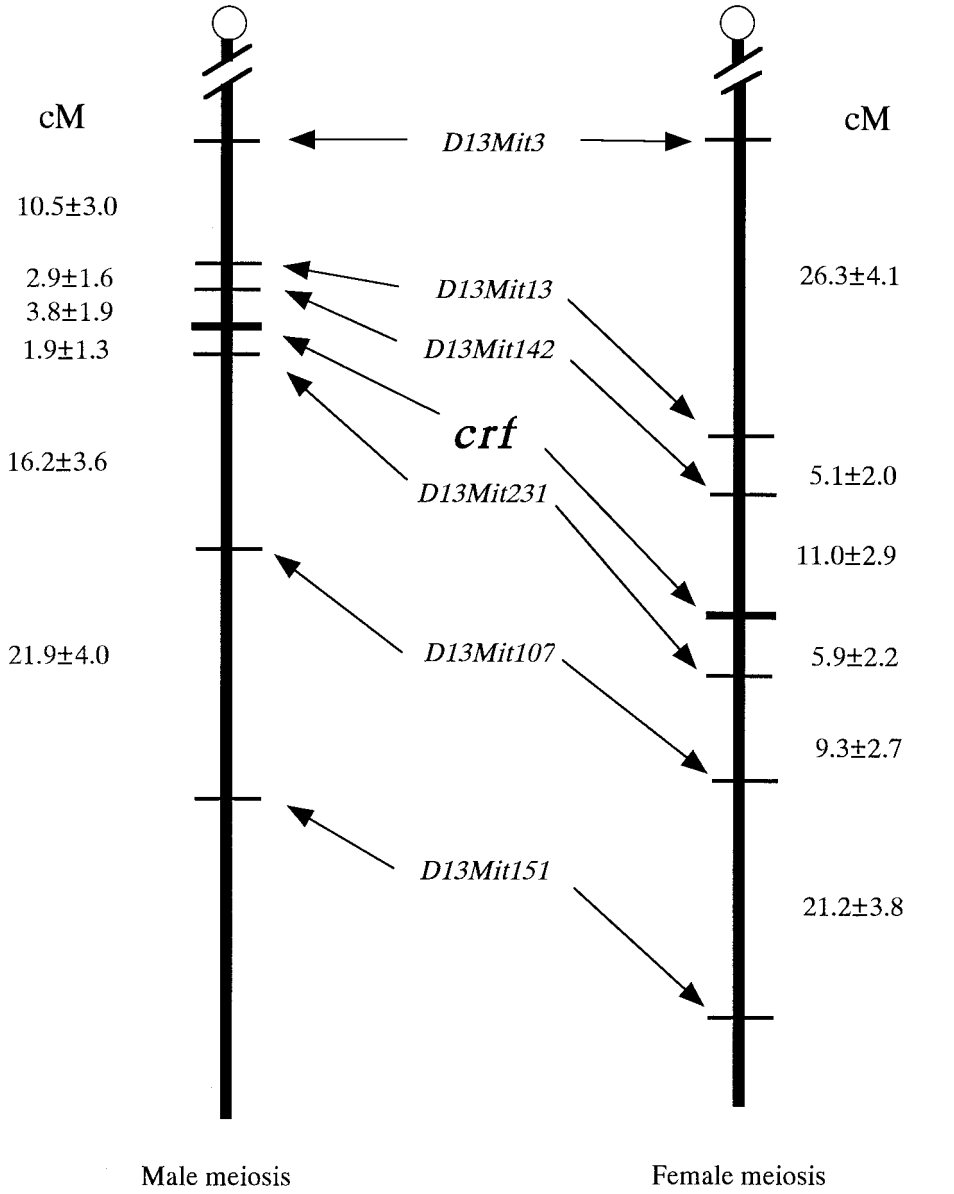

Figure 4. Sex-specific linkage map in proximal region of mouse chromosome 13. The distances between loci are shown as centiMorgans ± standard error. The distances are separately calculated from recombination frequencies in 105 backcross progeny from male F_1 hybrids mated to CRF females and in 118 backcross progeny from female F_1 hybrids mated to CRF males (recombinants/total progeny).

male meiosis. It is well documented that in mice as well as other animals there are sex-specific differences in recombination frequency, and in general recombination occurs less frequently during male meiosis than during female meiosis (Silver 1995). Therefore, to construct a high-resolution map for positional cloning of the *crf* gene, female F_1 should be chosen to produce backcross progeny.

Aside from the map position of the *crf* locus, it is intriguing that sex-specific differences in recombination frequencies were found in the proximal region between *D13Mit3* and *D13Mit231,* but in the distal region from *D13Mit231* to *D13Mit151* the recombination frequencies between sex were not different (Figure 4). The reason why some regions in the genome undergo recombination more frequently in the germ cells of one sex than the other is not fully understood. Recently it has been assumed that the genomic imprinted regions in which two parental alleles are differentially expressed in embryo genesis may be identical to the regions which undergo sex-specific recombination (Pàldi et al. 1995; Thomas and Rothstein 1991).

In conclusion, the *crf* mutation appears to increase lipid content in hair and lipid droplets in liver parenchyma cells, although the primary cause of the increase of lipid in these tissues remains unexplained, and an increased storage of the lipid material in hair tints the coat color in albino mice.

From the Institute for Experimental Animals (Hayakawa and Nikaido) and the Department of Biochemistry (Ohkawa), Kanazawa University, 13–1 Takara-machi, Kanazawa 920, Japan, and the Institute for Laboratory Animal Research, Nagoya University School of Medicine, Nagoya, Japan (Kitoh). T. Ohkawa is currently at the Japanese Red Cross Ishikawa Blood Center, Kanazawa, Japan. Address correspondence to Jun-ichiro Hayakawa at the address above or e-mail: hayakawa@med.kanazawa-u.ac.jp. We would like to thank Ms. Nobuko Saito for her excellent assistance with the genotyping *SSLP* and the staff of the Institute for Experimental Animals for their care of animals. This research was supported in part by a grant-in-aid for scientific research on priority areas (no. 06279101) and a grant-in-aid for scientific research (no. 08458274) from the Ministry of Education, Science, Sports and Culture, Japan.

References

Beechey CV and Searle AG, 1979. Crm at distal end of X. Mouse News Lett 60:47.

Hetherington CM, 1977. Recent spontaneous mutants. Mouse News Lett 56:35.

Manly KF, 1993. A Macintosh program for storage and analysis of experimental genetic mapping data. Mammal Genome 4:303–313.

Nikaido H, Horiuchi M, Hashimoto N, Saheki T, and Hayakawa J, 1995. Mapping of *jvs* (juvenile visceral steatosis) gene, which causes systemic carnitine deficiency in mice, on chromosome 11. Mammal Genome 6:369–370.

Pàldi A, Gyapay G, and Jami J, 1995. Imprinted chromosomal regions of the human genome display sex-specific meiotic recombination frequencies. Curr Biol 5:1030–1035.

Peters J and Searle AG, 1979. Fluorescence of sex-linked cream Crm. Mouse News Lett 61:37.

Silver LM, 1995. Mapping in the mouse: an overview. In: Mouse genetics. New York: Oxford University Press; 133–155.

Thomas BJ and Rothstein R, 1991. Sex, map, and imprinting. Cell 64:1–3.

Welch CL, Xia Y-R, Shechter I, Farese R, Mehrabian M, Mehdizadeh S, Warden CH, and Lusi AJ, 1996. Genetic regulation of cholesterol homeostasis: chromosomal organization of candidate genes. J Lipid Res 37:1406–1421.

Received May 13, 1997
Accepted October 20, 1997

Corresponding Editor: Neal Copeland

Clench: A New Autosomal Recessive Mutation in Japanese Quail

Y. Nakane and M. Tsudzuki

The clench (CL) is a new morphological mutation in Japanese quail (*Coturnix japonica*). The CL mutants rigidly clench their toes in both legs, which gives rise to a human fistlike appearance in the distal ends of the legs. Other parts of the CL body are quite normal. In spite of the severe toe abnormality, the CL mutants are normal in fertility, hatchability, and postnatal viability. Genetic analysis revealed that the CL mutation is an autosomal recessive with 100% penetrance. The proposed gene symbol is *cl*.

In September 1995, among the progeny from a pair of wild-type Japanese quail (*Coturnix japonica*) maintained at the Department of Laboratory Animal Science, College of Agriculture, Osaka Prefecture University, Sakai, Osaka, Japan, we found unusual chicks that exhibited permanently clenched toes. The same pair continued to produce similarly abnormal progeny. We separated the male and female of the original pair and 2 weeks later mated each of them to wild-type controls to obtain F_1s. Subsequently we mated the F_1 birds among themselves avoiding sib matings. Some of these matings segregated abnormal individuals, as did the original pair. Thus this abnormality was thought to be a hereditary trait. We named the trait clench (CL) and started genetic analysis. This article describes the clench trait and its mode of inheritance.

Materials and Methods

General care of quail is described elsewhere (Tsudzuki 1995). We reciprocally mated the CL mutants to control birds (UOP-WT line; Ito and Tsudzuki 1994) to obtain F_1 progeny. Subsequently we produced F_2 and backcross generations. Furthermore, to examine the penetrance of the mutant gene, we mated the CL mutant birds inter se. Segregation ratios of the normal and mutant were investigated at hatching. The data were analyzed by the chi-square test.

Results and Discussion

The abnormality in the CL mutant was limited to the toes. The other parts of the body were quite normal. The CL chicks rigidly clenched their toes in both legs, which gave rise to a human fistlike appearance in the distal ends of the legs (Figure 1). The CL adults more rigidly clenched their toes than the chicks. Both chicks and adults could stand and walk using the region around the first phalanx of the third and fourth toes. Furthermore, in spite of the severe abnormality in the toes, the CL mutant showed normal mating ability (Table 1).

Table 1. Fertility and hatchability in clench and normal quail

Matings[a]	Fertility	Hatchability
CL × CL	182/188[b] (96.8%)	133/182 (73.1%)
NOR × NOR	451/458[b] (98.5%)	341/451 (75.6%)

[a] CL and NOR mean clench and normal individuals, respectively.

[b] Total number of eggs set.

Table 2 shows the incidence of the CL mutant in mating experiments between the CL and control birds. All F_1 progeny from reciprocal matings were normal, which suggested autosomal recessive inheritance. Of F_2 progeny, 174 were normal and 66 were CL. This segregation ratio was in agreement with the expected 3:1 ratio ($\chi^2 = 0.800$, $.30 < P < .50$) based on the hypothesis that the CL trait is controlled by an autosomal recessive gene. At the backcross generation, normal and CL individuals segregated in a ratio of 275:266. This segregation ratio was in agreement with the expected 1:1 ratio ($\chi^2 = 0.150$, $.50 < P < .70$) on the basis of our hypothesis mentioned. Moreover, in the F_2 and backcross progeny, sex ratio was normal in both normal and CL individuals. These data apparently indicate that the CL trait is controlled by an autosomal recessive gene. We propose the gene symbol *cl* for the mutant gene controlling the CL trait. The penetrance of the *cl* gene seemed to be 100%, because all progeny from CL × CL matings were CLs.

In Japanese quail, approximately 50 morphological mutants have so far been reported in the literature (Cheng and Kimura 1990; Tsudzuki et al. 1998). Among them, however, there is no mutation that shows clenched toes. On the other hand, in chickens, there is a somewhat similar mutation known as crooked or curly toes (Fisher 1956; Hicks and Lerner 1949). Although some of the chicken crooked toes mutants mildly clench their toes inward, the majority show abnormal toes that are curled (crooked) laterally, which is obviously different from the quail CL mutants in all of which the toes are rigidly clenched inward. Hicks and Lerner (1949) did not describe a mode of inheritance of the trait, but Fisher (1956) showed that in the Kedu breed the crooked toes mutation is controlled by an autosomal recessive gene. Later Somes (1980) assigned the gene symbol *crt* to the gene. The penetrance of the *crt* gene is incomplete, which also differs from the quail *cl* gene that has 100% penetrance. The chickens showing hereditary arthrogryposis syndrome (Rigdon et al. 1965) also have abnormal toes that were curled laterally, as in the case of

Figure 1. Comparison of the toes of newly hatched normal (left) and mutant (right) chicks. The mutants rigidly clench their toes, resulting in a shape like a human fist.

Table 2. Incidence of the clench mutant at F_1, F_2, and backcross generations in mating experiments between the clench and control birds[a]

Matings[b]			No. of progeny observed	No. of progeny of[b]		Expected ratio[d]		
Male	×	Female	No. of matings	NOR	CL	NOR : CL	χ^2	P
NOR	×	CL	4	177	177	0	1:0	—	—
CL	×	NOR	4	108	108	0	1:0	—	—
Total			8	285	285	0	1:0	—	—
F_1	×	F_1	3	240	174	66	3:1	0.800	$.50 > P > .30$
F_1	×	CL	8	343	175	168	1:1	0.143	$.80 > P > .70$
CL	×	F_1	6	198	100	98	1:1	0.020	$.90 > P > .80$
Total			14	541	275	266	1:1	0.150	$.70 > P > .50$
CL	×	CL	4	167	0	167	0:1	—	—

[a] Observation was performed at hatching. There was no increased mortality noted among clench embryos.
[b] NOR and CL mean normal and clench individuals, respectively.
[c] Involving both newly hatched chicks and late dead embryos.
[d] Based on simple autosomal recessive inheritance.

Fisher (1956) and Hicks and Lerner (1949). This chicken mutation is also easily distinguishable from the quail CL mutation, because many of the chickens hatch with a normal external appearance and develop curled toes and/or spastic legs within 24–72 h. The quail CL mutants already have abnormal toes in embryonic stages and never show spastic legs. The quail CL mutation may be the first of this type of mutation in poultry. The arthrogryposis syndrome of chickens is histologically characterized by muscle necrosis in the legs. The cause of the quail CL mutant condition is unlikely to be muscle necrosis, because the two mutants show large differences in external phenotypes. Furthermore, the CL leg skeleton is quite normal involving phalanges. Thus, in the quail CL mutant, some abnormality might reside in the tendons controlling the toes.

From the Department of Laboratory Animal Science, College of Agriculture, Osaka Prefecture University, Sakai, Osaka 599-8531, Japan (Nakane), and the Laboratory of Animal Genetics, Faculty of Applied Biological Science, Hiroshima University, Kagamiyama, Higashi-Hiroshima, Japan (Tsudzuki). Address correspondence to Dr. Nakane at the address above or e-mail: ynakane@jyui.vet.osakafu-u.ac.jp.

References

Cheng KM and Kimura M, 1990. Mutation and major variants in Japanese quail. In: Poultry breeding and genetics (Crawford RD, ed). Amsterdam: Elsevier; 333–362.

Fisher H, 1956. Congenital crooked toes, an inherited defect in the domestic fowl. Arch Geflügelk 20:118–127.

Hicks AF Jr and Lerner IM, 1949. Hereditary crooked toes in chickens. Poult Sci 28:625–626.

Ito S and Tsudzuki M, 1994. Orange: a plumage color mutation accompanied by semi-lethality in Japanese quail. J Hered 84:145–147.

Rigdon RH, Schreiber MH, and Levy A, 1965. The arthrogryposis syndrome in chickens. Arch Pathol 79: 388–393.

Somes RG Jr, 1980. Alphabetical list of genes of domestic fowl. J Hered 71:168–174.

Tsudzuki M, 1995. Light down lethal: a new autosomal recessive down color mutation of Japanese quail. J Hered 86:305–307.

Tsudzuki M, Nakane Y, and Wada A, 1998. Hereditary multiple malformation in Japanese quail: a possible powerful animal model for morphogenetic studies. J Hered. 89:24–31.

Received June 19, 1997
Accepted December 13, 1997

Corresponding Editor: J. James Bitgood

Replication Banding and Sister-Chromatid Exchange of Chromosomes of Channel Catfish (*Ictalurus punctatus*)

Q. Zhang, W. R. Wolters, and T. R. Tiersch

A replication banding procedure using fluorouracil (FU) and bromodeoxyuridine (BrdU) was developed for use with cultured leukocytes of channel catfish (*Ictalurus punctatus*). Analyzable banding patterns were produced on chromosomes stained with a fluorochrome plus Giemsa (FPG) method. The consistency of the chromosomal bands was evaluated by computer-assisted image analysis. Banding patterns of representative chromosomes including those bearing nucleolus organizer regions (NOR) were reproducible. A standard RBG-banded karyotype (R bands by BrdU and Giemsa) was established with idiograms of each chromosome. We also developed procedures to study sister-chromatid exchange (SCE) and sister-chromatid differentiation (SCD) in cultured leukocytes, without addition of mutagenic substances. The average occurrence of SCEs in the absence of mutagens was 3.0 ± 1.0 (n = 60) chromosomes per cell and was not significantly different among fish (P = .26).

Studies of fish chromosomes have not been as successful or widespread as those in other vertebrate groups (Gold et al. 1990). A limiting factor has been technical difficulty in obtaining good chromosome spreads, because most species have a large number of small chromosomes. Because of this and minimal compartmentalization of the fish genome by base composition (Medrano et al. 1988), techniques for linear structural banding (e.g., quinacrine, Giemsa, and reverse bands) developed for higher vertebrates (Verma and Babu 1989) have succeeded rarely with fish chromosomes.

Dynamic methods using mitotically active cells, such as replication banding, are an alternative to structural banding. Techniques including RBG (replication bands by bromodeoxyuridine using Giemsa) procedures rely on the incorporation of a base analogue during DNA replication and postfixation modification of chromosome structure in the substituted regions (Ronne 1992). Therefore difficulties that relate to the structure or base composition of fish chromosomes can be bypassed with replication (R) banding. Replication banding of fish chromosomes has been reported in *Carassius auratus* (Zhang and Wu 1985); *Rutilus rutilus* and *Scardinius erythrophthalmus* (Hellmer et al. 1991); *Oncorhynchus mykiss* (Delany and Bloom 1984); *Salmo salar* (Pendas et al. 1993), and *Scorpaena procus* and *Scorpaena notata* (Giles et al. 1988) through intraperitoneal injection of bromodeoxyuridine (BrdU) into living fish. However, banding patterns have been better controlled with the use of cultured cells (Ronne 1992).

Sister-chromatid exchange (SCE) involves the breakage and reunion of chromosomal DNA (presumably between complementary regions) detectable after two or more rounds of replication in the presence of BrdU (Wolff 1982). Analysis of SCE is of interest because there appears to be a correlation between the frequency of SCE and exposure to mutagenic agents such as radiation or chemicals. Therefore SCE analysis can be valuable for the study of mutagenesis and environmental toxicology in fish (Kligerman 1979). Similar to the procedure used in replication banding, the presence of BrdU in cultures of cells for two consecutive generations yields sister chromatids that can be stained differentially [i.e., sister-chromatid differentiation (SCD)] to identify exchanged segments. Chromatids containing DNA strands with more BrdU incorporation will stain less intensely than chromatids with less incorporation because of the quenching action of BrdU (Verma and Babu 1989).

Computer-assisted chromosome analysis was first reported in fish in the mid-1980s (e.g., Gold et al. 1986). The introduction of newer technology has enabled handling of chromosome images imported directly from the light microscope by video camera (Bauchan and Campbell 1994). Computer-assisted analysis yields objective and quantitative estimates of banded areas of chromosomes (Drets et al. 1992). This technique remains unstudied for application in analysis of the weak bands that have been found in the chromosomes of most fish species.

Channel catfish is the most important food fish cultured in the United States, and genetic study of the species is generating wide interest (Wolters 1993). However, little information is available about chromosome structure, hindering basic research such as gene mapping in this species. The objectives of this study were to (1) develop a replication banding procedure for use with channel catfish chromosomes, (2) evaluate the consistency of the R-banding technique, (3) establish a standard RBG-banded karyotype and idiogram, and (4) estimate baseline frequency of SCD and SCE in cultured cells.

Material and Methods

Animals

The channel catfish used in this study were from a population maintained at LSU and spawned artificially in indoor systems (Tiersch et al. 1994). Eight fish (mean ± SD = 210 ± 55 g) were used for isolation of leukocytes and preparation of chromosomes for replication banding. Another five fish (500 ± 45 g) were used for investigation of SCD and SCE.

Leukocyte Culture

Leukocytes were isolated by the density centrifugation method (Zhang and Tiersch 1995). Culture media and incubation conditions were described previously (Zhang and Tiersch 1995). Mitotic activity of cultured cells was induced by incubating with final concentrations of 0.05 μg/ml phorbol 12-myristate 13-acetate (PMA) (Sigma Chemical Company, St. Louis, Missouri) and 0.5 μg/ml calcium ionophore A23187 (Sigma) (Lin et al. 1992), or with 5 μg/ml concanavalin A (Con A). After 24 h the media with PMA and A23187 were replaced with fresh media containing no mitogens; the cultures with Con A did not require a change of media at this step. Cells were incubated for another 48–72 h until the first round of mitotic activity occurred. Cultures were processed with the following procedures for replication banding and SCE and SCD analysis.

Replication Banding

DNA synthesis of cultured leukocytes was blocked with 5′-fluorouracil (FU; Sigma) at a final concentration 1.0×10^{-7} M. After 17 h the cells were pelleted and rinsed twice with Ca^{2+}- and Mg^{2+}-free phosphate buffered saline (CMF-PBS). The cells were cultured for another 5.5 h in fresh Leibovitz L15 medium (Gibco BRL, Life Technologies Inc., Gaithersburg, Maryland) with a mixture of 10^{-4} M BrdU, 6×10^{-6} M uridine (Sigma), and 4×10^{-7} M 5′-fluoro-2′-deoxyuridine (FrdU; Sigma). Twenty microliters of colchicine solution (100 μg/ml) was added to each culture at 30 min to 1 h before harvest. The cells were processed by a hypotonic treatment with 0.075 M KCl, followed by cold fixation in a mixture of methanol and acetic acid (3:1).

Chromosome staining was based on the fluorochrome plus Giemsa (FPG) method of Perry and Wolff (1974). After staining with Hoechst 33258 (150 μg/ml) for 25 min at room temperature, slides were placed on a styrofoam board, floated in a 60°C water bath, and irradiated with a long-wave (365 nm) ultraviolet (UV) light (115 V, 60 Hz, 0.3 A; Spectronic Corp., Westbury, New York) for 2 h from a distance of 10 cm. The slides were treated with 2× SSC for 4 h at 60°C, rinsed with distilled water (dH_2O), and dehydrated through a series of ethanol solutions (70%, 85%, 95%, and 100%). The slides were stained finally with 2% Giemsa in 0.01 M phosphate buffer (pH 6.8) for 10 min.

Evaluation of Replication Banding on Marker Chromosomes

Three distinctive chromosomes—1 (the largest chromosome), 6 (the largest metacentric chromosome), and 11 (the chromosome bearing the NOR) (Zhang 1996)—were used as representatives of each spread. The banding patterns of these chromosomes from different cells were compared to examine consistency of the technique. Slides were treated by the FPG procedure, and images of chromosomes were recorded as described below. The slides were destained with the mixture of methanol and acetic acid (3:1), rinsed with distilled water, dehydrated through the series of ethanol solutions, and air dried. The NOR were located using the silver staining procedure of Howell and Black (1980).

Computer-Assisted Chromosome Analysis

The process of karyotyping was assisted by the Optimas® (Bioscan, Inc., Edmonds, Washington) and Kary® (Pro Data, Oslo, Norway) computer software packages. Chromosome images were captured and recorded with an image analysis system (Zhang and Tiersch 1997) directly from a light microscope (Microphot-SA, Nikon Inc., Garden City, New York). For comparison, chromosomes were photographed with Kodak Technical Pan film 2415, the negatives were digitized using a slide scanner (SprintScan 35, Polaroid scanner model CS-2700, Needham Heights, Massachusetts), and the digitized images were stored on a 486 IBM compatible PC with a 1.2 GB hard drive, 8 Mbyte RAM, 2 Mbyte VRAM, and 66 MHz processor. Total lengths and arm lengths of chromosomes were measured by the "line measurement" function of the Optimas® software. The dark and light banding patterns of chromosomes were identified by densitometry and expressed with a luminance plot. The x-axis of the plot represented segments of chromosomes, and the y-axis represented the corresponding grayscale value ranging from 0 (black) to 255 (white). Images of metaphase spreads were imported into the Kary® software, which arranged chromosomes in descending order of size by automatic cutting and pasting to a template.

A standard karyotype was prepared by rearranging the chromosomes into groups based on relative length (%TCL) and cen-

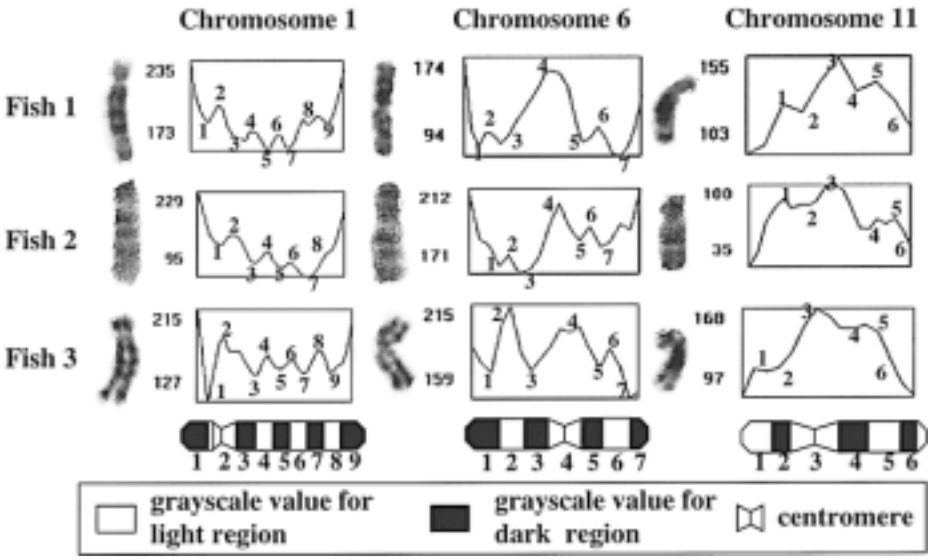

Figure 1. Computer-assisted analysis of replication banding patterns of representative chromosomes. Comparison of the luminance patterns of chromosome 1, 6, and 11 (the NOR-bearing chromosome) from cells of different fish. Arabic numbers indicated on the luminance plots correspond to the specific regions of the chromosome diagrammed within the idiograms.

tromeric index (CI) (Zhang 1996), which were calculated by the following formulas:

$$\%TCL = (\text{total length of each chromosome pair/total length of all chromosomes}) \times 100$$

$$CI\ (\%) = (\text{short-arm length/total length of chromosome}) \times 100.$$

An idiogram was prepared for each chromosome using the Microsoft PowerPoint® software (version 4.0).

Sister Chromatid Differentiation and Exchange

Bromodeoxyuridine (1.6×10^{-4} M final concentration) was added to cultured leukocytes incubated for 20 h before harvest. The method for preparation of chromosomes was the same as described above. Slides were treated with 5% $Ba(OH)_2$ for 7 min at 50°C and incubated overnight with 2× SSC buffer and 0.05% Triton X-100 (Mallinckrodt Specialty Chemicals Co., Paris, Kentucky) at 60°C. Prolonged staining in 5% Giemsa was required to reveal SCD and SCE. Twelve to fifteen spreads from each of five specimens were counted for SCE and SCD. One-way analysis of variance was used to analyze the frequency of occurrence of SCD or SCE among individual fish at a significance level of $P < .05$.

Results

Chromosomes prepared by FU/BrdU replication banding and stained with the FPG method exhibited serial bands with analyzable patterns (Figure 1). Each chromosome pair had a characteristic replication banding pattern and could be identified regardless of the state of contraction (Figure 1). Chromosome 1, the largest in the complement, had one dark band on the short arm and four well-defined dark bands on the long arm. Chromosome 6, the largest metacentric chromosome, had two dark bands on the short arm and two to three on the long arm. Chromosome 11, the NOR-bearing chromosome, possessed one minor dark band on the short arm and one or two dark bands on the long arm, with the major dark band adjacent to the centromere.

Individual chromosomes were identified based on an objective procedure: (1) dividing chromosomes into groups designated as A, B, C, D, E, F, G, or H based on %TCL and CI, and (2) pairing chromosomes within a group according to replication banding patterns (Zhang 1996). The final karyotype (Figure 2) was based on the analysis of 12 spreads and was summarized with an idiogram (Figure 3).

Sister-chromatid differentiation was found on most chromosomes (Figure 4a). However, SCE was observed only on one to five chromosomes per cell (Figure 4a–c). The occurrence of SCD ($P = .07$) was not significantly different among the five fish examined, nor was that of SCE ($P = .26$) (Table 1).

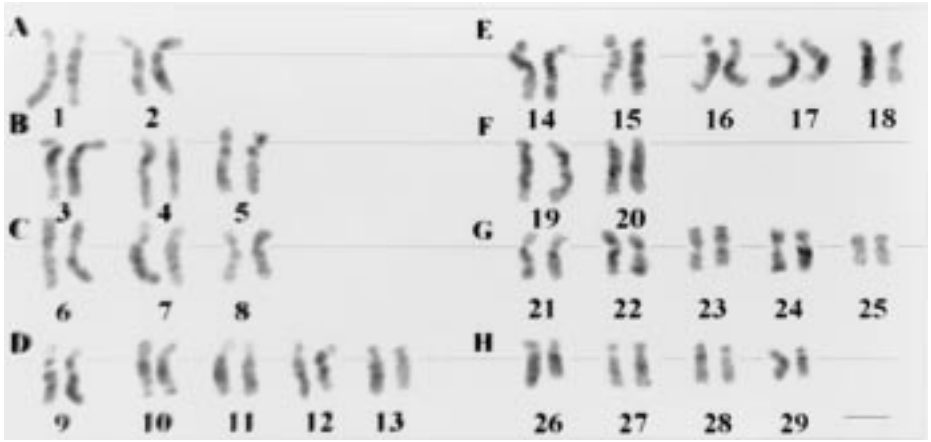

Figure 2. A standard RBG-banded karyotype (R bands by bromodeoxyuridine using Giemsa) of channel catfish. Abbreviations: A, large submetacentric; B, large subtelocentric; C, large and medium metacentric; D, medium submetacentric; E, medium subtelocentric; F, telocentric; G, small metacentric, and H, small submetacentric chromosomes. Bar = 10 μm.

Discussion

In this study replication banding procedures were developed for channel catfish using an in vitro culture technique. Three factors were critical for the success of the replication banding procedure: rapid growth of cultured cells, efficient arrest and release of the cell cycle, and control of intensity of the postlabeling treatment. The dynamic R bands were generated by differential incorporation of BrdU into replicating DNA segments. The uptake of BrdU is related to the replication status of cultured cells. The number of analyzable spreads was increased by addition of mitogens. Although Con A, pokeweed mitogen, and phytohemagglutinin M all have proliferative effects on in vitro culture of channel catfish leukocytes (Faulmann et al. 1983), a mixture of phorbol ester and calcium ionophore was found to be consistently mitogenic for catfish leukocytes (Lin et al. 1992). Consistent replication banding patterns rely on temporal and spatial control of BrdU incorporation, and

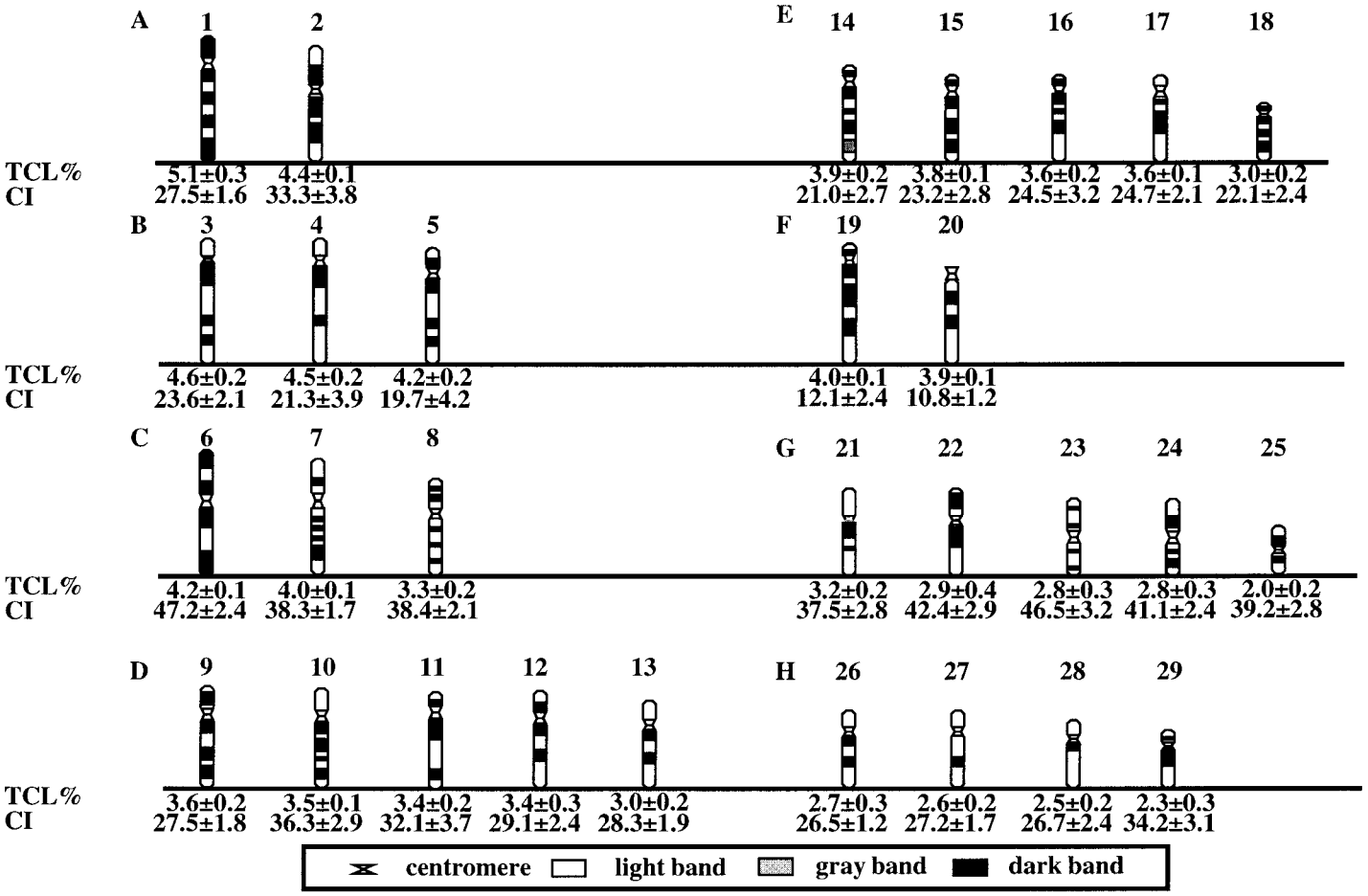

Figure 3. An ideogram of RBG-banded karyotype (R bands by bromodeoxyuridine using Giemsa) of channel catfish. The measurements were taken from chromosomes of 12 different spreads. Abbreviations: %TCL = percentage of total complement length, or relative length; CI = centromeric index.

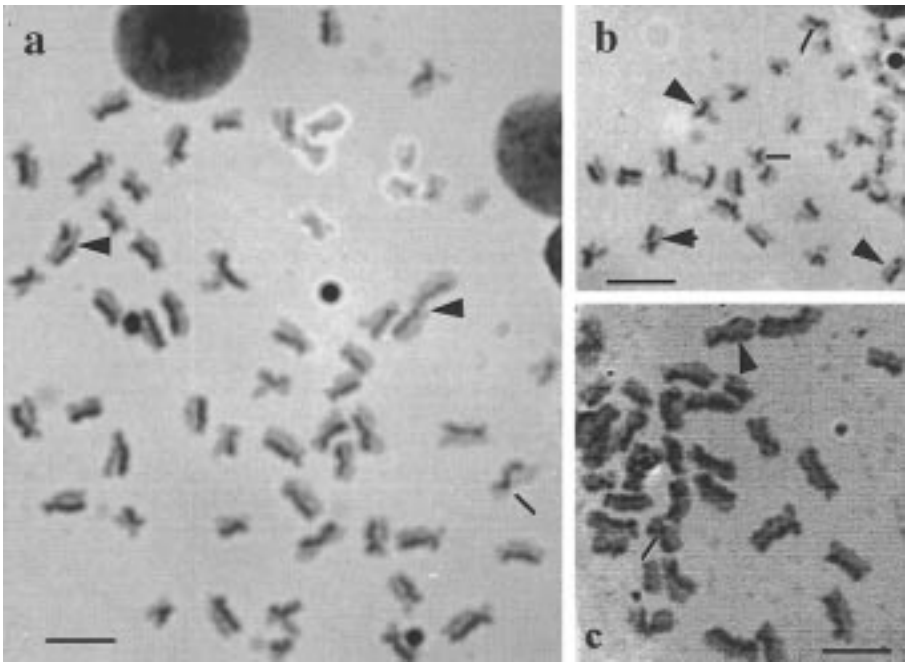

Figure 4. Sister-chromatid differentiation (SCD) and exchange (SCE) of channel catfish chromosomes. Arrows indicate representative SCE chromosomes; lines indicate position of centromeres. Bars = 10 μm.

this can be achieved by synchronization of cell populations. Several treatments were evaluated in this study, including use of the reversible S-phase inhibitors methotrexate (MTX) and FU, and high doses of thymidine and BrdU (data not shown). Although MTX has worked effectively in higher animals (Ronne 1992) and in some fishes such as eel (Liu 1988), it did not block mitosis in cultured channel catfish leukocytes. We also found that the addition of 0.3 mg/ml of thymidine did not synchronize cells effectively, and a similar result was found in cultures treated with high doses (70 μg/ml) of BrdU. In contrast, FU was able to block cultures and was easily released by the BrdU-based mixture. The resultant spreads were arrested mostly in prometaphase.

The final consideration of replication banding was the postlabeling treatment. The FPG is a popular staining procedure to reveal BrdU-labeled regions. Various modifications have been developed from the original methods for use in different species. In this study a prolonged incuba-

Table 1. The occurrence of sister-chromatid differentiation (SCD) and exchange (SCE) in chromosomes of channel catfish (2*N* = 58)

Fish	Number of chromosomes per spread	
	SCD	SCE
1	56 ± 1	3 ± 1
2	55 ± 1	2 ± 1
3	56 ± 2	2 ± 1
4	58 ± 1	4 ± 1
5	57 ± 1	2 ± 1
Mean ± SD	57 ± 2	3 ± 1

The number of chromosomes per cell (mean ± SD) bearing SCD ($P = .07$) or SCE ($P = .26$) were not significantly different among the five individuals examined.

tion with 2× SSC was utilized to generate differentiated bands. The double-staining method using Hoechst 33258 and actinomycin D was developed originally to identify structural bands on human chromosomes. This direct method was not effective for channel catfish chromosomes, while a similar method using Hoechst staining was able to produce replication bands on rainbow trout chromosomes (Delany and Bloom 1984). Other direct methods such as staining with acridine orange revealed replication bands in cyprinid fishes (Hellmer et al. 1991), but did not produce reproducible bands in this study, presumably resulting from a different packaging of DNA and associated protein molecules.

Establishment of an effective evaluation method for replication R-banded chromosomes was another important consideration of this study. Unlike structural bands, most replication bands, especially on fish chromosomes, are continuous and do not have clear borders. Computer-assisted processing of replication-banded chromosomes was efficient and reproducible, and the results were more informative than those of subjective methods. Comparisons among different spreads were enabled by use of marker chromosomes, which were identified by distinctive morphology and banding patterns. The chromosomes bearing the NOR of channel catfish were consistently located on short arms of a pair of medium-sized submetacentrics (Zhang 1996) and could be used as an internal reference to gauge the contraction level of metaphase spreads. The variation found among individual karyotypes was not due to differences in banding pattern but was mostly due to the difficulty in identifying centromeric regions of chromosomes.

In this study the SCE of channel catfish chromosomes were produced by alkaline treatment followed by prolonged exposure to 2× SSC buffer. The incorporation of atomic Br derived from BrdU enhances the binding of DNA with nonhistone proteins by formation of additional hydrogen bonds and makes the BrdU-incorporated chromosomal region more compact and less degradable by alkali treatment (Zhou et al. 1989). Based on this principle, a modified C-banding method that produces highly resolved centromeric C bands on channel catfish chromosomes (Zhang 1996) was used in this study. Our method (designed after failure to reveal SCE or SCD with routine FPG staining techniques) was found to be effective for use in analyzing chromosomes incorporated with low levels of BrdU.

To our knowledge, this is the first report of a cytogenetic map of channel catfish providing a foundation for physical mapping in this species. Fluorescence in situ hybridization (FISH) is a common technique for identification of chromosomal location of DNA sequences. Simultaneous recognition of hybridization signal and identification of individual chromosomes has been reported in mammalian species with techniques combining replication banding and FISH (Larramendy et al. 1993). Techniques allowing use of in situ polymerase chain reaction for detection of a single-locus gene have been developed for channel catfish (Zhang et al. 1997), although individual identification of chromosomes remains problematic. Further studies are required to standardize these techniques for physical mapping in this species. The development of an in vitro BrdU incorporation technique for producing replication banding and SCE could allow analysis of phylogenetic relationships or identification of catfish sex chromosomes as reported in amphibians (Schempp and Schmid 1981).

From the School of Forestry, Wildlife, and Fisheries, Louisiana Agricultural Experiment Station, Louisiana State University Agricultural Center, Baton Rouge, LA 70803 (Zhang and Tiersch) and the U.S. Department of Agriculture, Agricultural Research Service, Catfish Genetics Research Unit, Stoneville, Mississippi (Wolters). Q. Zhang is currently at the Department of Veterinary Science, Louisiana State University, Baton Rouge, Louisiana. This study was funded in part by USDA, Agricultural Research Service Cooperative Agreement CRIS 6402-31000-002-02S, USDA special grant 93-34310-9057, and the Louisiana Catfish Promotion and Research Board. We thank J. Ratcliff for technical assistance and J. Avault, R. Chabreck, R. Cooper, D. Shih, and M. Stine for critical review. This manuscript was approved by the Director of the Louisiana Agricultural Experiment Station as manuscript 96-22-0158. Address correspondence to Dr. Tiersch at the address above of e-mail: ttiersch@agctr.lsu.edu.

References

Bauchan GR and Campbell TA, 1994. Use of an image-analysis system to karyotype diploid Alfalfa (*Medicago sativa* L). J Hered 85:18–22.

Delany ME and Bloom SE, 1984. Replication banding patterns in the chromosomes of the rainbow trout. J Hered 75:431–434.

Drets ME, Obe G, Monteverde FJ, Folle GA, Medina II, De Galvez G, Duarte JE, and Mechoso BH, 1992. Computerized graphic and light microscopic analyses of T-banded chromosome segments of Chinese-hamster ovary cells and human-lymphocytes. Biol Zentralblatt 111:204–214.

Faulmann E, Cuchens MA, Lobb CJ, Miller NM, and Clem LW, 1983. An effective culture system for studying in vitro mitogenic responses of channel catfish lymphocytes. Trans Am Fish Soc 112:673–679.

Giles V, Thode G, and Alvarez MC, 1988. Early replication bands in two scorpion fishes, *Scorpaena porcus* and *S. notata* (Order Scorpanneiformes). Cytogenet Cell Genet 47:80–83.

Gold JR, Amemiya CT, and Ellison JR, 1986. Chromosomal heteromatin differentiation in North American cyprinid fishes. Cytologia 51:557–566.

Gold JR, Li YC, Shipley NS, and Powers PK, 1990. Improved methods for working with fish chromosomes with a review of metaphase chromosome banding. J Fish Biol 37:563–575.

Hellmer A, Voiculescu I, and Schempp W, 1991. Replication banding studies in 2 cyprinid fishes. Chromosoma 100:524–531.

Howell WM and Black DA, 1980. Controlled silver staining of nucleolus organizer regions with a protective colloidal developer: a one step method. Experientia 36: 1014–1015.

Kligerman AD, 1979. Introduction of sister chromatid exchanges in the central mudminnow following in vivo exposure to mutagenic agents. Mutation Res 64:205–217.

Larramendy ML, Nylund SJ, Armstrong E, and Knuutila S, 1993. Simultaneous detection of high-resolution R-banding and fluorescence *in-situ* hybridization signals after fluorouracil-induced cellular synchronization. Hereditas 119:89–94.

Lin GL, Ellsaesser CF, Clem LW, and Miller NW, 1992. Phobol ester/calcium ionophore activate fish leukocytes and induce long-term cultures. Dev Comp Immunol 16:153–163.

Liu L, 1988. Analysis of high-resolution G-banding pattern in fish chromosomes treated by BrdU. Acta Genet Sinica 15:117–121.

Medrano L, Bernardi G, Couturier J, Dutrillaux B, and Bernardi G, 1988. Chromosome banding and genome compartmentalization in fishes. Chromosoma 96:178–183.

Pendas AM, Moran P, and Garciavazquez E, 1993. Replication banding-patterns in Atlantic salmon (*Salmo salar*). Genome 36:440–444.

Perry P and Wolff S, 1974. New Giemsa method for differential staining of sister chromatids. Nature 251:156–158.

Ronne M, 1992. Synchronization, banding and *in-situ* hybridization: A short laboratory manual. In Vivo 6:49–58.

Schempp W and Schmid M, 1981. Chromosome banding in Amphibia VI: BrdU-replication patterns in Anura and demonstration of XX/XY sex chromosomes in *Rana esculenta.* Chromosoma 83:697–710.

Tiersch TR, Goudie CA, and Carmichael GJ, 1994. Cryopreservation of channel catfish sperm: storage in cryoprotectants, fertilization trials, and growth of channel catfish produced with cryopreserved sperm. Trans Am Fish Soc 123:580–586.

Verma RS and Babu A, 1989. Human chromosomes:

manual of basic techniques. New York: Pergamon Press.

Wolff S, 1982. Sister chromatid exchange. New York: John Wiley.

Wolters WR, 1993. Channel catfish breeding and selection programs: constraints and future prospects. In: Selective breeding of fishes in Asia and the United States (Main KL, Reynolds B, eds). Honolulu, Hawaii: Oceanic Institute; 82–95.

Zhang Q, 1996. Cytogenetic and molecular analysis of the channel catfish (*Ictalurus punctatus*) genome (PhD dissertation). Baton Rouge, Louisiana: Louisiana State University.

Zhang Q, Cooper RK, and Tiersch TR, 1997. Detection of a single-locus gene on channel catfish chromosomes by *in-situ* polymerase chain reaction. Comp Biochem Physiol 118B:793–796.

Zhang Q and Tiersch TR, 1995. Cryopreservation of leucocytes of channel catfish for subsequent cytogenetic analysis. J Fish Biol 47:1016–1025.

Zhang Q and Tiersch TR, 1997. Chromosomal inheritance patterns of intergeneric hybrids of ictalurid catfishes: Odd diploid numbers with equal parental contributions. J. Fish Biol 51:1073–1078.

Zhang R and Wu H, 1985. A study of sex chromosome in *Carassius auratus* by BrdU-Hoechst 33258-Giemsa techniques. Acta Genet Sinica 12:373–378.

Zhou M, Li Y, Zhou T, and Yu X, 1989. A BrdU-BSG method for G-banding in fish chromosomes and an ideogram of G-banded karyotype of silver carp. Acta Genet Sinica 16:184–187.

Received July 29, 1997
Accepted December 10, 1997

Corresponding Editor: Martin Tracey

Genetic Differences in Male Development Time Among Populations of the Endangered Gila Topminnow

T. N. Cardwell, R. J. Sheffer, and P. W. Hedrick

Timing of male sexual maturity was compared in a common laboratory environment for populations from the four watersheds in which the Gila topminnow (*Poeciliopsis o. occidentalis*) still remains in Arizona. One population, Monkey Spring, was found to have an approximately 50% later development of male sexual maturity. Monkey Spring is the only population of the four whose natural habitat has both a constant and warm, year-round temperature and year-round reproduction. Year-round reproduction is a common strategy in tropical fish species in warm constant environments. Our findings are consistent with the hypothesis that the other three populations—Bylas Springs, Cienega Creek, and Sharp Spring—have adapted to temporally variable environments and seasonally limited reproduction with earlier male maturation. This genetic difference in a fitness-related trait lends support to the recommendation that Gila topminnows from different watersheds be managed and conserved separately.

The Gila topminnow (*Poeciliopsis o. occidentalis*) is a small, live-bearing fish (Poeciliidae) once common throughout lower elevations of the Gila River drainage in Arizona and New Mexico, and in Sonora, Mexico (Hubbs and Miller 1941), but now endangered and limited to a small fraction of its former range (U.S. Fish and Wildlife Service 1993). The Gila topminnow has been the subject of an ongoing series of investigations to determine the pattern and amount of molecular genetic variation over the few existing, and now quite isolated, populations and the possible association of genetic variation and fitness over these populations.

Published molecular genetic surveys have reported little or no variation among or within few extant natural Gila topminnow populations. For example, of 25 allozyme loci surveyed, only two were variable and only one population, Sharp Spring, was polymorphic for these loci while three other populations, Bylas Spring, Cienega Creek, and Monkey Spring, were monomorphic (Vrijenhoek et al. 1985). Recently Quattro et al. (1996) found that these four populations all had the same mitochondrial DNA haplotype using low-resolution six-cutter restriction enzymes.

Quattro and Vrijenhoek (1989) found differences in fitness measures between Sharp Spring and Monkey Spring, with Monkey Spring appearing to have lower fitness for all traits examined and suggested that there was a positive correlation of allozyme variation and fitness. However, their overall survival values were quite low, indicating that their laboratory environment was highly stressful to the fish and probably influenced the other fitness measures as well. In contrast, when the same fitness measures were examined by Sheffer et al. (1997), also in laboratory-reared fish, they showed a very high overall survival and no significant difference in survival among populations. Sheffer et al. (1997) also found that Monkey Spring males were significantly larger at 12 weeks than fish from three other populations.

Observations during the research reported in Sheffer et al. (1997) suggested that there may be differences in timing of male sexual maturity among the populations, a trait with potentially important fitness consequences. The present experiment was set up to quantify any differences among populations in the development of male secondary sex characteristics in a common, controlled environment. If differences are observed in a common environment, this indicates that there are genetic differences for this fitness trait among the populations.

Fish stocks were initiated in 1994 (Sheffer et al. 1997) from 20 pregnant females from four locations in Arizona—Bylas Spring, Cienega Creek, Sharp Spring, and Monkey Spring (Figure 1)—representing the four major watersheds in which natural populations of Gila topminnows are still extant. The first three locations are subject to large summer-winter temperature fluctuations. In contrast, Monkey Spring at its outflow is a warm spring and is chemically and thermally (27.4 $\pm$ 0.6°C) invariant (Schoenherr 1974). Monkey Spring is separated from other surface drainages by a 10 m high, natural travertine dam and modern diversion into an irrigation system.

Since summer 1994, stocks of approximately 1000 adults from each of these populations have been maintained in large, circular raceways under constant conditions. Seven gravid females were removed at random from each stock in July 1995 (after approximately three generations in captivity) and placed, one fish each, in 10 gal aquaria with the intent of obtaining five or more tanks of fish from each population. Broods of four or more juveniles were used in the study, making it likely that there would be one or more males in the brood. All the aquaria were maintained at the same light cycle (14 h of daylight), temperature (26°C), and water quality. Pregnant females from different populations were randomly placed in aquaria.

After birth of a brood, the female was removed and offspring were kept in sibling groups of four to nine individuals. They were observed daily until the start of gonopodial development (which is an external signal of the initiation of male sexual development), termed initiation age (defined by elongation of anterior anal fin rays 3–5 in males). Once development started, male fish were observed (by T.N.C.) in a petri dish held upright against the side of the tank, every 4 days until gonopodial development was completed. Completion age is indicated by a fully fused and clear gonopodial tip which signals male sexual maturity. Initiation and completion age were analyzed for significant differences among populations with ANOVA and Tukey multiple-comparisons tests.

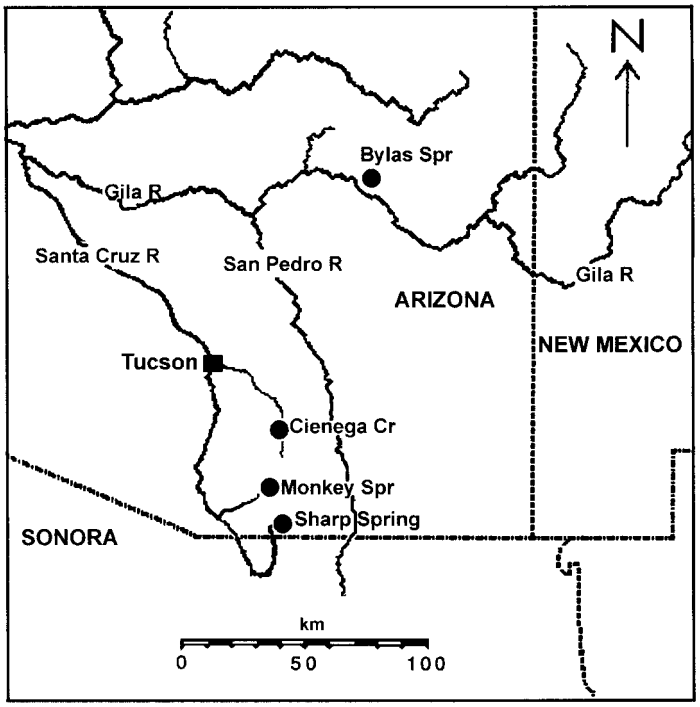

Figure 1. Map indicating four sample sites (solid circles) for Gila topminnow populations.

Table 1. Mean initiation and completion ages and duration of development for each tank

Population	Tank	Mean initiation age (*N*)	Mean completion age (*N*)	Duration of development
Bylas Spring	A	21.0 (2)	57.0 (2)	36.0
	B	26.0 (1)	54.0 (1)	28.0
	C	26.0 (1)	54.0 (1)	28.0
	D	25.0 (4)	51.0 (4)	26.0
	E	25.0 (1)	69.0 (1)	44.0
	F	29.8 (4)	58.0 (3)	28.3
	G	32.0 (2)	66.0 (2)	34.0
	Mean	26.8 (1.0)	57.2 (1.7)	30.4
Cienega Creek	A	24.8 (5)	64.6 (5)	39.8
	B	26.0 (2)	59.0 (2)	33.0
	C	23.8 (4)	64.0 (4)	40.3
	D	19.5 (2)	47.0 (2)	27.5
	E	21.0 (4)	47.0 (4)	26.0
	Mean	23.3 (0.9)	57.6 (3.0)	34.4
Sharp Spring	A	21.0 (1)	52.0 (1)	31.0
	B	31.3 (4)	54.0 (4)	22.8
	C	22.0 (2)	55.0 (2)	33.0
	D	28.3 (4)	72.0 (4)	43.8
	E	29.3 (3)	59.7 (3)	30.3
	Mean	27.9 (1.4)	60.6 (3.8)	32.7
Monkey Spring	A	34.0 (1)	82.0 (1)	48.0
	B	35.4 (7)	91.3 (6)	55.9
	C	36.0 (2)	92.0 (2)	56.0
	D	56.0 (5)	104.0 (2)	48.0
	E	27.7 (3)	64.3 (3)	36.7
	Mean	39.8 (3.0)	86.8 (4.6)	47.0

The number of males *N* at each stage and the standard error of the means are also given. Age is given in days.

Results for individual tanks from the different populations are given in Table 1. The first tank initiated development at 19.5 days (Cienega Creek tank D) and the first tanks completed development at 47 days (Cienega Creek tanks D and E). Monkey Spring tanks A–D were last to initiate development and were the last to complete development. Of the 22 tanks, the five Monkey Spring tanks had the four latest initiation ages and completion ages and the four longest durations of development. On average, mean initiation age, mean completion age, and duration of development were 53%, 48%, and 45% longer, respectively, in Monkey Spring than the average of the other three populations.

Overall differences among populations in age of initiation and completion were highly statistically significant ($P < .001$). There were no significant differences in either initiation or completion age among Bylas Spring, Cienega Creek, and Sharp Spring, but Monkey Spring fish differed significantly from the other three populations ($P < .001$ for each comparison). Variation within populations among tanks was not a significant source of variation in initiation of maturation, but it was significant among tanks within populations for completion ages ($P < .05$). Regression of duration of development on initiation age was significant ($P < .01$), explaining 29% of the variance in duration.

The highly significant difference between the Monkey Spring population and the other populations in time to male sexual maturity, when raised in a common environment, indicates that there are genetic differences for this fitness-related trait between Monkey Spring fish and those from the other populations. This difference corresponds with the interpopulation fitness study by Sheffer et al. (1997) which found that 12-week-old, laboratory-reared Monkey Spring males were significantly larger than male offspring from the other three populations (male growth ceases after sexual maturity, so late male development is consistent with larger size).

The most obvious explanation for the large genetic difference in male sexual development between Monkey Spring and other populations is that they have been under different selection pressures. Southern Arizona is the northernmost extent of the geographic range of *P. occidentalis* (Rosen and Bailey 1963). Tropical derivation (tendency to breed year-round) of the Gila topminnow, along with a natural barrier separating warm Monkey Spring from the other populations in contrast with selection against year-round breeding in seasonally variable temperature habitats, could account for the genetic differences in male sexual maturation between Monkey Spring and other natural populations.

Although spring and summer surges in reproduction exist in all natural populations, the constant-temperature habitat of Monkey Spring supports year-round reproduction while the seasonally variable temperature habitats, such as Bylas Spring, Cienega Creek, and Sharp Spring, do not (Schoenherr 1974). Because of the year-round reproduction at Monkey Spring, some females are available for mating all year, which reduces selection against later starting, slower developing, and consequently larger males. On the other hand, male fish at temperature-variable sites are under selection pressure against late development because reproduction ceases from late fall to spring. This also imposes a trade-off in these locations between earlier development with potentially lower mating success because of smaller size or completion of development next spring with more mating success as a larger male. However, overwintering in cold temperatures poses survival risks and may increase potential costs of delayed male development. In other words, the slower male development time in Monkey Spring fish is consistent with predictions from life-history and sexual competition considerations.

We should note that the influence of environment on sexual development is well documented in fishes. Day length, temperature (Conover and Kynard 1981), and so-

cial interactions (Borowsky 1973, 1978, 1987; Braddock 1945) are all possible modifiers of developmental timing in the secondary sex characteristics. Some studies have found significant effects of the presence of other males on timing of development (Borowsky 1973, 1978, 1987). In this experiment, temperature, day length, and water quality were controlled. Per aquarium density and the numbers of male siblings in the same aquarium were kept as constant as possible but are two other possible sources of variation in developmental timing. Although we do not have enough observations per population and a wide enough range of values to statistically examine this effect, it does not appear to be significant.

Our observation of a large genetic difference in a fitness-related trait between Monkey Spring fish and those from the other populations supports the suggestion of Simons et al. (1989) that "at least one representative lineage is preserved from each of the four geographic areas in Arizona." It is also consistent with the recommendation (Sheffer et al. 1997; U.S. Fish and Wildlife Service 1993) that Gila topminnows from different watersheds be managed and conserved separately.

From the Department of Biology, Arizona State University, Tempe, AZ 85287–1501. We acknowledge the National Science Foundation and the Howard Hughes Medical Institute for support and Larry Nienabur for care of the topminnows. We appreciate the comments of W. L. Minckley. Address correspondence to Dr. Hedrick at the address above or e-mail: hedrick@hedricklab.la.asu.edu.

References

Borowsky RL, 1973. Social control of adult size in males of *Xiphophorus variatus.* Nature 245:332–335.

Borowsky RL, 1978. Social inhibition of maturation in natural populations of *Xiphophorus variatus* (Pices: Poeciliidae). Science 201:933–935.

Borowsky RL, 1987. Agonistic behavior and social inhibition of maturation in fishes of the genus *Xiphophorus* (Poeciliidae). Copeia 1987:792–796.

Braddock JC, 1945. Some aspects of the dominance-subordination relationship in the fish *Platypoecilius maculatus.* Physiol Zool 18:176–195.

Conover DO and Kynard BE, 1981. Environmental sex determination: interaction between temperature and genotype in a fish. Science 213:577–579.

Hubbs CL and Miller RR, 1941. Studies of the order Cyprinodontes, XVII. Genera and species of the Colorado River system. Occas Papers Mus Zool, Univ Mich 433: 1–9.

Quattro JM, Leberg PL, Douglas ME, and Vrijenhoek RC, 1996. Molecular evidence for a unique evolutionary lineage of endangered Sonoran desert fish (genus *Poeciliopsis*). Conserv Biol 10:128–135.

Quattro JM and Vrijenhoek RC, 1989. Fitness differences among remnant populations of the endangered Sonoran topminnow. Science 245:976–978.

Rosen DE and Bailey RM, 1963. The Poeciliid fishes (Cyprinodontiformes), their structure, zoogeography, and systematics. Bull Am Mus Nat Hist 126:1–176.

Schoenherr AA, 1974. Life history of the topminnow *Poeciliopsis occidentalis* (Baird and Girard) in Arizona and an analysis of its interaction with the mosquito fish *Gambusia affinis* (Baird and Girard) (PhD dissertation). Tempe: Arizona State University.

Sheffer RJ, Hedrick PW, Minckley WL, and Velasco, AL 1997. Fitness in the endangered Gila topminnow. Conserv Biol 11:162–171.

Simons LH, Hendrickson DA, and Papoulias D, 1989. Recovery of the Gila topminnow: a success story? Conserv Biol 3:11–15.

U.S. Fish and Wildlife Service, 1993. Draft Gila topminnow recovery plan. Albuquerque, New Mexico: U.S. Fish and Wildlife Service.

Vrijenhoek RC, Douglas ME, and Meffe GK, 1985. Conservation genetics of endangered fish populations in Arizona. Science 229:400–402.

Received September 16, 1997
Accepted December 13, 1997

Corresponding Editor: Martin Tracey

A Genetic Marker in the Growth Hormone Receptor Gene Associated With Body Weight in Chickens

X. P. Feng, U. Kuhnlein, R. W. Fairfull, S. E. Aggrey, J. Yao, and D. Zadworny

A genomic clone spanning 16 kb of the GH receptor gene was mapped and used as a probe for identifying restriction fragment length polymorphisms (RFLPs) in chickens. Several strains of meat-type and egg laying chickens were found to segregate for an *Hin*dIII RFLP located in the intron preceding exon 4. The polymorphic *Hin*dIII site overlapped with a poly(A) signal. Association of the *Hin*dIII RFLP with traits was analyzed in a random-bred White Leghorn strain in three generations using either selective or random genotyping. Both methods revealed significant association of the *Hin*dIII$^+$ allele (presence of the poly(A) signal) with an increased juvenile body weight (130 days of age). In two meat-type strains divergently selected for size of the abdominal fat pad, the *Hin*dIII$^+$ allele was coselected with leanness. The results indicate the presence of a genetic variant of the GH receptor gene which affects growth and abdominal fat deposition and which is relatively frequent in egg laying as well as in meat-type chickens.

The growth hormone (GH) axis affects many metabolic processes such as reproduction, growth, aging and immune responsiveness. In poultry it has been shown that GH levels are associated with the rate of growth, mature body weight, fatness and egg production (Anthony et al. 1990; Burke and Marks 1982; Picaper et al. 1986; Scanes et al. 1984). It has also been reported that the number of hepatic GH receptors (GHR) is affected by selection for growth or feed efficiency (Vanderpooten et al. 1993).

Whether these differences in GH or GHR levels are due to genetic variations in either one of the two genes or in other regulatory genes of the GH axis is not known. However, in some sex-linked dwarf chickens, stunted growth and reduced immune responsiveness appear to be the consequences of mutations in the *GHR* gene (Agarwal et al. 1994; Burnside et al. 1991; Duriez et al. 1993; Huang et al. 1993; Pinard and Monvoisin 1994). This observation and the hypothesis by Robertson (1985) that genes which segregate for alleles with major effects are likely to also segregate for alleles with minor effects prompted us to search for genetic markers in the *GHR* gene which are associated with growth.

Materials and Methods

Isolation and Characterization of a Cosmid Clone of the *GHR* Gene

A cosmid library constructed from genomic DNA of a Cornish White Rock chicken was purchased from Stratagene (Stratagene, La Jolla, California). The genomic DNA had been partially digested with *Sau*3AI and inserted into the *Bam*HI site of the cosmid vector pWE15. Screening of 5×10^4 colonies with the radiolabeled full-length chicken *GHR* cDNA as a probe (Burnside et al. 1991) yielded one positive clone.

A restriction map of the cosmid clone was constructed by analyzing the restriction fragment lengths and the hybridization signals obtained with probes for the T3 and T7 promoters which flank the vector and with individual subfragments (Figure 1A). The clone contained two vector segments interspersed with two chicken genomic DNA fragments. One of these (16.3 kb) hybridized to the GHR cDNA, while the other (10.5 kb) presumably represented an unrelated genomic DNA fragment.

The smallest contiguous segment of the cosmid clone which hybridized to the cDNA clone consisted of two adjacent *Hin*dIII fragments. The segment was 5.1 kb in length and located near one of the ends of the cosmid vectors (Figure 1B).

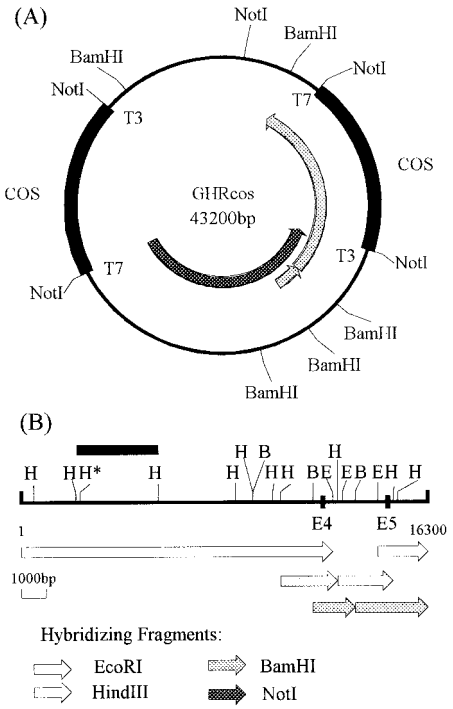

Figure 1. **(A)** Restriction map of the cosmid clone established by hybridizing partial digests and double digests with the T3 and T7 promoter sequences and/or selected restriction fragments. **(B)** Location of the restriction sites *Hin*dIII (H), *Bam*HI (B), and *Eco*RI (E) in the insert containing part of the *GHR* gene. Arrows indicate the restriction fragments which hybridized with the *GHR* cDNA. The black bars indicate the locations of exon 4, exon 5, and the *Hin*dIII fragment which revealed the *Hin*dIII RFLP. The polymorphic *Hin*dIII site (present in the cosmid clone) is marked with an asterisk (*).

Southern blots with the two *Eco*RI subfragments of the *GHR* cDNA isolated by Burnside et al. (1991) revealed that the cosmid clone only hybridized with the 5′ fragment (nucleotide position 0–1400), but not with the 3′ fragment (nucleotide position 1400–2030). Thus the cosmid clone encompassed 5‘ portions of the *GHR* gene. Sequence analysis of the two hybridizing *Hin*dIII fragments revealed that they contained exon 4 and exon 5 of the chicken cDNA (Burnside et al. 1991). Exon 2 (the exon preceding exon 4, since the human equivalent of the human exon 3 is not present in the chicken) appeared to be absent, since an oligonucleotide probe corresponding to exon 2 did not hybridize to the cosmid clone. It indicates that the intron between exon 2 and exon 4 is larger than reported by Agarwal et al.(1994). Large introns are present in the human *GHR* gene between exons 2 and 3 (≥14 kb) and between exons 3 and 4 (27 kb) (Godowski et al. 1989). Thus the cosmid clone appeared to contain 16 kb of the *GHR* gene, spanning exons 4 and 5 and including 12 kb of the intron up-stream of exon 4.

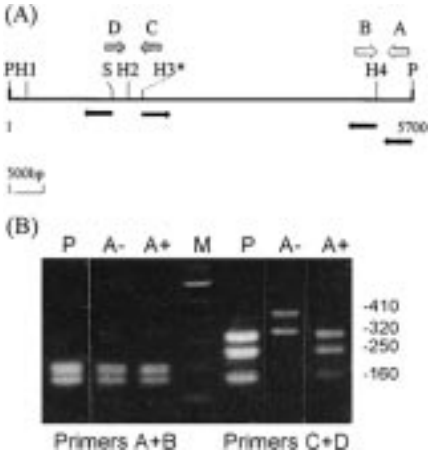

Figure 2. **(A)** Strategy for developing a PCR assay for the *Hin*dIII RFLP. A *Pst*I fragment which contained the polymorphic *Hin*dIII fragment was subcloned from the cosmid clone and mapped. Restriction sites are *Pst*I (P), *Hin*dIII (H), and *Sal*I (S). The fragment H which revealed the *Hin*dIII RFLP in Southern blots is encompassed by H3 and H4. Primer sequences for the three candidate polymorphic sites H2, H3, and H4 were obtained by sequencing the 3′ end of the *Pst*I clone and the 3′ end and the 5′ end of the fragment H3-H4. The sequence of primer D was determined by directional cloning of the fragment H1-S into pUC18 and sequencing of the 3′ end. **(B)** *Hin*dIII digests of the PCR products obtained with the primer pairs A/B and C/D using the *Pst*I subclone (lanes 1 and 5) or genomic DNA from female chickens with genotype H^- (lanes 2 and 6) or H^+ (lanes 3 and 8). Lane 4 is a molecular weight marker. The *Hin*dIII RFLP is located in the fragment amplified by primers C and D.

Southern Blotting

DNA was extracted from blood as described by Jeffreys and Morton (1987) and dissolved in 5 mM Tris-HCL, 0.1 mM EDTA (pH 7.5). Five micrograms of DNA was digested overnight with 25 units of restriction enzyme. DNA fragments were separated by electrophoresis in a 1% agarose gel for 20 h at 1 V/cm and transferred onto Zeta probe membrane (Bio-Rad) by alkali blotting (Reed and Mann 1985). Hybridization was carried out with the ^{32}P-labeled fragments of the *GHR* genomic clone followed by autoradiography. Prehybridization, hybridization, and washing were performed according to Kuhnlein et al. (1989).

PCR Assays

The primer sequences used to locate the *Hin*dIII RFLP (Figure 2) were as follows: A: 5′-CCACTGAATTTGAAGCAGCAG-3′; B: 5′-TTTCCTTTGTTGCACATGCCC-3′; C: 5′-GGCTCTCCATGGGTATTAGGA-3′; and D: 5′-GCTGGTGAACCAATCTCGGTT-3′. About 125 ng of DNA was used as template in 50 μl of a reaction mixture containing 1.25 μM of each primer, 5 μl of 10× reaction buffer (10 mM Tris-HCL, pH 9.0, 1.5 mM $MgCl_2$, 50 mM KCL), 5 mM of each dNTP, 5% formamide, and 1.25 units of *Tth* DNA polymerase (Pharmacia). Amplification was carried out for 35 cycles in a thermal cycler (Perkin Elmer Cetus Corp, Norwalk, Connecticut). Each cycle consisted of 30 s at 92°C, 80 s at 59°C, and 90 s at 72°C. Primers C and D revealed the *Hin*dIII RFLP.

Results

Characterization of a *Hin*dIII RFLP in the *GHR* Gene and Development of a PCR Assay

Pooled or individual *Hin*dIII fragments of the *GHR* cosmid insert were used in an initial search for polymorphisms at *Msp*I, *Taq*I, *Pst*I, and *Hin*dIII restriction sites. White Leghorn strains derived from five different genetic origins and meat-type birds from two genetic origins all segregated for a polymorphism at a *Hin*dIII site, indicating that this RFLP is quite common. No polymorphisms were observed with any of the three other restriction enzymes.

The RFLP was only revealed by one of the *Hin*dIII fragments (Figure 1B). It resulted in a single band shift, indicating that the RFLP coincided with one of the ends of the hybridizing fragment (data not shown). In order to establish PCR assays the sequences surrounding the two ends were determined. For this purpose a clone encompassing the entire *Hin*dIII fragment had to be isolated. Southern blotting of a *Pst*I digest of the cosmid clone with the *Hin*dIII fragment as a probe revealed a single band of 5.7 kb. It was subcloned, a restriction map established, and the sequences of the flanking regions determined as indicated in Figure 2A.

Primers of each end of the polymorphic *Hin*dIII fragment were designed and the PCR products analyzed by gel electrophoresis (Figure 2B). The PCR products obtained with genomic DNA revealed that the *Hin*dIII RFLP coincided with the 5′ end of the *Hin*dIII fragment. The analysis also revealed an additional *Hin*dIII site located 250 bp upstream of the polymorphic *Hin*dIII site. The proximity of the two sites explains why the *Hin*dIII RFLP was only detected with a single rather than with two fragments of the *Hin*dIII digest of the cosmid clone.

Restriction mapping of the genomic DNA using the 5.7 kb *Pst*I fragment P (Figure 2A) as a probe revealed that in the vicinity of the *Hin*dIII RFLP, the genomic DNA from White Leghorns (strain 7) had the same arrangement of *Pst*I and *Hin*dIII sites as the cosmid clone originating from Cornish hens (data not shown). Hence there was no rearrangement within the 5.7

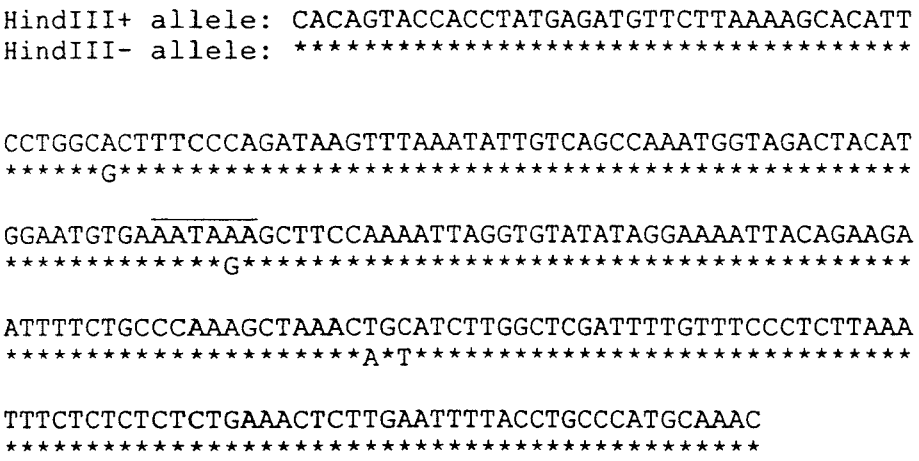

Figure 3. Sequence comparison of two *Hin*dIII$^+$ and two *Hin*dIII$^-$ *GHR* alleles from strain 7 and strain S. Strain 7 is a White Leghorn strain established from four North American commercial strains in 1960 (Gowe et al. 1993). Strain S is a White Leghorn strain developed at Cornell in 1939 and kept as a closed breeding population (Cole and Hutt 1973). PCR products obtained with primers C and D were digested with *Sal*I (see Figure 2), cloned in the 5′ to 3′ direction by ligating into pUC18 linearized with *Sal*I and *Sma*I and sequenced from the reverse primer. The sequence shown is the reverse complementary sequence which coincides with the 5′ to 3′ direction of the *GHR* gene. Alleles of the same RFLP genotype in both strains had identical sequences. The poly(A) site AATAAA which overlaps with the *Hin*dIII site AAGCTT is overlined.

kb *Pst*I fragment during cloning of the *GHR* gene.

The PCR products obtained with DNA from two chickens each of the White Leghorn strain 7 and strain S were directionally cloned into pUC18 and sequenced from the reverse primer. In both strains the loss of the restriction site was caused by an A to G transition. It resulted in the loss of a poly(A) signal that overlapped with the *Hin*dIII site (Figure 3). In addition, the transition at the *Hin*dIII site was accompanied by a transition and a transversion 60 bp downstream and a transition 60 bp upstream of the *Hin*dIII site.

Influence of Selection for Meat Traits and Egg Traits on the Incidence of the *GHR* RFLP

Analysis of two meat strains derived from a common genetic base, but divergently selected for the size of the abdominal fat pad (Leclercq 1988), revealed that the frequency of the *Hin*dIII$^+$ allele was significantly higher in the lean line than the fat line (Table 1). In two other meat-type strains (strain 30 and 31; Sabour et al. 1992) derived from a common genetic base, the *Hin*dIII$^+$ allele occurred at a high frequency in both strains. Nevertheless, selection for body weight, feed efficiency, and egg production over nine generations appears to have led to a further increase of the incidence of the *Hin*dIII$^+$ allele (Table 1).

The influence of selection for egg production traits in egg layers (White Leghorns) was analyzed in a set of three strains consisting of a control strain and two strains selected for several egg production traits (Gowe et al. 1993). Although there was a tendency for an increase in the frequency of the *Hin*dIII$^+$ allele, the increase was not significant (Table 1).

Table 1. Influence of selection on the frequency of the *GHR* alleles

Strain[a]	Frequency of the *Hin*dIII$^+$ allele
Fat-line ($N = 15$)	0.27[b]
Lean-line ($N = 15$)	0.93[b]
Strain 30 ($N = 21$)	0.91
Strain 31 ($N = 23$)	1.00
Strain 7 ($N = 39$)	0.36
Strain 8 ($N = 44$)	0.45
Strain 9 ($N = 29$)	0.52

[a] The fat and lean lines were derived from a common genetic base which included a large cross section of founder birds. The two strains were divergently selected for the size of the abdominal fat pad (Leclercq 1988). They were imported to McGill University in 1982 and maintained for five generations without selection using between 60 and 70 sires and an equal number of dams to propagate each strain (Fotouhi et al. 1993). Strains 30 and 31 were derived from a strain developed from seven different meat-type stocks and were maintained without selection (strain 30) or selection for body weight at 28 days, feed efficiency, and egg production (Chambers et al. 1984; Sabour et al. 1992). Strains 7, 8, and 9 are White Leghorns (egg layers) derived from a common genetic base and kept without selection (strain 7) or selected for egg production traits (Gowe et al. 1993). Strain 8 was selected for egg production to 273 days per hen housed (hence there was indirect selection pressure for low mortality and early onset of egg laying), while strain 9 was selected for the rate of egg production per day hens were alive from the onset of egg laying to 273 days.

[b] $P < .05$ (chi-square test).

Trait Association of *GHR* Genotype in White Leghorns

Changes in allele frequencies in selected strains may be due to genetic drift rather than response to selection. To gain more evidence for variants in the *GHR* gene which affect traits, an association study of the *GHR* RFLP with traits was carried out in the three White Leghorn strains (7, 8, and 9). An initial screen was carried out by selective genotyping in one or two generations for each strain (Table 2). It indicated differences in the *GHR* RFLP frequencies for juvenile body weight in strain 7 ($P < .05$) and strain 9 ($P < .1$). In both of these strains the *Hin*dIII$^+$ allele was associated with a higher juvenile body weight.

The association of the *GHR* RFLP with body weight was reanalyzed by linear regression in the next generation of strain 7 in a sample size of 285 females. It was significant for juvenile body weight, confirming the result obtained by selective genotyping in the previous two generations (Table 3).

Discussion

A marker located in an intron of the *GHR* gene was found to be associated with body weight in White Leghorn chickens. This association does not appear to be due to spurious combinations of the marker and other genes affecting growth, since it was observed in three successive generations. However, close linkage with a neighboring gene cannot be excluded. Nevertheless, since several types of dwarfism in chickens and other species are due to defects in the *GHR* gene, such an alternative is less likely (Agarwal et al. 1994; Duriez et al. 1993; Goossens et al. 1993; Huang et al. 1993).

The human *GHR* gene is very large, encompassing at least 87 kb (Godowski et al. 1989). Much of this length stems from the exceedingly large second intron (>14 kb) and third intron (25 kb). Based on the analysis of our *GHR* cosmid clone, the second intron of the chicken *GHR* gene (equivalent to human introns 2 and 3 since exon 3 is absent in chickens) is also large, exceeding 12 kb. Our *Hin*dIII RFLP is located 7 kb upstream of exon 3 and coincides with a poly(A) signal. Three other poly(A) signals have been reported in the *GHR* gene, two located in the untranslated 3′ region of the *GHR* gene and one in exon 5, giving rise to the three main *GHR* transcripts of 4.3 kb, 3.2 kb, and 0.8 kb, respectively (Agarwal et al. 1993; Oldham et al. 1993). Whether this fourth poly(A) signal is functional remains to be determined. However, its potential effect on the

Table 2. Selective genotyping of the *GHR* locus

Trait	Extremes	Frequency of the *Hind*$^+$ allele Strain 7	Strain 8	Strain 9
Age at first egg	Early	0.35	0.67[#]	0.54[#]
	Late	0.29	0.60	0.31
Body weight at 130 days	High	0.54**	0.87	0.52*
	Low	0.29	0.78	0.29
Body weight at 365 days	High	0.35	n.d.[a]	0.49
	Low	0.23	n.d.	0.52
Egg weight at 365 days	High	0.32	0.87[#]	0.31
	Low	0.46	0.71	0.44
Rate of egg laying	High	n.d.	n.d.	0.31
	Low	n.d.	n.d.	0.44
Residual feed consumption (g)	High	0.42	0.80[#]	n.d.
	Low	0.45	0.73	n.d.

Between 15 and 20 chickens which ranked at the extremes of the trait distribution were analyzed. The frequencies given are from one hatch ([#]) or from two hatches two generations apart (1989 and 1992). The rate of egg laying was measured from age at first egg and 457 days, adjusted for mortality (hen-day rate). Residual feed consumption is the amount of feed which could not be accounted for by body mass gain, body mass, and egg mass. It was measured between day 247 and 268 days (Fairfull and Chambers 1984). The average female population sizes were 305 for strain 7, 970 for strain 8, and 1,050 for strain 9.

[a] n.d. = no data.

** $P < .05$; * $P < .1$ (chi-square test).

Table 3. Least square means of traits depending on the *GHR* genotype

Trait	*GHR* RFLP *Hind*III$^+$	*Hind*III$^-$	P^a
Age at first egg (days)	165.9	167.4	.51
Body weight (g) at			
130 days	1,338	1,289	.046
265 days	1,754	1,734	.58
365 days	1,786	1,767	.65
Egg weight at 365 days (g)	59.4	60.5	.18
Residual feed consumption (g) 247–268 days	569	590	.45

Based on a sample size of 285.

[a] Significance based on SAS General Linear Models procedures.

abundance or the size distribution of *GHR* transcripts must be minor, since its abolition has a relatively small effect on growth. Alternatively, the effect on growth may be due to linked mutations rather than the mutation at the putative poly(A) site. Analysis of *Hind*III alleles from two genetically very distant strains (strain S kept as a closed breeding population since 1939 and strain 7 founded from commercial leghorns in 1956) showed that in both strains the *Hind*III mutation was associated with three additional base changes within a stretch of 240 nucleotides.

In analogy with the stunted growth in chickens with a defective *GHR* gene, one might speculate that the *Hind*III$^-$ allele is associated with an increased GHR activity. The coselection of the *Hind*III$^+$ allele with leanness in the experimental strains of Leclercq (1988) is compatible with such a scenario (Vasilatos-Younken 1995). However, direct measurements of the kinetics of GHR and other components of the GH axis during development in different tissues are required. Toward this end we have started to select chickens on the basis of markers in the *GHR* and *GH* genes, while maintaining diversity of the remaining genetic background. These selection experiments indicate that selection for the *Hind*III$^+$ allele indeed results in an increased body weight of the magnitude predicted by the linear regression analysis (unpublished data).

Our results seem to bear out the postulate of Robertson (1985) that genes which segregate for rare alleles that have major effects on a trait (i.e., dwarfism) are likely to also segregate for other more common variants that have minor effects. When searching for quantitative trait genes it may therefore be expedient to first identify genes responsible for extreme phenotypes (outliers) and then search for more frequent variants in such genes in elite breeding populations.

From the Department of Animal Science, McGill University, Ste. Anne de Bellevue, Quebec, Canada H9X 3V9 (Feng, Kuhnlein, Aggrey, Yao, and Zadworny), and the Centre for Food and Animal Research, Agriculture Canada, Ottawa, Canada (Fairfull). This research was supported by grants from the Natural Sciences and Research Council of Canada, Agriculture Canada, and Shaver Poultry Breeding Farms Ltd. We are thankful for the technical support by L. Volkov and the staff of the Centre for Food and Animal Research. We further thank Dr. Burnside for generously supplying a chicken GHR cDNA clone. Address correspondence to Dr. Kuhnlein at the address above or e-mail: kuhnleinu@agradm.lan.mcgill.ca.

References

Agarwal SK, Cogburn LA, and Burnside J, 1994. Dysfunctional growth hormone receptor in a strain of sex-linked dwarf chicken: evidence for a mutation in the intracellular domain. J Endocrinol 142:427–434.

Anthony N, Vasilatos-Younken R, Emmerson DA, Nestor KE, and Bacon WL, 1990. Pattern of growth and plasma growth hormone in turkeys selected for increased egg production. Poult Sci 69:2057–2063.

Burke WH and Marks HL, 1982. Growth hormone and prolactin levels in nonselected and selected broiler lines of chickens from hatch to eight weeks of age. Growth 46:283–295.

Burnside J, Liou SS, and Cogburn LA, 1991. Molecular cloning of the chicken growth hormone receptor complementary deoxyribonucleic acid: mutation of the gene in sex-linked dwarf chickens. Endocrinology 128: 3183–3192.

Chambers JR, Bernon DE, and Gavora JS, 1984. Synthesis and parameters of new populations of meat-type chickens. Theor Appl Genet 69:23–30.

Cole RK and Hutt FB, 1973. Selection and heterosis in Cornell White Leghorns: a review with special consideration of inter-strain hybrids. Anim Breed Abstr 41:103–118.

Duriez B., Sobrier ML, Duquesnoy P, Tixier-Boichard M, Decupyere E, Coquerell G, Zeman M, Goosens M, and Amselem S, 1993. A naturally occurring growth hormone mutation: in vivo and in vitro evidence for the functional importance of the WS motif common to all members of the cytokine receptor superfamily. Mol Endocrinol 7: 806–814.

Fairfull RW and Chambers JR, 1984. Breeding for feed efficiency: poultry. Can J Anim Sci 64:513–527.

Fotouhi N, Karatzas CN, Kuhnlein U, and Zadworny D, 1993. Identification of growth hormone receptor DNA polymorphisms which respond to divergent selection for abdominal fat content in chickens. Theor Appl Genet 85:931–936.

Godowski PJ, Leung PW, Meacham LR, Galagani JP, Hellmiss R, Keret R, Rotwein PS, Parks JS, Laron Z, and Wood WI, 1989. Characterization of the human growth hormone receptor gene and demonstration of partial gene deletion in two patients with Laron-type dwarfism. Proc Natl Acad Sci USA 86:8083–8087.

Goossens M, Amselem S, Duquesney P, and Sobrier M-L, 1993. Molecular genetics of Laron-type GH insensitivity syndrome. Recent Progr Horm Res 48: 165–178.

Gowe RS, Fairfull RW, McMillan I, and Schmidt GS, 1993. A strategy for maintaining high fertility and hatchability in a multiple-trait egg stock selection program. Poult Sci 72:1433–1448.

Huang H, Cogburn LA, Agarwal SA, Marks HL, and Burnside J, 1993. Overexpression of a truncated growth hormone receptor in the sex-linked dwarf chicken: evidence of a splice mutation. Mol Endocrinol 7:1392–1398.

Jeffreys A.J and Morton DB, 1987. DNA fingerprints of dogs and cats. Anim Genet 18: 1–15.

Kuhnlein U, Gavora JS, Spencer JL, Bernon DE, and Sabour M, 1989. Incidence of endogenous viral genes in two strains of White Leghorn chickens selected for egg production and resistance to Marek's disease. Theor Appl Genet 77:26–32.

Leclercq B, 1988. Genetic selection of meat-type chickens for low abdominal fat content. In: Leanness in domestic birds (Leclercq B and Whitehead CC, eds). London: Butterworth; 25–40.

Oldham ER, Bingham B, and Baumbach WR, 1993. A functional polyadenylation signal is embedded in the chicken growth hormone receptor RNA. Mol Endocrinol 7:1379–1390.

Picaper G, Leclercq B, Saadoun A, and Mongin P, 1986. A radio immune assay of chicken growth hormone using growth hormone produced by recombinant DNA technology: validation and observations of plasma hormone variations in genetically fat and lean chickens. Reprod Nutr Dev 26:1105–1114.

Pinard M-H and Monvoisin J-L, 1994. Effects of sex-linked dwarf gene and of major histocompatibility complex (MHC) types on immune response in White Leghorn chickens. Proc 5th World Congr Genet Appl Livestock Prod 20:238–241.

Reed KC and Mann DA, 1985. Rapid transfer of DNA from agarose gels to nylon membranes. Nucleic Acids Res 13:7207–7221.

Robertson DS, 1985. A possible technique for isolating genic DNA for quantitative traits in plants. J Theor Biol 117:1–10.

Sabour MP, Chambers JR, Grunder AA, Kuhnlein U, and Gavora JS, 1992. Endogenous viral gene distribution in populations of meat-type chickens. Poult Sci 71:1259–1270.

Scanes CG, Harvey S, March JA, and King DB, 1984. Hormones and growth in poultry. Poult Sci 63:2062–2074.

Vanderpooten A, Janssens W, Buyse J, Leenstra F, Berghman L, Decuypere E, and Kuhn ER, 1993. Study of the hepatic growth hormone receptor at different ages in chickens selected for a good feed conversion and a fast weight gain. Domest Anim Endocrinol 10: 199–206.

Vasilatos-Younken R, 1995. Proposed mechanisms for the regulation of growth hormone action in poultry: metabolic effects. J Nutr 125:1783S–1789S.

Received March 14, 1997
Accepted December 13, 1997

Corresponding Editor: Lyman Crittenden

A Cosmid Specific for Sequences Encoding a Microtubule-Associated Protein, MAP1B, Contains a Polymorphic Microsatellite and Maps to Bovine Chromosome 20q14

A. Eggen, S. Solinas-Toldo, and R. Fries

A clone for the bovine gene MAP1B was isolated from a bovine cosmid library with a probe obtained by cross-species PCR. The single positive cosmid clone was localized by FISH to chromosome region 20q14. Analysis of the cosmid revealed the presence of a microsatellite motif with a two-allele polymorphism detectable by PCR amplification of genomic DNA. However, the analysis of this polymorphism in a bovine family affected by SMA indicated absence of very close linkage of the phenotype for bovine SMA with MAP1B.

Mapping of eukaryotic genomes includes two types of loci: type I and type II (O'Brien 1991). Type I represent conserved coding sequences. They are often not or only slightly polymorphic and therefore uninformative for systematic mapping of segregating loci. However, type I loci are the basis for the construction of comparative genome maps. Such maps, besides being of general biological interest, will be useful in identifying marker loci and candidate genes for economic trait loci (ETL) in a given region of the genome through the delineation of conserved synteny segments (Fries 1993; Womack 1987). However, the mapping of ETLs will be accomplished through linkage analysis using type II marker loci. These loci are highly polymorphic but do not represent coding sequences. The high degree of polymorphism, abundance, and even distribution in the eukaryotic genomes make (CA)*n* repetitive segments (so called microsatellites) the type II markers of choice (Beckmann and Weber 1992; O'Brien et al. 1993; Stallings et al. 1991). The result from two types of marker being used in the mapping process is two types of maps. Mapping would be more efficient if it was possible to combine the type I and type II characteristics in one marker, for example, by identifying a highly polymorphic microsatellite site in or close to a coding sequence. We have recently characterized a polymorphic microsatellite in the bovine gene for the $p21^{ras}$ activator (RASA) (Eggen et al. 1992; Fries et al. 1990). While this microsatellite marker was identified via sequence database search, we now present a more general approach consisting of the screening of a cosmid library with a probe for a coding gene and the subsequent search for a microsatellite in positive clones by screening with the (CA)*n* microsatellite motif. Due to the frequent occurrence of microsatellites in eukaryotic genomes, it is hypothesized that most cosmid inserts (encompassing about 40 kb) contain at least one microsatellite, most often of the $(CA)_n$ type. We chose a probe for the gene encoding a microtubule-associated protein, MAP1B, to demonstrate the feasibility of establishing a marker with both type I and type II characteristics and to identify a candidate marker for the bovine spinal muscular atrophy condition (El-Hamidi et al. 1989). It maps to the long arm of human chromosome 5 in close proximity to the spinal muscular atrophy (SMA) locus (Lien et al. 1991) Similar pathology between human and bovine spinal muscular atrophy suggests that homologous loci might be involved in the pathogenesis of the bovine and human form. Demonstration of linkage of MAP1B to the bovine form would corroborate the genetic homology of the bovine and human myopathy, whereas absence of linkage would indicate genetic heterogeneity. In this article we report the cloning of a bovine cosmid containing MAP1B sequence, its assignment to a bovine chromosome using fluorescence in situ hybridization, identification of a (CA)*n* microsatellite, and the analysis of the polymorphism in a bovine family affected by SMA.

Material and Methods

Construction of a Cosmid Library

High molecular weight bovine DNA was extracted from a Holstein-Friesian bull according to Dillela and Woo (1985). Partially digested (*Sau*3A) and dephosphorylated DNA was ligated into the *Bam*HI site of the SuperCos1 cloning vector (Stratagene; Evans et al. 1989).

Cross-Species PCR

PCR reactions were performed on total bovine genomic DNA using primers designed to obtain MAP1B-specific amplification from human DNA. The primers MAP1B-P1 (5′CCG AAT TCG CCC TGC TGT TAT ATT TTT C3′) and MAP1B-P2 (5′CTA AAC AAA TTG TCC ATG AAC TGC AGG G3′) amplify a 400 bp fragment from exon 1 of the human MAP1B gene (position 800–1,200 bp), and the primer MAP1B-P3 (5′CCG AAT CCC TTT CAG TGT CTG TTG TGC3′) together with MAP1B-P4 (5′CCC TGC AGA GGC CTC TAC CTG AGA TAC3′) amplify another 400 bp fragment from the same exon (position 4,800–5,200 bp) (Lien LL, personal communication). A PCR reaction for the amplification of bovine DNA consisted of A 200 ng template DNA, the upper and the lower primer at 250 nM, each dNTP at 200 μM, 2.5 U *Taq* DNA polymerase (Boehringer, Mannheim), and the reaction buffer with 2.0, 1.75, 1.5, 1.25, 0.75, or 0.5 mM $MgCl_2$. The cycling profile was 94°C, 5 min; 30 cycles of 94°C, 30 s; 60°C, 30 s; 72°C, 30 s; followed by a final extension at 72°C, 10 min. One fourth of the product was analyzed on ethidium bromide stained 2% agarose, 1× TBE gel.

Sequencing

The PCR product was electrophoresed through a low gelling temperature agarose gel (Sigma, type VII) and the gel slice containing the specific amplification product was removed. Sequencing was performed directly in the low gelling temperature agarose with a modified dideoxynucleotide termination technique (Sanger et al. 1977; Steffen et al. 1991).

Isolation of a MAP1B-Specific Cosmid Clone

The cosmid library was screened using one of the MAP1B-specific PCR probes. The PCR product was purified and isolated as described above then labeled using the random priming kit of Boehringer (Mannheim). Colony hybridization was performed as described in Sambrook et al. (1989). Prehybridization and hybridization was performed in formamide (50%), SSC (6×), and Blotto (0.05×) in the presence of denatured salmon sperm DNA (100 μg/ml) at 40°C for 2–3 h and 24 h, respectively.

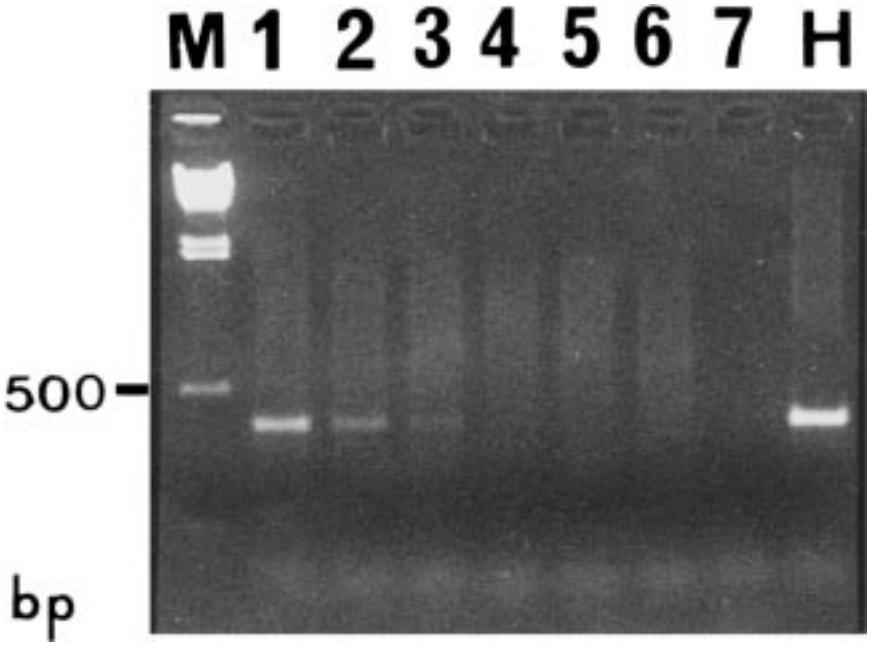

Figure 1. Cross-species PCR of bovine and human genomic DNA with the primers MAP1B-P1 and MAP1B-P2 derived from the sequence of the human MAP1B gene. PCR reactions loaded in lanes 1–6 contained 2.0, 1.75, 1.5, 1.25, 0.75, and 0.5 mM $MgCl_2$, respectively. A control PCR without DNA was loaded in lane 7 and the amplification product of human genomic DNA in lane H.

In situ Hybridization

Chromosome spreads were prepared from primary fibroblast cultures established from male bovine fetuses. Q-banding of the chromosomes was performed prior to hybridization by dipping the slides in a solution of 0.005% quinacrine mustard for 30 s at room temperature (QFQ-banding). Well-spread metaphases with distinctive banding pattern were photographed using a Leitz Diaplan microscope equipped for fluorescence and Kodak Technical Pan films. The MAP1B-specific cosmid was labeled with biotin-16-dUTP (Boehringer Mannheim) and hybridized as described by Solinas-Toldo et al. (1993). The chromosomes carrying label were identified using the photographs taken earlier of the QFQ-banded preparations. Assignment of the hybridization site to a specific band was based on measurement of the overall length of the chromosome and the distance of the signal from the centromere. Calculation of the average fractional length of signal position from the centromere (FL_{cen}) and direct application of this value to the corresponding chromosome of the standard ideogram (ISCNDA 1989) was described by Solinas-Toldo et al. (1993).

Isolation of a Microsatellite

In order to detect the presence of a microsatellite motif, 2 μg of MAP1B-specific cosmid DNA was digested individually with different restriction enzymes (*Pst*I, *Eco*RI, *Sac*I, *Hin*fI, *Sau*3A, *Pvu*II, *Msp*I, *Hae*III, *Xho*I, *Hin*dIII, and *Taq*I), electrophoresed on a 1% agarose gel, blotted onto a nylon membrane, and hybridized overnight in a solution containing Na_2PO_4 (0.5 M, pH 7.2), BSA (1%), SDS (7%), and a $(GT)_{10}$ oligonucleotide labeled by nick translation using the kit of Boehringer, Mannheim. After autoradiography, the positive *Pst*I band was subcloned: 1 μg of the cosmid was digested with *Pst*I, run on a 1% low gelling temperature agarose gel. The band of interest was cut out of the gel and ligated into the pBluescript II SK+ vector digested with *Pst*I and dephosphorylated. To confirm the presence of inserts, some recombinants were tested as follows: a few cells from each colony were lysed in boiling water (100 μl) and 5 μl were used as substrate for PCR with primers complementary to the T3 and T7 promoter sequences of pBluescript II in a 100 μl reaction. Thirty cycles of the PCR were carried out under standard conditions at 94°C (15 s), 45°C (15 s), and at 72°C (30 s), followed by a final incubation at 72°C for 10 min. The amplified product was cut out of the gel and sequenced as previously described.

PCR Visualization of the Polymorphism

For amplification of the MAP1B microsatellites, an upper, MAP1B-P5 (5′TAC TGA TTC TGA CTG ATT ATG TCT3′), and a lower primer, MAP1B-P6 (5′GGC TGT GCC TCG ATA GAT GGT GCG3′) were designed from the obtained sequence. The PCR was carried out as described by Fries et al. (1990) with the following modification: the 30 amplification cycles were performed with denaturation at 94°C (30 s), annealing at 60°C (30 s), and polymerization at 72°C (30 s). The amplified DNA fragments were resolved on a polyacrylamide gel (6%, 7 M urea) at a constant power of 45 W for 2 h 30 min.

SMA Diagnosis

The SMA condition was diagnosed by H. Stocker and P. Ossent (Klinik für Geburtshilfe, Jungtier- und Eutererkrankungen, and Institut für Veterinärpathologie der Universität Zürich) as described in Stocker et al. (1992). Parentage was verified by blood group testing.

Cloning of a MAP1B-Specific Cosmid

To obtain bovine MAP1B-specific sequences, PCR was carried out on bovine DNA using two primer pairs derived from human sequences. Each of these cross-species PCR systems yielded amplification products of about 400 bp at an optimized MgCl2 concentration (Figure 1). This size was expected based on the human sequence and was a first indication of MAP1B specificity of the amplified fragments. However, both fragments were sequenced to determine their identity. Comparison of the resulting sequences (EMBL accession numbers Z29519 and Z29520) with the corresponding mouse sequence (X51396) revealed homologies of 88% and 86%, respectively. The more homologous fragment was used to screen 350,000 recombinant cosmids. A single positive colony was isolated. The two PCR systems derived from human sequences encoding MAP1B were applied on DNA isolated from this clone and yielded fragments of the expected size, indicating that this cosmid most likely contained bovine sequences encoding MAP1B. *Eco*RI digestion of this cosmid revealed 10 fragments amounting to a total insert size of 38 kb.

Chromosomal Localization of the MAP1B-Specific Cosmid

After hybridization and two rounds of signal amplification, 27 metaphases were scored. Twenty metaphase spreads showed a signal on both homologous chromosomes 20 as, for example, shown in Figure 2. In seven metaphases only one of the two homologous chromosomes was labeled. The FL_{cen} value amounted to 0.32

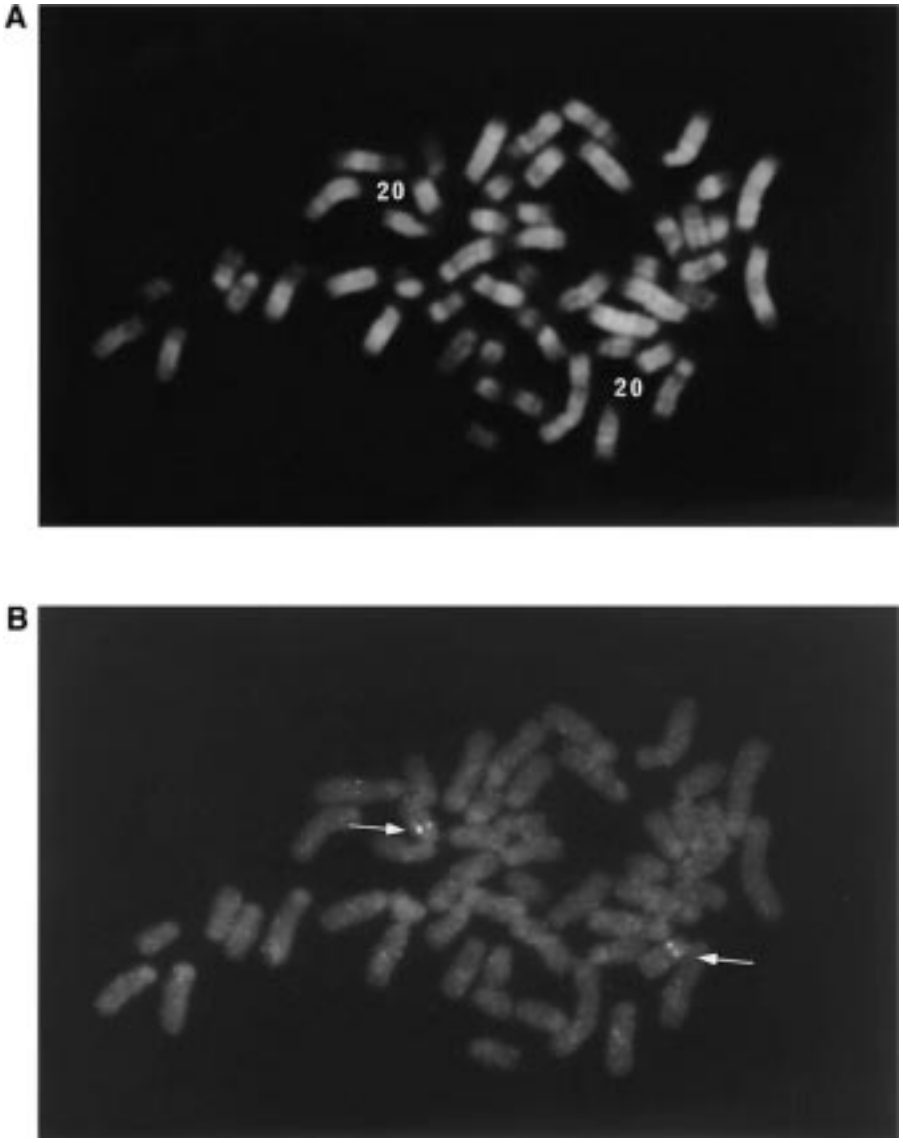

Figure 2. Bovine metaphase showing QFQ-banding of the chromosomes prior to in situ hybridization **(A)** and propidium iodide staining after hybridization **(B)**. The arrows indicate the specific hybridization signal.

(±0.042) and assigned the hybridization site to band 20q14. The mapping of MAP1B to chromosome 20 represents the first assignment to this chromosome.

Identification of a (CA)$_n$ Microsatellite in the MAP1B-Specific Cosmid

Southern blotting and hybridization of DNA from the MAP1B-specific DNA with a (CA)*n*-specific probe identified a distinct 450 bp *Pst*I fragment. This fragment was subcloned, and its partial sequencing revealed the presence of a $(CA)_{12}$ microsatellite (Figure 3). The PCR with primers designed from flanking sequences was carried out using DNA samples of 20 unrelated bovine animals (Brown Swiss). Two fragments, encompassing 277 and 279 nucleotides, respectively, corresponding to two alleles with frequencies of 82% and 18%, respectively, were detected as shown in Figure 4. The PIC (Botstein et al. 1980) value was 0.25.

5'-TTTTTTTAATTACTGATTCTGACTGATTATGTCTTTTAAGGATGGGCTGCTTCAGTGGTTTGCATTTGACTA
TATCCAGGTGATGCTGAAATCTTTGAAAGCAAAATGTCATTTTCTAGATATATAATTTTTTAGGATGCTTATAG
GGTCTCGTCTCCACAGAACTAATACTCATCTAAAGACACATA**CACACACACACACACACACACACACA**GGCTCT
CTCCTGATTTCAGAAAGGGCCGACTATGGCTAAATTTAAAAACACACGCACCATCTATCGAGGCACAGCCAT
TACCAAGCCCCATAAAACCCGAGAGCCCTTTACACCTGCACACAGCTGGCCCTTCTCGCTCACACACCTGA
ATGTGGCCCAAACAGCGGCCTAGG-3'

Figure 3. MAP1B microsatellite and flanking sequences. The sequences corresponding to the two primers MAP1B-P5 and MAP1B-P6 are underlined. The microsatellite sequence is in boldface.

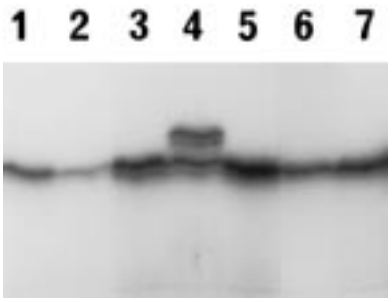

Figure 4. Representative autoradiogram showing the two alleles identified at the MAP1B microsatellite locus. Animals 1, 2, 3, 5, 6, and 7 are homozygous for allele 277 and animal 4 is heterozygous 277/279.

Analysis of the MAP1B-Specific Microsatellite in a Bovine Family Affected by SMA

All SMA affected animals were paternally and maternally derived from the same carrier animal (Figure 5). A grandson of this animal, an obligate carrier of the SMA defect, was typed 277/277 at the MAP1B microsatellite locus. Under the hypothesis of very close linkage of SMA with MAP1B (as is the case in humans), all SMA affected animals should have received allele "277" together with the SMA defect from either parent. However, due to the low PIC of the microsatellite marker, only 3 of 10 SMA animals were informative, that is, one of the parents was heterozygous at the microsatellite locus. Two of these animals were homozygous having received allele "277" from either parent, and one was heterozygous (277/279), having received 277 from only one parent. This indicated absence of at least very close linkage of the bovine SMA disorder with MAP1B.

Discussion

We have cloned a cosmid containing bovine MAP1B-specific sequences using a cross-species PCR approach and have assigned this cosmid to domestic cow chromosome 20q14 using FISH. Cross-species PCR based on human sequences, cosmid cloning, and FISH (requiring large insert probes) may indeed be the method of choice for the efficient regional mapping of type I loci in cattle and other species. The fact that a polymorphic microsatellite could also be detected in this cosmid demonstrates that by using cosmid cloning it should often be possible to combine the type I and type II characteristics in one marker. However, the low PIC value of the

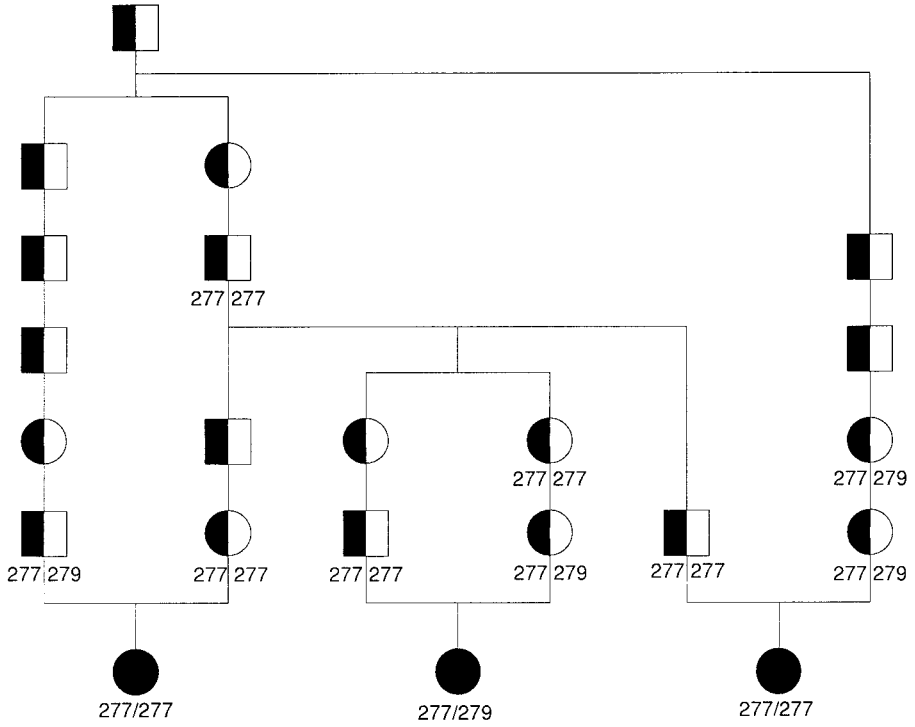

Figure 5. Pedigree with SMA affected and carrier animals and MAP1B microsatellite genotypes. Male family members are represented by squares, females by circles; affected members are represented by solid symbols and carriers by half-solid symbols.

observed microsatellite reduces the usefulness of this locus in linkage studies. In any case, the microsatellite marker was not sufficiently polymorphic to prove linkage of MAP1B with SMA or to conclusively demonstrate absence of linkage, respectively. It will be necessary to apply other approaches for the detection of polymorphic markers within the MAP1B-specific cosmid, such as using other microsatellite motifs, RFLP screening using the entire cosmid as probe (Steele and Georges 1991; White and Lalouel 1988), or the generation of poly(A) markers in SINE-repetitive elements (Economou et al. 1990).

If MAP1B is not closely linked to SMA in cattle, a defect different from the one assigned to human chromosome 5q11.2–13.3, causing Werdnig-Hoffmann type SMA, would have to be assumed to cause the bovine form of SMA. Spinal muscular atrophies are caused by pathological changes of the motor neurons, which can have many possible primary causes (Brady 1993; Troyer et al. 1992). It is therefore quite possible that human Werdnig-Hoffmann type SMA and bovine SMA, even though very similar in appearance, may indeed be different diseases.

The mapping of MAP1B in cattle adds to the comparative vertebrate genome map. Previous comparative studies concerning loci from human 5q13–14 have established homology with murine chromosome 13 and bovine chromosomes 10 and 7 (O'Brien et al. 1993). The result of this study indicates yet another linkage disruption, as MAP1B was assigned to bovine chromosome 20. Therefore, in spite of the tendency of a higher degree of conservation between the human and bovine than between the human and the murine genomes (Threadgill and Womack 1990a,b), it will be important to use extrapolation of synteny to the bovine genome cautiously, and species-specific confirmation of extrapolations is recommended in each instance.

From the Swiss Federal Institute of Technology, ETH Zentrum, Zurich, Switzerland. A. Eggen is currently at the Laboratoire de Génétique Biochimique et de Cytogénétique, INRA, Jouy-en-Josas, France. We especially thank Prof. G. Stranzinger for his continuous interest and generous support in this work, Prof. L. Kunkel and L. Lien for providing the sequences of the human MAP1B primers, and H. Stocker and P. Ossent for the SMA diagnosis. This work was made possible by grants from the Swiss National Science Foundation (31-27743.89) and the Swiss Federal Institute of Technology (0-20-216-88). We are grateful to Dr. Michael Bishop (USDA, Clay Center, Nebraska) for the critical reading of the manuscript. Address correspondence to Dr. Eggen at the address above.

References

Beckmann JS and Weber JL, 1992. Survey of human and rat microsatellites. Genomics 12:627–631.

Botstein D, White RL, Skolnick M, and Davis RW, 1980. Construction of a genetic linkage map in man using restriction fragment length polymorphisms. Am J Hum Genet 32:314–331.

Brady ST, 1993. Motor neurons and neurofilaments in sickness and in health. Cell 73:1–3.

Dillela AG and Woo SLC, 1985. Cosmid cloning of genomic DNA. Focus 7(2):1–5.

Economou EP, Bergen AW, Warren AC, and Antonarakis SE, 1990. The polydeoxyadenylate tract of Alu repetitive elements is polymorphic in the human genome. Proc Natl Acad Sci USA 87:2951–2954.

Eggen A, Solinas-Toldo S, Dietz AB, Womack JE, Stranzinger G, and Fries R, 1992. RASA contains a polymorphic microsatellite and maps to bovine syntenic group U22 on chromosome 7q2.4-qter. Mammal Genome 3:559–563.

El-Hamidi M, Leipold HW, Vestweber JGE, and Saperstein G, 1989. Spinal muscular atrophy in brown Swiss calves. J Vet Med A 36:731–738.

Evans GA, Lewis K, and Rothenberg BE, 1989. High efficiency vectors for cosmid microcloning and genomic analysis. Gene 79:9–20.

Fries R, 1993. Mapping the bovine genome: methodological aspects and strategy, Anim Genet 24:111–116.

Fries R, Eggen A, and Stranzinger G, 1990. The bovine genome contains polymorphic microsatellites. Genomics 8:403–406.

ISCNDA, 1989. International system for cytogenetic nomenclature of domestic animals. Cytogenet Cell Genet 53:65–79.

Lien LL, Boyce FM, Kleyn P, Brzustowicz LM, Menninger J, Ward DC, Gilliam TC, and Kunkel LM, 1991. Mapping of human microtubule-associated protein 1B in proximity to the spinal muscular atrophy locus at 5q13. Proc Natl Acad Sci USA 88:7873–7876.

O'Brien SJ, 1991. Mammalian genome mapping: lessons and prospects. Curr Opin Genet Dev 1:105–111.

O'Brien SJ, Womack JE, Lyons LA, Moore KJ, Jenkins NA, and Copeland NG, 1993. Anchored reference loci for comparative genome mapping in mammals. Nat Genet 3:103–112.

Sambrook J, Fritsch EF, and Maniatis T, 1989. Molecular cloning: a laboratory manual, 2nd ed. Cold Spring Harbor, New York: Cold Spring Harbor Laboratory Press.

Sanger F, Nicklen S, and Coulson AR, 1977. DNA sequencing with chain-terminating inhibitors. Proc Natl Acad Sci USA 74:5463–5467.

Solinas-Toldo S, Fries R, Steffen P, Neibergs HL, Barendse W, Womack JE, Hetzel DJS, and Stranzinger G, 1993. Physically mapped, cosmid-derived microsatellite markers as anchor loci on bovine chromosomes. Mammal Genome 4:720–727.

Stallings RL, Ford AF, Nelson D, Torney DC, Hildebrand CE, and Moysis RK, 1991. Evolution and distribution of (GT)n repetitive sequences in mammalian genomes, Genomics 10:807–815.

Steele MR and Georges M, 1991. Generation of bovine multisite haplotypes using random cosmid clones. Genomics 10:889–904.

Steffen P, Eggen A, and Fries R, 1991. Method for isolating microsatellites by the consequent use of PCR [abstr]. Cytogenet Cell Genet 58:2153–2154.

Steffen P, Eggen A, Dietz A, Womack JE, Stranzinger G, and Fries R, 1992. Isolation and mapping of polymorphic microsatellites in cattle. Anim Genet 24: 121–124.

Stocker H, Ossent P, Heckmann R, and Oertle C, 1992. Spinale muskelatrophie bei Braunvieh-Kälbern. Schweiz Arch Tierheilk 134:97–104.

Threadgill DW and Womack JE, 1990a. Syntenic conservation between humans and cattle. I. Human chromosome 9. Genomics 8:22–28.

Threadgill DW and Womack JE, 1990b. Syntenic conservation between humans and cattle. II. Human chromosome 12. Genomics 8:29–34.

Troyer D, Leipold HW, Cash W, and Vestweber J, 1992. Upper motor neurons and descending tract pathology in bovine spinal muscular atrophy. J Comp Pathol 107:305–317.

White R and Lalouel JM, 1988. Chromosome mapping with DNA markers. Sci Am 258:20–28.

Womack JE, 1987. Comparative gene mapping: a valuable new tool for mammalian developmental studies. Dev Genet 8:281–293.

Corresponding Editor: James Womack

Inheritance of a Disease Lesion Mimic Mutant in Soybean

J. Chung, P. E. Staswick, G. L. Graef, D. S. Wysong, and J. E. Specht

Disease lesion mimic mutants have been identified in several plant species, including one that affects the primary root in soybean [*Glycine max* (L.) Merr.]. These mutants display chlorotic and/or necrotic lesions despite the absence of any detectable pathogen. A soybean mutant exhibiting this phenotype in its leaves was observed as a single M_2 plant among the bulked progeny of about 150,000 M_1 plants grown from mutagenized (i.e., gamma-irradiated) seed of the determinate cultivar Hobbit 87. Leaves of the identified mutant plant became more necrotic and chlorotic as they aged, eventually undergoing an earlier than normal leaf senescence. No pathogen was detectable in the affected leaves. The selfed progeny of the mutant bred true for this phenotype. Reciprocal crosses were made between the mutant and its Hobbit 87 parent. The mutant also was crossed to a determinate isoline of the cultivar Harosoy. The F_1 phenotype and the F_2 and $F_{2:3}$ segregation data indicated that the mutant behaved as a single recessive allele, designated *dlm* (an acronym for disease lesion mimic). About two-thirds of the F_2 plants classified as nonmutant displayed a faint freckling on some of their leaves, but this was not a reliable indicator of heterozygosity at the *Dlm* locus based on F_3 progeny tests. Disease lesion mimicry mutants may be useful in basic research aimed at better understanding disease hypersensitive response and programmed cell death in plants.

In several plant species, mutants have been identified whose leaves exhibit chlorotic or necrotic symptoms generally associated with pathogen attack, yet no pathogens can be detected in the affected leaf tissue (Dietrich et al. 1994). The term "disease lesion mimicry" was coined to describe such mutants, primarily because the leaf lesions produced by a mimicry mutant frequently emulate the leaf lesions produced in wild-type leaves infected by a bacterial or fungal pathogen (Johal et al. 1995; Walbot et al. 1983).

Although little is known about the fundamental mechanisms involved in disease lesion mimicry, or even the basic function of the wild-type allele at each mutant mimicry locus, various models for lesion initiation and propagation have been proposed. The progression of lesion initiation and expansion in most lesion mimic mutants is developmentally regulated (Johal et al. 1995). Generally the lesions first appear in the developmentally oldest leaves and then appear in subsequent leaves as these also reach a similar age. Dietrich et al. (1994) delineated two classes of mimicry mutants. In the determinate type, lesion initiation occurred spontaneously at some particular leaf age, but lesion expansion was slow and was eventually checked. However, in the indeterminate type, lesion initiation was triggered by some pathogenic, chemical, or developmental signal, but once initiated, lesion expansion was rapid and unchecked, leading to large chlorotic areas that eventually coalesced and resulted in premature leaf death. Dietrich et al. (1994) suggested that lesion mimic mutants of both classes were defective in some molecular function or biochemical pathway in hypersensitive disease response and/or programmed cell death.

While conducting mutagenesis in the soybean (for the purpose of generating new mutants for stem growth habit), a mutant with an unusual phenotype was discovered. That phenotype, which was initially thought to be a disease susceptibility, was subsequently recognized as disease lesion mimicry when no causal organism could be found in the mutant's tissues. Kosslak et al. (1996) recently reported a disease lesion mimicry mutant affecting primary root tissue in the soybean [*Glycine max* (L.) Merr.], but we could find no reports in the literature of soybean mutants displaying disease lesion mimicry in the leaves. The objective of the research described here was to determine the nature of the inheritance of the soybean leaf mutant.

Materials and Methods

All genetic studies were conducted in field nurseries and greenhouses located on the University of Nebraska East Campus. In May 1991, seed of the determinate soybean cultivar Hobbit 87 was exposed to 50 krad of gamma irradiation and immediately planted in the field. The resultant M_1 plants (approximately 150,000) were harvested in bulk in the fall of 1991. The bulked M_2 seed (approximately 1,000,000) was planted in the field in May 1992. After emergence, plants were inspected on a weekly basis. M_2 plants that developed unusual phenotypes were tagged and a description of the phenotype recorded on the tag. A single M_2 plant, bearing the tagged notation "late-appearing, chlorophyll deficiency with brown spots," was gathered in the fall of 1992, along with about 350 other tagged M_2 plants. All tagged plants were threshed individually and their $M_{2:3}$ seed progenies were planted in the field in May 1993, with the "brown spot" mutant planted in row 93-h1054. All M_3 plants in row 93-h1054 displayed the mutant phenotype and were individually threshed to initiate the genetic studies. Seed of $M_{3:4}$ progenies were planted in a greenhouse in October 1993, along with seeds of Hobbit 87. Using physical emasculation, reciprocal crosses were made between an M_4 mutant plant and a Hobbit 87 plant. F_1 seeds derived from those reciprocal crosses were planted in May 1994 in a campus field along with seed collected from the two greenhouse-grown parents. The F_1 plants were individually harvested to collect F_2 seed. As part of an independent study project, a student planted 24 F_2 plants of the Hobbit 87 $\times$ M_4 mutant, 24 F_2 plants of a reciprocal mating, and 4 plants of each parent were grown to maturity in the 1994–1995 winter greenhouse. A photoperiod of 14 h day/10 h night was supplied by an overhead panel of high-intensity, 400 W metal halide lights. The thermoperiod was 25°C/15°C (day/night). After reaching the R_4 reproductive stage (i.e., end of pod elongation), the leaves of the F_2 plants and parents were examined, and those with the mutant phenotype were red-tagged. About two-thirds of the F_2 plants classified as normal were observed to have a barely discernible freckling in some (but not all) of their leaves. These F_2 plants were white-tagged to establish a pedigree trace. All 48 F_2 plants and parental plants were harvested individually at maturity. About 30 F_3 seed from each of the 48 F_2 plants, and from each of the two

parents, were planted in the field in May 1995. After the R_4 stage, the $F_{2:3}$ plant rows were classified as (1) true-breeding for the normal phenotype, (2) segregating for the mutant phenotype, and (3) true-breeding for the mutant phenotype. The number of normal and mutant F3 plants in the segregating rows also was recorded.

The 93-h1054 mutant had also been mated with a determinate isoline of the cultivar Harosoy in 1994, as part of a larger linkage study. A single F_1 plant was grown and phenotyped in the 1994–1995 winter greenhouse. The 84 F_2 plants and their $F_{2:3}$ progenies were grown and phenotyped in the summers of 1995 and 1996, respectively.

Results and Discussion

In early to mid-August 1993, older leaves of all plants in the M_3 progeny of the original M_2 plant began developing freckled appearance (i.e., small necrotic spots, each surrounded by a chlorotic halo). The yellowish-green halo areas rapidly expanded and eventually coalesced, such that by late August nearly all leaves on each plant turned yellow, then a dark brown. Premature leaf drop followed, resulting in the M_3 progeny row 93-h1054 undergoing plant senescence that was several days earlier than that of a nearby row of Hobbit 87.

Because the freckled, chlorotic appearance of the mutant leaves seemed to be a reflection of pathogenicity, we initially presumed that this mutant was simply susceptible to some pathogen. To determine what pathogen might be causal agent, symptomatic leaves from several M_3 mutant plants were taken to the University of Nebraska Plant and Pest Diagnostic Clinic. An exhaustive examination revealed no histochemical evidence of pathogenicity. Clinic personnel suggested that an abiotic factor was perhaps the likely cause of the phenotype.

Mutant plants were grown during the winter of 1993–1994 in a greenhouse. As the plants began flowering, aging leaves began to exhibit, on their upper surfaces, reddish-brown spots that were surrounded by a greenish-yellow halo (Figure 1). On the lower surfaces, narrow but elongated lesions formed along the veins. Some of the larger lesions consisted of concentric brown/yellow rings of dead tissue. These lesions were typical of a soybean disease commonly known as "target spot," caused by the fungus *Corynespora cassiicola* (Athow 1987). However, neither this nor any other pathogen was detectable in affected mutant leaves that were again submitted for a pathological analysis. The absence of pathogenicity finally led us to conclude that this soybean mutant was exhibiting disease lesion mimicry (Walbot et al. 1983).

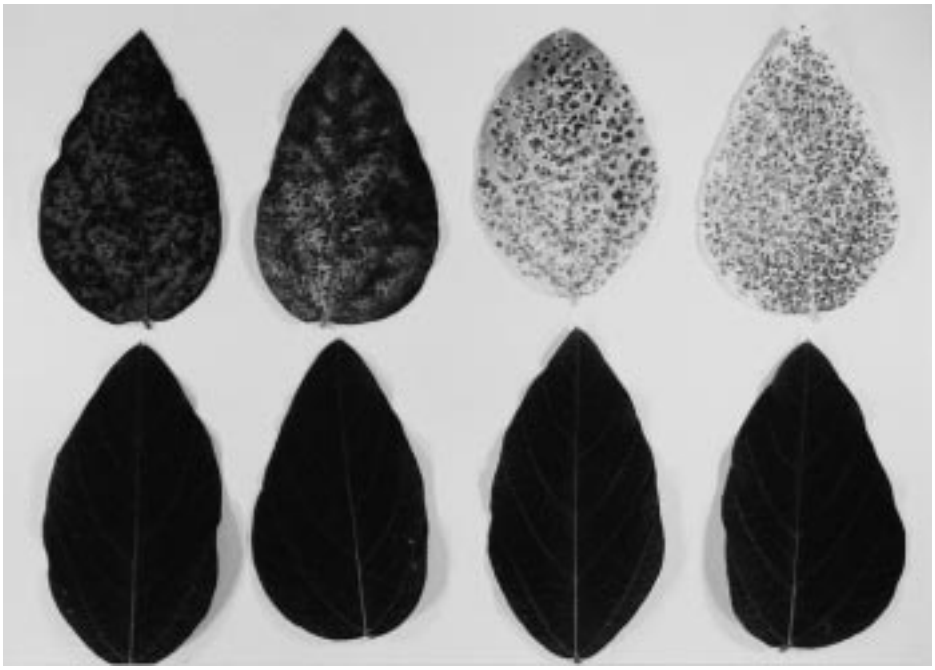

Figure 1. Fully expanded leaves from the disease lesion mimicry mutant (top) and from its wild-type counterpart (bottom). Leaves are ordered (left to right) based on a developmental age (young to old) reflecting stem node position (upper to lower).

F_1 plants from the matings between the mutant and Hobbit 87 had a normal phenotype, irrespective of whether the mutant served as the female or male parent in the mating (Table 1). The observed F_2 segregation of normal versus mutant in the reciprocal crosses was 18:6 and 17:7, both of which fit a monogenic 3:1 ratio. Mutant F_2 plants produced only mutant F_3 progeny, whereas normal F_2 plants produced all normal progeny, or progeny with normal and mutant segregants. The 8:10 and 7:10 ratios of homozygous dominant versus heterozygous F_2 plants in the reciprocal crosses fit a 1:2 ratio. Finally, the 172:46 and 178:49 counts of normal and mutant plants in the segregating $F_{2:3}$ families also fit a 3:1 ratio. The F_1 phenotype and the F_2 and F_3 segregation data indicated that the mutant phenotype was conditioned by a recessive nuclear allele. The F_2 populations in the reciprocal matings with Hobbit 87 were obviously small. However, the proposed genetic model was verified in a separate population derived from the mating of the mutant with another parent. In that mating (Table 1) the F_1 phenotype was normal, the F_2 segregation fit a 3:1 ratio, mutant F_2 plants bred true, and the number of normal F_2 plants classified as homozygotes and heterozygotes fit a 1:2 ratio.

About two-thirds of the normal F_2 plants produced in the reciprocal matings involving Hobbit 87 exhibited a faint freckling on one or more of their leaves, suggesting that this might be indicative of heterozygosity at the mutant locus. Of the 20 F_2 plants in the Hobbit 87 matings (10 in each cross) that were subsequently shown in the F_3 generation to be heterozygotes for the mutant gene, 17 (8 in one cross, 9 in its reciprocal) exhibited faintly freckled leaves (Table 1). However, faint freckling was also observed in 7 (4 in one cross, 3 in its reciprocal) of the 18 normal F_2 homozygotes. Faint freckling was not easily distinguishable from other forms of leaf spotting, so even if faint leaf freckling did characterize heterozygous F_2 plants, its penetrance is too marginal to serve as a reliable indicator of heterozygosity at the mutant locus.

The gene symbol *dlm* (disease lesion mimicry) was chosen for the recessive mutant allele and has been approved by the Soybean Genetics Committee (Diers B, personal communication). We are currently attempting to position the *Dlm* locus on the soybean molecular linkage map (Shoemaker and Specht 1995). Researchers interested in examining the mutant phenotype or in cloning the mutant gene need

Table 1. Inheritance of a soybean disease lesion mimic mutant phenotype in the F_1, F_2, and F_3 generations derived from reciprocal matings of the mutant with the cultivar Hobbit 87 and from a mating of the mutant with the cultivar Harosoy

Mating and generation	Plant or family phenotypes			Hypothesized phenotypic ratio	χ^2 test value	Probability of a greater χ^2
	Normal	Segregating	Mutant			
Hobbit 87 × mutant						
F_1 plants	5	—	—	All	—	—
F_2 plants	18(12)[a]	—	6	3:1	0.000	1.000
$F_{2:3}$ families from nonmutant F_2 plants	8(4)	10(8)	—	1:2	0.999	0.317
F_3 plants in the segregating families	172	—	46	3:1	1.768	0.184
Mutant × Hobbit 87						
F_1 plants	5	—	—	All	—	—
F_2 plants	17(12)[a]	—	7	3:1	0.222	0.637
$F_{2:3}$ families from nonmutant F_2 plants	7(3)	10(9)	—	1:2	0.999	0.317
F_3 plants in the segregating families	178	—	49	3:1	1.403	0.238
Mutant × Harosoy						
F_1 plants	1	—	—	All	—	—
F_2 plants	64	—	20	3:1	0.063	0.801
$F_{2:3}$ families from nonmutant F_2 plants	22	42	—	1:2	0.008	0.929

[a] Parentheses enclose the number of F_2 plants that were observed to have a faint freckling phenotype on one or more of their leaves.

only send a seed request to the corresponding author. Seed of the mutant will be deposited in the soybean genetic type collection (Nelson RL, curator, USDA-ARS, University of Illinois).

From the Departments of Agronomy (Chung, Staswick, Graef, and Specht) and Plant Pathology (Wysong), University of Nebraska, Lincoln, Nebraska. Published as paper no. 11860, Journal Series, Nebraska Agricultural Research Division project no. 12-194. Research partially funded by grants received from the Nebraska Soybean Development, Utilization, and Marketing Board. Address correspondence to Dr. Specht, 322 Keim Hall, Department of Agronomy, University of Nebraska, Lincoln, NE 68583-0915, or e-mail: agro0010@unlvm.unl.edu.

References

Athow KL, 1987. Fungal diseases. In: Soybeans: improvement, production, and uses, 2nd ed (Wilcox JR, ed). Madison, Wisconsin: American Society of Agronomy; 687–727.

Dietrich RA, Delaney TP, Uknes SJ, Ward ER, Ryals JA, and Dangl JL, 1994. Arabidopsis mutants simulating disease resistance response. Cell 77:565–577.

Johal GS, Hulbert SH, and Briggs SP, 1995. Disease lesion mimics of maize: a model for cell death in plants. BioEssays 17:685–692.

Kosslak RM, Dieter JR, Ruff RL, Chamberlin MA, Bowen BA, and Palmer RG, 1996. Partial resistance to rootborne infection by *Phytophthora sojae* in three allelic necrotic root mutants in soybean. J Hered 87:415–422.

Shoemaker RC and Specht JE, 1995. Integration of the soybean molecular and classical genetic linkage groups. Crop Sci 35:436–446.

Walbot V, Hoisington DA, and Neuffer MG. 1983. Disease lesion mimics in maize. In: Genetic engineering of plants (Kosuge T and Meredith C, eds). New York: Plenum; 431–442.

Received April 7, 1997
Accepted October 20, 1997

Corresponding Editor: Gary E. Hart

Inheritance of a Rusty-Leaf Trait in Peanut

W. D. Branch

A rusty-leaf mutant was found previously in the cultivated peanut (*Arachis hypogaea* L.). Crosses involving the rusty-leaf genotype were made both between and within subspecies of *A. hypogaea* to determine its inheritance. The F_1, F_2, and F_3 data indicated that two complementary recessive genes, designated rl_1 and rl_2, control the rusty-leaf characteristic. No maternal or cytoplasmic effects were detected among progenies from reciprocal hybridization.

Hammons (1973) first reported the occurrence of a spontaneous mutant peanut (*Arachis hypogaea* L.) with a rusty-leaf phenotype that he found to be inherited as a recessive characteristic. Rusty-leaf was discovered as an off-type plant in a foundation seed increase field of Virginia Bunch 67 (Hammons RO, personal communication). Since its original discovery in 1967, the rusty-leaf genotype has bred true to type. Virginia Bunch 67 is an older peanut cultivar that was developed by pure-line selection from a mixed sample of small and large seed and released by the Georgia Agricultural Experiment Stations around 1945 (Higgins and Bailey 1955).

Plants of both rusty-leaf and Virginia Bunch 67 have semi-erect or decumbent growth habits, medium maturity, and pink testa color. However, rusty-leaf plants have a light- or pale-green color with small, white speckled areas on the youngest leaflets giving it a rusty appearance. The most mature leaves conversely appear more normal green in color on the same plant. The contrast between inside and outside of the canopy can frequently resemble early spider-mite damaged foliage.

Previously several different chlorophyll-deficient and other abnormal leaf colors have been evaluated extensively to further knowledge of peanut genetics (Murthy and Reddy 1993; Wynne and Coffelt 1982). The objective of this genetic study was to gain insight into the inheritance of another unusual leaf trait, rusty-leaf.

Materials and Methods

Reciprocal crosses were made in the greenhouse between rusty-leaf and two

Table 1. F_2 plant segregation for leaf color among four peanut cross combinations

Cross	No. of families	F_2 leaf color		χ^2	
		Normal	Rusty	(15:1)	*P*
Rusty-leaf × Georgia Browne	3	888	67	0.956	.25–.50
Georgia Browne × rusty-leaf	3	962	71	0.685	.25–.50
Rusty-leaf × Georgia Red	2	276	16	0.296	.50–.75
Georgia Red × rusty-leaf	2	274	13	1.450	.10–.25
Total				3.387	.25–.50
Pooled	10	2,400	167	0.286	.50–.75
Homogeneity				3.101	.25–.50

Table 2. F_3 progeny segregation for leaf color from F_2 normal leaf peanut plants

Cross	$F_{2:3}$ leaf color progeny			χ^2	
	Normal	(15:1)	(3:1)	(7:4:4)	*P*
Rusty-Leaf × Georgia Browne	24	8	8	3.302	.10–.25
Rusty-Leaf × Georgia Red	23	9	8	1.933	.25–.50
Total				5.235	.25–.50
Pooled	47	17	16	4.716	.05–.10
Homogeneity				0.519	.75–.90

peanut cultivars, Georgia Browne (Branch 1994) and Georgia Red (Branch and Hammons 1987), both of which have dark green leaf color. The parental lines rusty-leaf and Georgia Browne represent crosses within *A. hypogaea* subsp. *hypogaea*; whereas rusty-leaf and Georgia Red represent cross combinations between subsps. *hypogaea* and *fastigiata.*

The F_1, F_2, and F_3 populations were space-planted in field nursery plots during 1994, 1995, and 1996, respectively, at the agronomy research farm near the Georgia Coastal Plain Experiment Station, Tifton, Georgia. Phenotypic classification was based upon individual plants, and segregation data were analyzed by the CHISQA computer program (Hanna et al. 1978).

Results and Discussion

The leaf color of each F_1 plant for all cross combinations was classified as normal, indicating that rusty-leaf color is recessive to normal green. These results agree with the earlier observation by Hammons (1973).

The F_2 segregation from each cross fit a 15 normal green:1 rusty-leaf color ratio (Table 1). No significant differences were detected among crosses or between reciprocal crosses, which suggest the absence of cytoplasmic or maternal effects. Total, pooled, and homogeneity chi-square values also fit a 15:1 ratio. These results suggest that two complementary recessive genes control the rusty-leaf trait. Similar digenic inheritance has commonly been found in the cultivated peanut (Murthy and Reddy 1993; Wynne and Coffelt 1982).

Individual F_2 plant selections were made within two cross combinations (rusty-leaf × Georgia Browne and rusty-leaf × Georgia Red) for subsequent progeny row testing in the F_3 generation. F_3 progeny from F_2 plants with rusty-leaf color bred true to type. Segregation of $F_{2:3}$ progeny from F_2 plants with normal leaf color fit a 7 non-segregating (all normal green):4 segregating (15 normal green:1 rusty):4 segregating (3 normal green:1 rusty) expected ratio (Table 2). These F_3 results verify the F_2 findings for digenic inheritance.

The data from this genetic study indicate that two recessive genes control the rusty-leaf trait. The symbols rl_1 and rl_2 are proposed for the genes conditioning the rusty-leaf trait found in the cultivated peanut.

From the Department of Crop and Soil Sciences, University of Georgia, Coastal Plain Experiment Station, Tifton, GA 31793–0748. Contribution from the University of Georgia, College of Agricultural and Environmental Sciences.

References

Branch WD, 1994. Registration of 'Georgia Browne' peanut. Crop Sci 34:1125–1126.

Branch WD and Hammons RO, 1987. Registration of 'Georgia Red' peanut. Crop Sci 27:1090.

Hammons RO, 1973. Genetics of *Arachis hypogaea.* In: Peanuts—culture and uses. Stillwater, Oklahoma: American Peanut Research and Education Association; 135–173.

Hanna W, Mullinix B, and Grimes L, 1978. Computer programs for analyses of inheritance and linkage data. Crop Sci 18:517.

Higgins BB and Bailey WK, 1955. New varieties and selected strains of peanuts. Bulletin NS 11. Athens: University of Georgia Agricultural Experiment Stations.

Murthy TGK and Reddy PS, 1993. Cytogenetics and genetics of groundnuts. Andover, England: Intercept.

Wynne JC and Coffelt TA, 1982. Genetics of *Arachis hypogaea* L. In: Peanut science and technology. Yoakum, Texas: American Peanut Research and Education Society; 50–94.

Received June 17, 1997
Accepted October 20, 1997

Corresponding Editor: Fredrick Bliss

In situ Hybridization Mapping of Genes in *Hordeum vulgare* L.

G. Butnaru, J. Chen, P. Goicoechea, and J. P. Gustafson

Linkage maps of barley (*Hordeum vulgare* L.) containing genomic and cDNA sequences and functional genes have been constructed which cover a large genetic distance throughout the entire genome. It was decided to physically locate three genes from the barley linkage map to sites on chromosomes within the barley genome. In situ hybridization (ISH) with biotin-labeled DNA probes was used to determine the physical chromosome location of the genes for nitrate reductase, carboxypeptidase, and α-amylase within the barley genome. The results indicated all of the genes studied hybridized to barley chromosomes 5H and 6H, and that the gene order on the physical map was similar to that observed on the genetic map. The major difference between the genetic map location of nitrate reductase and carboxypeptidase on chromosome 5H was the locations observed for each gene on the 5H short and long arms. The hybridization site of nitrate reductase on the short and long arms of chromosome 5H and the hybridization site for carboxypeptidase on the short arm of 5H was not observed on any genetic map. However, these sites were observed by ISH in the same location on different cultivars. The additional hybridization sites are probably due to the presence of silenced homologous sequences, or to unrelated sequences that show considerable homology. The nitrate reductase hybridization sites were also detected on the satellite, and the short and long arms of chromosome 6H.

Understanding the genetic control and manipulation of economic traits in cereals has always been a major goal of breeding programs and has led to improved breeding strategies, germplasm, and ultimately higher yield. For the past several years it has been the aim of many research programs to develop high-density linkage maps using genes and a variety of codominant and dominant molecular markers. Maps are being used to establish linkages between molecular markers and agriculturally important traits that are difficult to evaluate using standard breeding methodologies. The linkages between molecular markers and genes affecting valuable traits give the breeder a powerful tool in selecting for the desired agronomic trait.

Several RFLP maps of barley (*Hordeum vulgare* L.) have been constructed which cover a large genetic distance on all seven barley chromosomes (Becker et al. 1995; Giese et al. 1994; Graner et al. 1991; Heun et al. 1991; Jensen 1987; Kasha et al. 1995; Kleinhofs et al. 1993; Langridge et al. 1995; Qi et al. 1996; Röder et al. 1993). The maps and data can be found listed in the

Table 1. The detection of the physical location of the α-amylase gene on barley chromosome 6H

Varieties	Number of cells	Arm ratio	Gene location detections %[a]	Distance from centromere (%)
Long arm				
Apex	758	1.22 ± 0.03	35 (4.6%)	51.1 ± 3.0
Steptoe	898	1.23 ± 0.01	44 (4.9%)	48.9 ± 0.5
Steptoe[b]	147	1.23 ± 0.15	14 (9.5%)	56.2 ± 10.8
Total	1,803		93 (5.2%)	52.1[c]

[a] Percentage distance from the centromere to the telomere ± standard deviation.

[b] Hybridization at 42°C while all others are at 37°C.

[c] Average gene location over all measurements.

GrainGenes barley database (http://wheat.pw.usda.gov/ggpages/newggmaps.html#barley).

There are several possible techniques for locating DNA sequences to physical sites on chromosomes. First, the most involved procedure would be "chromosome walking" using DNA sequencing and pulsefield gel electrophoresis (PFGE), or a combination of both (Ganal et al. 1989; Siedler and Graner 1991). Second would be to produce deletion or recombinant chromosome stocks for the markers of interest and thus map specific markers to specific deletions (Gill et al. 1993; Hohmann et al. 1995; Rogowsky et al. 1993; Werner et al. 1992). If the deletions involved are large then markers can only be mapped in a relative sense. In addition, the markers can only be mapped in the genetic background used to create the deletion or recombinant chromosome stocks. Third, low- and single-copy DNA sequences can be physically mapped in relation to centromeres by in situ hybridization (ISH) (Dong and Quick 1995; Gustafson and Dillé 1992; Lehfer et al. 1993; Leitch and Heslop-Harrison 1993; Song and Gustafson 1995; Wang et al. 1995). In situ hybridization appears to represent an appropriate method to physically map DNA sequences because it can be accomplished using any species or variety.

In situ hybridization of low- and single-copy sequences has proven to be difficult in plants and works best with large, single-copy or multiple-copy probes (Ambros et al. 1986; Busch et al. 1995; Chen and Gustafson 1995; Clark et al. 1989; Dong and Quick 1995; Gustafson and Dillé 1992; Gustafson et al. 1990; Huang et al. 1988; Lehfer et al. 1993; Leitch and Heslop-Harrison 1993; Song and Gustafson 1995; Wang et al. 1995). In order to fully exploit the benefits of merging genetic maps, it is desirable that an ISH procedure be able to physically map RFLP probes shorter than 1–2 kb. Hybridization frequencies are very low when mapping such small single-copy markers. With ISH, only one DNA molecule embedded into the cellular context is analyzed in each chromatic; as compared to millions of naked DNA copies hybridized using Southern analysis. A major advantage of ISH is that probe polymorphism is not required for the location of a DNA sequence to a particular chromosome as it is with linkage maps.

In situ hybridization techniques have already been used to ascertain the physical location of repeated and low-copy sequences and functional genes in barley (Clark et al. 1989; Lehfer et al. 1993; Leitch and Heslop-Harrison 1993; Pedersen et al. 1995), wheat (*Triticum aestivum* L. em Thell.) (Chen and Gustafson 1995; Mukai and Gill 1991; Rayburn and Gill 1985), rye (*Secale cereale* L.) (Busch et al. 1995; Gustafson et al. 1988, 1990), rice (*Oryza sativa* L.) (Gustafson and Dillé 1992; Song and Gustafson 1995), and parsley (*Petroselinum crispum* L.) (Huang et al. 1988). In addition, ISH has been utilized for the identification of alien chromosome segments in various species (Lapitan et al. 1986; Nkongolo et al. 1993; Schwarzacher et al. 1992) ranging in size up to a wheat-rye centric break and fusion translocation. The use of ISH to determine the relative physical location of genes or molecular markers on chromosomes should lead to a better understanding of the differences between the genetic and physical chromosome structure and genome organization.

This study was designed to establish the physical location within the barley genome of the α-amylase (α-*Amy*), carboxypeptidase (*Cxp*), and nitrate reductase (*Nar*) genes, and to determine the location of any secondary hybridization sites of homologous DNA sequences for the three genes.

Materials and Methods

The barley varieties utilized were Steptoe, a six-row barley (from T. Blake, Montana State University) and Apex, a two-row barley (from M. Maluszynski, International Atomic Energy Agency, Vienna, Austria). The cDNA clones bNRp30a, pMI8A, and pMI8B for nitrate reductase, α-*Amy1* for α-amylase, and *Cxp* for carboxypeptidase, respectively, were supplied by A. Klienhofs, Washington State University.

The creation of protoplast slides, hybridization, detection, and visualization of biotinylated probes to chromosomes followed the procedures of Gustafson and Dillé (1992). The hybridization's were carried out at both 37°C and 42°C to determine whether temperature effects hybridization detection levels and/or hybridization site location. The experiment was a blind independent experiment, in that neither J. Chen and G. Butnaru had any prior knowledge of either the chromosome or genetic map location of any of the three genes to be analyzed. The detection measurements of the hybridized sites for all of the gene complexes for α-amylase were duplicated by G. Butnaru and J. Chen on different in situ hybridized slides using root tips from different seeds at the same hybridization temperatures to establish if there was any experimenter bias that affected the measurements. The arm ratios and detection location measurements were made using phase-contrast microscopy and a Zeiss Photomicroscope III coupled with a Hamamatsu image enhancement system on all chromosomes showing a hybridization site. The measurements were taken directly from the monitor screen using a set of electronic calipers. The physical map localization was calculated as a percent of the arm length from the centromere. Several detection's were measured for each probe at each physical location and standard deviations were calculated.

Results and Discussion

The α-amylase gene was physically located on the long arm (L) of barley chromosome 5H (5HL) 52.1% from the centromere (Table 1; Figures 1A and 2). This arm location is in agreement with previous reports derived from genetic mapping studies (Linde-Laursen 1982; Nielsen and Frydenberg 1974; Shin et al 1990). The physical location of the α-*Amy1* locus (51.1% versus 48.9%) was slightly different when the varieties Apex and Steptoe, respectively, were compared at a 37°C hybridization temperature. However, there were no significant differences between the arm location from variety to variety, or from sci-

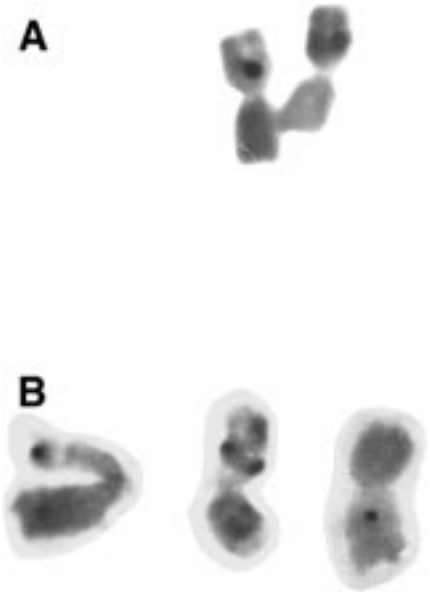

Figure 1. **(A)** In situ hybridized mitotic metaphase chromosomes of Steptoe showing α-*Amy1* hybridized to sites on barley chromosome arms 6HL. **(B)** In situ hybridized mitotic metaphase chromosomes of Apex showing *Nar1* hybridized to the three sites on barley chromosome 6H.

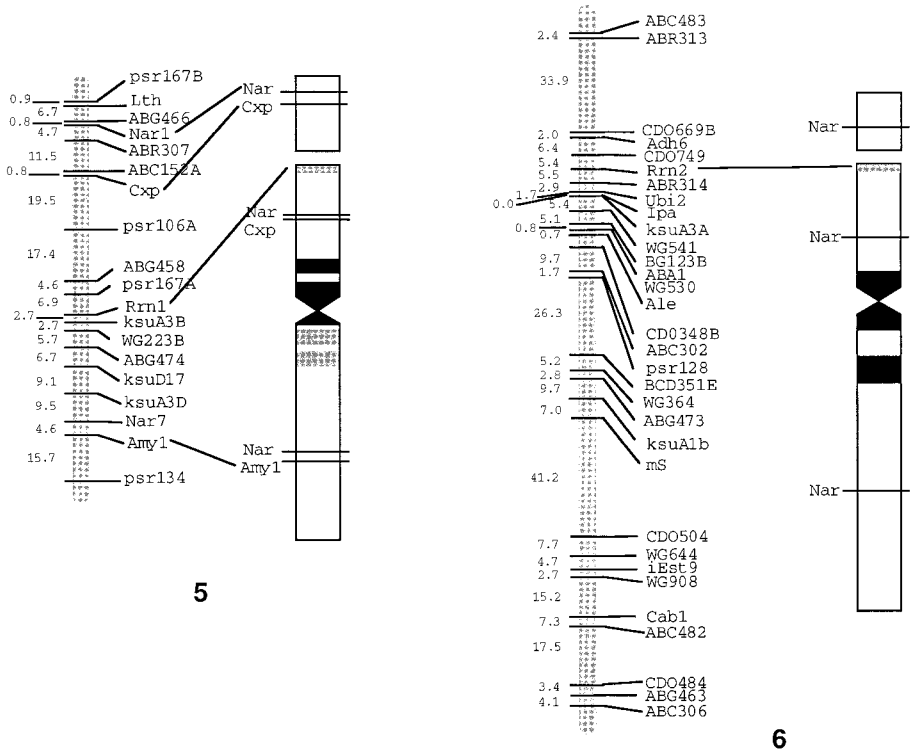

Figure 2. A comprehensive picture showing the physical location of RFLP markers for barley chromosomes 5H and 6H.

entist to scientist analyzing the slides. In addition, no differences were observed for the α-*Amy1* hybridization site when the hybridization temperature was raised from 37°C to 42°C. The difference in the α-*Amy1* location, as a percentage of the arm distance from the centromere, on 5HL in Steptoe when the hybridizations were carried out at 37°C versus 42°C, 48.9 ± 0.5% versus 56.2 ± 10.8%, respectively, might be due to the 42°C hybridization temperature (higher stringency level). The standard deviations for all probes studied at 42°C hybridization's were higher than at 37°C (Tables 1, 2, 3, and 4), which could be due to the effects of temperature altering the chromosome structure during the period of hybridization. However, even with the high standard deviations, a significant difference was observed in the increase in detection percentage when the hybridization temperature was raised from 37°C to 42°C, 4.9% versus 9.5%, respectively.

The *Cxp3* locus was detected on barley chromosome 5H (Table 2; Figure 2). A detection site was located 46.8% of the distance from the centromere on the short arm (S), which agrees with the genetic mapping of the *Cxp3* locus in barley to 5HS (Kleinhofs et al. 1988). In addition, a second detection site was observed on the 5HS satellite 81.5% of the distance from the centromere. However, the detection levels observed on the satellite were extremely low.

The analysis of the *Nar1* gene location showed similar results to that observed with the *Cxp3* locus. Two nitrate reductase genes have been genetically located on the satellites of barley chromosome arms 6HS and 5HS (Kleinhofs et al. 1988; Melzer et al. 1988). Surprisingly the present data showed a higher percentage of detection on chromosome arm 5HL (4.9%) versus that observed on chromosome arm 5HS (1.4%) (Table 3; Figures 1B and 2). Chromosome arm 5HL is known to be the location of a different nitrate reductase gene (*Nar7*), therefore this study suggests that the nitrate reductase cDNA clone bNRp30a, under the stringency conditions utilized, was capable of limited cross-hybridizing with the *Nar7* locus.

A detection site was also observed on the 5H satellite very close to the observed *Cxp3* site. The ISH data suggests that the main site of nitrate reductase might be located on chromosome arm 5HL approximately 50.0% of the distance from the centromere. This differs from the Southern analysis data of Kleinhofs et al. (1988).

Table 2. The detection of the physical location of the carboxypeptidase gene on barley chromosome 6H

Varieties	Number of cells	Arm ratio	Gene location detections (%)[a]	Distance from centromere (%)
Short arm				
Apex	270	1.22 ± 0.03	13 (4.8%)	42.7 ± 6.2
Steptoe	1,716	1.23 ± 0.03	31 (1.8%)	51.5 ± 4.0
Steptoe[b]	433	1.23 ± 0.14	24 (5.5%)	46.1 ± 7.8
Total	2,419		68 (2.8%)	46.8[c]
Satellite				
Apex	270	1.22 ± 0.03	2 (0.7%)	85.3 ± 2.1
Steptoe	1,716	1.23 ± 0.03	4 (0.2%)	84.1 ± 1.6
Steptoe[b]	433	1.23 ± 0.14	10 (2.3%)	75.1 ± 8.2
Total	2,419		16 (0.6%)	81.5[c]

[a] Percentage distance from the centromere to the telomere ± standard deviation.

[b] Hybridization at 42°C while all others are at 37°C.

[c] Average gene location over all measurements.

Table 3. The detection of the physical location of the nitrate reductase gene on barley chromosome 6H

Varieties	Number of cells	Arm ratio	Gene location detections (%)[a]	Distance from centromere (%)
Long arm				
Apex	284	1.22 ± 0.05	15 (5.3%)	49.4 ± 6.6
Steptoe	854	1.23 ± 0.02	42 (4.9%)	47.6 ± 5.1
Steptoe[b]	300	1.18 ± 0.11	14 (4.4%)	53.0 ± 12.5
Total	1,438		71 (4.9%)	50.0[c]
Short arm				
Apex	284	1.22 ± 0.05	5 (1.8%)	59.2 ± 12.6
Steptoe	854	1.23 ± 0.02	6 (0.7%)	36.1 ± 1.1
Steptoe[b]	300	1.18 ± 0.11	9 (3.0%)	46.0 ± 11.2
Total	1,438		20 (1.4%)	47.1[c]
Satellite				
Apex	284	1.22 ± 0.05	3 (1.1%)	86.7 ± 6.1
Steptoe	854	0	0	
Steptoe[b]	300	0	0	
Total	1,438		3 (0.2%)	86.7[c]

[a] Percentage distance from the centromere to the telomere ± standard deviation.

[b] Hybridization at 42°C while all others are at 37°C.

[c] Average gene location over all measurements.

In the current barley genome, linkage maps indicate the presence of one functional gene location each for carboxypeptidase and nitrate reductase. The alternative site(s) observed in the present study by ISH could be the result of several alternative events. First, totally unrelated DNA sequences may be homologous enough to show some level of detection at the relatively low stringency level utilized in the ISH technique. Second, relic genes that have lost function may be present elsewhere in the genome. Third, additional sites may have been not mapped during RFLP analysis because of a lack of polymorphisms. Finally, variation in copy number of any DNA sequence at a site could also have a significant effect on the ISH detection percentage for that particular sequence. All of the above alternatives could be true and suggest that a high ISH detection percentage might not necessarily locate the active site of the gene in question, but could be detecting any one of the above. In situ hybridization, at present, is not an appropriate technique for determining which of a number of sites may represent an active member of a dispersed set of related sequences. Therefore placing the physical location of an active gene to a specific site could be subject to error. Additional differences in the location of *Cxp3* and *Nar1* from variety to variety (Table 2) could also result from deletions, duplications, inversions, and translocations that have been observed between barley varieties. It appears that ISH combined with linkage mapping is the best approach for locating a functional gene.

The *Nar1* detection levels observed on chromosome 5H were lower than those on 6H, which is probably indicative of low levels of homology of the nitrate reductase probe to the related DNA sequences located on chromosome 5H (Table 4). It is interesting to note that the detection sites on both 6H and 5H for nitrate reductase were in similar locations on each chromosome with the sites on the satellites showing the least homology.

When comparing the physical location of DNA sequences between varieties, differences can be seen. The physical differences are not large, but the *Nar1* site on 5HS is in a slightly different physical location depending on the barley cultivar analyzed, that is, Apex or Steptoe (Table 3). In addition, the α-*Amy1* site on 5HS in Apex and Steptoe (Table 4) shows some variation. All of these sites are ones of extremely low detection levels and could be sites of DNA sequences showing some degree of homology, or are relic silenced gene sites that have evolved and have changed part of their sequence as compared to the active site.

Table 4. The detection of the physical location of a nitrate reductase site on barley chromosome 5H

Varieties	Number of cells	Arm ratio	Gene location detections (%)[a]	Distance from centromere (%)
Long arm				
Apex	273	1.85 ± 0.04	5 (1.8%)	47.6 ± 7.1
Steptoe	764	1.99 ± 0.10	13 (1.7%)	50.2 ± 11.6
Steptoe[b]	300	1.57 ± 0.08	5 (1.7%)	48.0 ± 16.0
Total	1,337		23 (1.7%)	48.6[c]
Short arm				
Apex	273	1.85 ± 0.04	2 (0.7%)	28.5 ± 3.0
Steptoe	764	1.99 ± 0.10	12 (1.6%)	44.8 ± 3.6
Steptoe[b]	300	1.57 ± 0.08	7 (2.3%)	48.0 ± 7.2
Total	1,337		21 (1.5%)	40.4[c]
Satellite				
Apex	273	1.85 ± 0.04	2 (0.7%)	80.8 ± 10.0
Steptoe	764	1.99 ± 0.10	2 (0.3%)	82.6 ± 10.6
Steptoe[b]	300		0	0
Total	1,337		4 (0.5%)	81.7[c]

[a] Percentage distance from the centromere to the telomere ± standard deviation.

[b] Hybridization at 42°C while all others are at 37°C.

[c] Average gene location over all measurements.

From the Department of Genetics, Banat's University of Agricultural Sciences, Timisoara, Romania (Butnaru), the College of Life Science, Wuhan University, Wuhan, Hubei, People's Republic of China (Chen), CIMA-Arkaute, Vitoria, Spain (Goicoechea), and the USDA Agricultural Research Service, Plant Genetics Research Unit and Plant Science Unit, University of Missouri, Columbia, MO 65211 (Gustafson). This article reports the results of research only. Mention of a proprietary product does not constitute an endorsement or a recommendation for its use by the USDA or the University of Missouri. This article is a contribution of the USDA, Agricultural Research Service, and the Missouri Agricultural Experiment Station, journal series no. 12,654. J.P.G. would like to thank the North American Barley Mapping Project (NABMP) for financial support. Address correspondence to Dr. Gustafson at the address above.

References

Ambros PF, Matzke MA, and Matzke AJM, 1986. Detection of a 17 kb unique sequence (T-DNA) in plant chromosomes by in situ hybridization. Chromosoma 94:11–18.

Becker J, Vos P, Kuiper M, Salamini F, and Heun M, 1995. Combined mapping of AFLP and RFLP markers in barley. Mol Gen Genet 249:65–73.

Busch W, Herrmann RG, and Martin R, 1995. Refined physical mapping of the Sec-1 locus on the satellite of chromosome 1R of rye (*Secale cereale*) Genome 38: 889–893.

Clark M, Karp A, and Archer S, 1989. Physical mapping

of the B-hordein loci on barley chromosome 5 by in situ hybridization. Genome 32:925–929.

Chen JM, and Gustafson JP, 1995. Physical mapping of genetically mapped RFLP clones in homoeologous group 7 chromosomes of wheat by in situ hybridization. Heredity 75:225–233.

Dong HA and Quick J, 1995. Detection of a 2.6 kb single/low copy DNA sequence on chromosomes of wheat *(Triticum aestivum* L.) and rye (*Secale cereale* L.) by fluorescence in situ hybridization. Genome 38:246–249.

Ganal MW, Young ND, and Tanksley SD, 1989. Pulse field gel electrophoresis and physical mapping of large DNA in the *TM-2a* region of chromosome 9 in tomato. Mol Gen Genet 215:395–400.

Giese H, Holm-Jensen AG, Mathiassen H, Kjaer B, Rasmussen SK, Bay H, and Jensen J, 1994. Distribution of RAPD markers on a linkage map of barley. Hereditas 120:267–273.

Gill KS, Gill BS, and Endo TR, 1993. A chromosome region-specific mapping strategy reveals gene-rich telomeric ends in wheat. Chromosoma 102:374–381.

Graner A, Jahoor A, Schondelmaier J, Siedler H, Pillen K, Fishbeck G, Wenzel G, and Herrmann RG, 1991. Construction of a RFLP map of barley. Theor Appl Genet 83:250–256.

Gustafson JP, Butler E, and McIntyre CL, 1990. Physical mapping of a low-copy DNA sequence in rye (*Secale cereale* L.). Proc Natl Acad Sci USA 87:1899–1902.

Gustafson JP, Dera AR, and Petrovic S, 1988. Expression of modified ribosomal RNA genes in wheat. Proc Natl Acad Sci USA 85:3943.

Gustafson JP and Dillé JE, 1992. The chromosome location of *Oryza sativa* recombination linkage groups. Proc Natl Acad Sci USA 89:8646–8650.

Heun M, Kennedy AE, Anderson JA, Lapitan NLV, Sorrells ME, and Tanskley SD, 1991. Construction of a restriction fragment length polymorphism map for barley (*Hordeum vulgare*). Genome 34:437–447.

Hohmann U, Graner A, Endo TR, Gill BS, and Herrmann RG, 1995. Comparison of wheat physical maps with barley linkage maps for group 7 chromosomes. Theor Appl Genet 91:618–626.

Huang PL, Hahlbrock K, and Somseich IE, 1988. Detection of a single-copy gene on plant chromosome by in situ hybridization. Mol Gen Genet 211:143–147.

Jensen J, 1987. Linkage map of barley chromosome 4. In: Barley genetics (Yasuda S and Konishi T, eds). Nakasange Okayama: Sanyo Press; 189–199.

Kasha KJ, Kleinhofs A, Kilian A, Saghai Maroof M, Scoles GJ, Hayes PM, Chen FQ, Xia X, Li X-Z, Biyashev RM, Hoffman D, Dahleen L, Blake TK, Rossnagel BG, Steffenson BJ, Thomas PL, Falk DE, Laroche A, Kim W, Molnar SJ, and Sorrells ME, 1995. The North American barley map on the cross HT and its comparison to the map on cross SM. In: The plant genome and plastome: their structure and evolution (Tsunewaki K, ed). Tokyo: Kodansha Scientific Ltd.; 73–88.

Kleinhofs A, Chao S, and Sharp PJ, 1988. Mapping of nitrate reductase genes in barley and wheat. Proceedings of the Seventh International Wheat Genetics Symposium, Cambridge, U.K.; 541–546.

Kleinhofs A, Killian A, Kudrna D, and NABGMP, 1993. The NABGMP Steptoe × Morex mapping progress report. Barley Genet Newslett 23:79–83.

Langridge P, Karakousis A, Collins N, Kretchmer J, and Manning S, 1995. A consensus linkage map of barley. Mol Breed 1:389–395.

Lapitan NLV, Sears RG, Rayburn AL, and Gill BS, 1986. Wheat-rye translocations. Detection of chromosome breakpoints by in situ hybridization with a biotin-labeled DNA probe. J Hered 77:415–419.

Lehfer H, Busch W, Martin R, and Herrmann RG, 1993. Localization of the B-hordein locus on barley chromosomes using fluorescence in situ hybridization. Chromosoma 102:428–432.

Leitch IJ and Heslop-Harrison JS, 1993. Physical mapping of the 18S-5.8S-26S rRNA genes in barley by in situ hybridization. Genome 35:1013–1018.

Linde-Laursen I, 1982. Linkage map of the long arm of barley chromosome 3 using C-bands and marker genes. Heredity 49:27–35.

Melzer JM, Kleinhofs A, Kudrna DA, Warner RL, and Blake TK, 1988. Genetic mapping of the barley nitrate reductase-deficient nar 1 and nar 2 loci. Theor Appl Genet 75:767–771.

Mukai Y, Endo TR, and Gill BS, 1990. Physical mapping of 5S rRNA multigene family in common wheat. J Hered 81:290–295.

Mukai Y and Gill BS, 1991. Detection of barley chromatin added to wheat by genomic in situ hybridization. Genome 34:448–452.

Nielsen G and Frydenberg O, 1974. Linkage between the loci Amy 1 (α-amylase), o (orange lemma) and Xn (xantha seedling). Barley Newslett 4:53–54.

Nkongolo KK, Lapitan NLV, Quick JS, and Muhlmann MD, 1993. An optimized fluorescence in situ hybridization procedure for detecting rye chromosomes in wheat. Genome 36:701–705.

Pedersen C, Giese H, and Linde-Laursen I, 1995. Towards an integration of the physical and the genetic chromosome maps of barley by in situ hybridization. Hereditas 123:77–99.

Qi X, Stam P, Lindhout P, 1996. Comparison and integration of four barley genetic maps. Genome 39:379–394.

Rayburn AL and Gill BS, 1985. Use of biotin-labeled DNA probes to map specific DNA sequences on what chromosomes. J Hered 76:78–81.

Röder MS, Lapitan NLV, Sorrells ME, and Tanskley SD, 1993. Genetic and physical mapping of barley telomeres. Mol Gen Genet 238:294–303.

Rogowsky PM, Sorrells ME, Shepherd KW, and Landridge P, 1993. Characterization of wheat-rye recombinants with RFLP and PCR probes. Theor Appl Genet 85:1023–1028.

Siedler H and Graner A, 1991. Construction of physical maps of the *Hor1* locus of two barley cultivars by pulse field gel electrophoresis. Mol Gen Genet 226:177–181.

Shin JS, Chao S, Corpuz L, and Blake T, 1990. A partial map of the barley genome incorporating restriction fragment length polymorphism, polymerase chain reaction, isozyme, and morphological marker loci. Genome 33:803–810.

Schwarzacher T, Anamthawat-Jonsson K, Harrison GE, Islam AKMR, Jia JZ, King IP, Leitch AR, Miller TE, Reader SM, Rogers WJ, Shi M, and Heslop-Harrison JS, 1992. Genomic in situ hybridization to identify alien chromosomes and chromosome segments in wheat. Theor Appl Genet 84:778–786.

Song YC and Gustafson JP, 1995. The physical location of fourteen RFLP markers in rice (*Oryza sativa* L.). Theor Appl Genet 90:113–119.

Wang ZX, Kurata N, Saji S, Katayose Y, and Minobe Y, 1995. A chromosome specific repetitive DNA sequence in rice (*Oryza sativa* L.). Theor Appl Genet 90:907–913.

Werner JE, Endo TR, and Gill BS, 1992. Toward a cytogenetically based physical map of the wheat genome. Proc Natl Acad Sci USA 89:11307–11311.

Received June 19, 1997
Accepted December 13, 1997

Corresponding Editor: Halina Skorupska

Comparison of Genetic Diversity Between *Cunninghamia konishii* and *C. lanceolata*

T.-P. Lin, C.-T. Wang, and J.-C. Yang

Genetic diversity within and genetic differentiation among five geographic areas of *Cunninghamia konishii* were investigated using young shoots of 120 clones as materials. Nine loci, comprising six polymorphic loci (*Pgm-2, Pgi-1, 6Pgd-2, Skdh-1, Skdh-2, Aat-2*) from five enzyme systems were analyzed by starch-gel electrophoresis. The average percentage of polymorphic loci per geographic area was 62.3% at the 99% criterion for polymorphism. Mean expected heterozygosity ranged from 0.191 to 0.239 in the different areas. On average there were 1.98 alleles per locus; the effective number of alleles per locus ranged from 1.39 to 1.54. Partitioning the genetic variability into within- and among-population components with *F* statistics led to an estimate of within-population variation of 97.1% of the total variation. Treating *C. konishii* and *C. lanceolata* as one panmistic population each, the expected heterozygosity was 0.251 and 0.343, respectively. Other genetic parameters were also consistently lower in *C. konishii* than those observed for *C. lanceolata.* Genetic differentiation between these two species (F_{ST}) was only 0.057, thus 94% of the genetic variation resided within species. In fact, the allozyme phenotypes found in *C. konishii* were within the variation of *C. lanceolata* indicating that *C. konishii* is a variety of *C. lanceolata* even though they have been separated for a long period. Genetic drift was found to be significant in populations of *C. konishii.*

Cunninghamia konishii Hay. (=*C. lanceolata* (Lamb.) Hook. var. *konishii* (Hay.) Fujita) is an endemic conifer of Taiwan, and closely related to *C. lanceolata* (Lamb.) Hook., a species which only occurs in mainland China. Old growth of *C. konishii* represents a source of valuable timber in Taiwan. It is usually found scattered within forests of *Chamaecyparis* at elevations of 1300–2800 m (Liu 1966), and is also in association with *Taiwania cryptomerioides, Pseudotsuga wilsoniana,* and *Pinus* spp. *C. konishii* has been used in reforestation programs on national forest land over the past 15 years and man-made plantations of this species occupy about

10,000 ha. *C. lanceolata* was introduced from China and has been widely cultivated at low elevations, especially on private forest land.

Genetic variation in seed samples of *C. lanceolata* was found to be quite high (Muller-Starck and Liu 1989). The number of alleles per locus was 4.15, the percentage of polymorphic loci was 88%, and the expected heterozygosity was 0.299. The high level of genetic diversity observed in *C. lanceolata* was further confirmed recently by studying seed samples from 16 populations from mainland China (Yeh et al. 1994). Since the studies mentioned above were based on trees from man-made plantations, it will be interesting to investigate genetic variation of *C. konishii* from natural forests.

In this study the population genetic structure of *C. konishii* was investigated using young leaf tissue. The relationship between *C. konishii* and *C. lanceolata* is unclear, the comparison between these two species will be welcomed by scientists who wish to know how well they are related at the allozyme level despite the high similarity in vegetative morphology.

Materials and Methods

Seed and Young Leaf Tissue Collection

In 1994 wind-pollinated seeds from 18 individual trees (families) were collected from the seed orchard at Chuyuanshan, Tungsyh, Taiwan, at an elevation of 700 m. It was established between 1968 and 1974, and is composed of 25 grafted clones planted over 10 ha. Clones originated from an old-growth forest of *C. konishii* in central Taiwan.

In April 1996 and 1997 young leaf tissues from 120 clones were collected from a clonal garden established in June 1978 at the Lienhuachih Station, Taiwan Forestry Research Institute (TFRI). The original clones (139) were collected from major old-growth forests of *C. konishii.* The original sites for these clones are shown in Figure 1. These locations were grouped into five areas based on their separation by rivers and/or high mountains. Area 1 is separated from areas 2 and 3 by mountains over 3000 m, which decline at the north ends. Areas 4 and 5 are also separated by the central mountain range. Areas 2 and 3 are separated by valleys. However, the significance of barrier to gene flow between them is not clear. Also in 1996 and 1997, young leaf tissues of 160 trees of *C. lanceolata,* originating from 44 seed sources in China, were collected from another garden at the Lienhuachih Station, TFRI. This garden was established in May 1981.

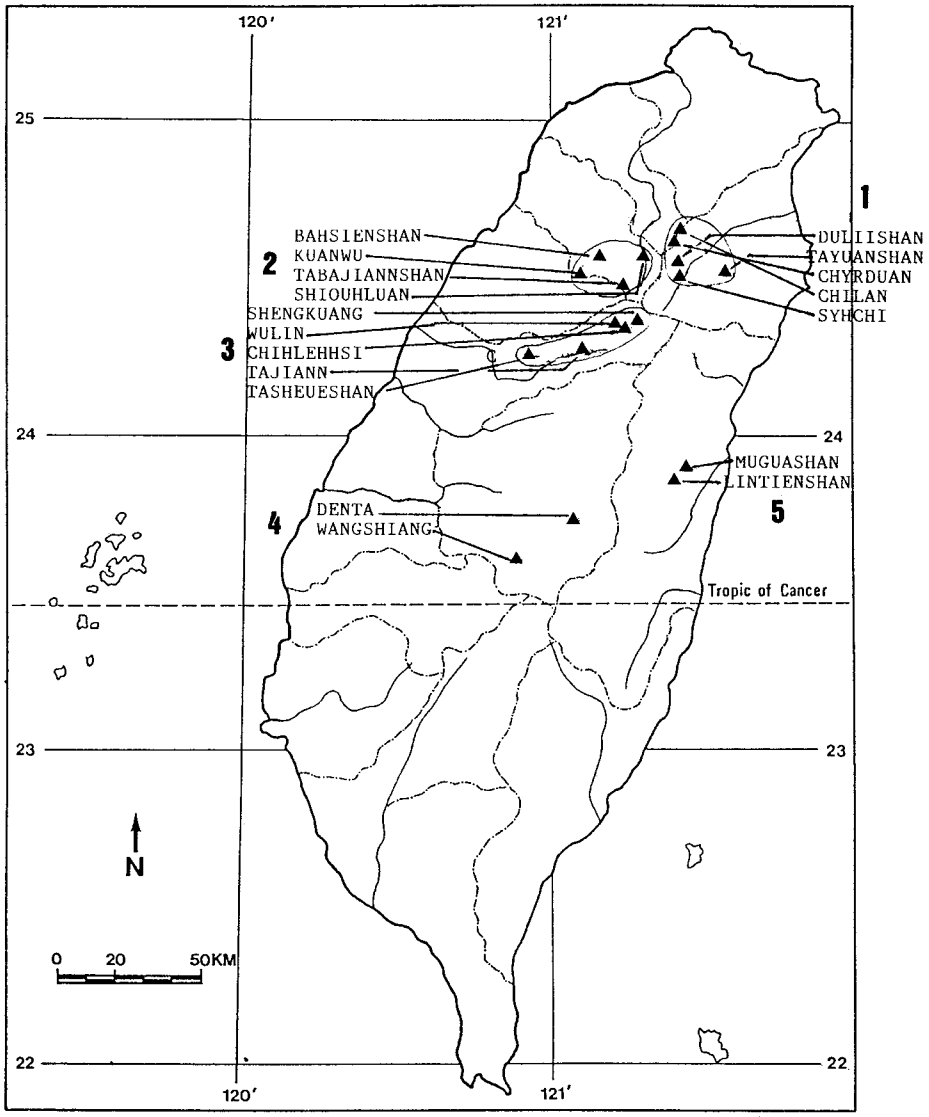

Figure 1. Map of Taiwan which showing the location of five geographic areas of *Cunninghamia konishii.*

Electrophoresis

Horizontal starch-gel electrophoresis was used for separating isozymes: IDH (isocitrate dehydrogenase, EC 1.1.1.42), 6PGD (6-phosphogluconic dehydrogenase, EC 1.1.1.43), PGI (phosphogluco-isomerase, EC 5.3.1.9), SKDH (shikimate 5-dehydrogenase, EC 1.1.1.25), PGM (phosphoglucomutase, EC 5.4.2.2), FEST (fluorescent esterase, EC 3.1.1.1), MDH (malate dehydrogenase, EC 1.1.1.37), G6PD (glucose-6-phosphate dehydrogenase, EC 1.1.1.49), and AAT (L-aspartate aminotransferase, EC 2.6.1.1). Young leaf tissues and gametophytes were ground with extraction buffer according to the procedures described in Feret (1971). Electrophoresis and staining followed the procedure described in Cheliak and Pitel (1984). Aspartate aminotransferase (*Aat*) was resolved by polyacrylamide vertical slab gel electrophoresis (Davis 1964). The zone specifying the most anodally migrating variants was designated as 1, the next as 2, and so on. Within each zone, the most anodally migrating variants was designated as a, the next as b, and so on.

Data Analysis

The inheritance of allozyme polymorphism in haploid tissue from heterozygous trees was tested for confirmation with the expected 1:1 ratio. Allozyme genotypes from the young leaf tissue of individual trees from each geographic area were used in conjunction with the POPGENE computer package (Yeh and Boyle 1996) for estimates of allele frequencies, mean number of alleles per locus, effective num-

Table 1. Average number of alleles per locus, effective number of alleles per locus, percentage of polymorphic loci, and expected and observed heterozygosities for each area of *C. konishii*

	Geographic area[a]					
	1	2	3	4	5	Mean
Sample size	38	36	14	16	16	
Avg. no. of alleles/locus	2.11	2.11	1.78	1.89	2.00	1.98
Effective no. of alleles/locus	1.54	1.46	1.39	1.51	1.50	1.48
% polymorphic loci[b]	66.7	66.7	55.6	55.6	66.7	62.3
Mean H_e	0.214	0.231	0.191	0.239	0.219	0.219
Mean H_o	0.174	0.190	0.187	0.227	0.174	0.190

[a] Area 1, Denta-Wangshiang; 2, Tasheueshan-Tajiann; 3, Mugua-Lintienshan; 4, Chilan-Syhjih; 5, Kuanwu-Bahsienshan.
[b] The frequency of the most common allele is less than 0.99.

ber of alleles per locus (N_e), percentage of polymorphic loci, mean observed (H_o) and expected (H_e) heterozygosities, and Wright's *F* coefficient for all loci.

Results

Nine enzyme systems tested could be resolved clearly enough for inheritance studies. The 14 loci resolvable from the megagametophyte tissues of *C. konishii* were *Idh-1, Pgi-1, Pgm-1, Pgm-2, Skdh-1, Skdh-2, 6Pgd-1, 6Pgd-2, Aat-2, Mdh-1, Fest-1, Fest-2, Fest-3,* and *G6pd-1.* In summary, no significant deviation from the expected 1:1 segregation ratio was found, indicating that most allozymes exhibited distinct, codominant expression and simple Mendelian segregation in their mode of inheritance.

Six of the nine enzyme systems from young leaf tissue of *C. konishii* were resolved well enough for genetic diversity analysis: *Idh-1, Pgm-1, Pgm-2, Pgi-1, 6Pgd-1, 6Pgd-2, Skdh-1, Skdh-2,* and *Aat-2. Idh-1, Pgm-1,* and *6Pgd-1* were monomorphic, while *Pgm-2 a* and *c* were rare alleles in *C. konishii.*

Genetic Diversity

Measures of genetic diversity are listed in Table 1. Of the six polymorphic loci of *C. konishii, Skdh-2* and *6Pgd-2* had a mean heterozygosity greater than 0.5 over the five geographic areas. *Aat-2* had a mean H_e greater than 0.3. *Pgi-1* and *Skdh-1* had a mean H_e ranging from 0.1 to 0.2. The last polymorphic locus, *Pgm-2,* had a mean H_e of less than 0.1. At the population level, the five areas had similar H_e values, and the overall average heterozygosity was 0.219. The average number of alleles per locus for the five areas ranged from 1.78 to 2.11, with an average of 1.98. Effective numbers of alleles per locus varied from 1.39 to 1.54, with an average of 1.48. The percentage of polymorphic loci per individual varied from 55.6% to 66.7%, with an average of 62.3%.

Genetic Differentiation

In *C. konishii* the F_{IS} values for all five enzyme systems were positive (0.107; data not shown). This probably is not due to inbreeding but a spatial Wahlund effect. Each area is actually composite collections of genotypes from throughout rather widespread locations. Any differences in allele frequencies between the actual collection sites within an area will produce the appearance that there is a deficiency of heterozygotes. The extent of genetic differentiation among areas (F_{ST}) averaged 0.029. Thus more than 97% of the genetic variation resided within areas. Unbiased genetic distances between pairs of areas were very small and ranged from 0 to 0.08 (data not shown). There was no significant correlation between genetic and geographic distances for all pairs of areas.

Comparison of Genetic Diversity Between *C. konishii* and *C. lanceolata* at the Species Level

Eight loci in six enzyme systems of both species were resolved well enough for genetic diversity comparison (Table 2). *Pgm-1* did not consistently stain for young leaf tissue of *C. lanceolata.* Major alleles within each locus were the same for both species. *Idh-1a, Idh-1b, Pgi-1a, Pgi-1c, Pgi-1e,* and *Skdh-2d* were rare alleles in *C. lanceolata* and were all absent from *C. konishii. Pgm-2a* was the only allele found in some areas of *C. konishii* but not in *C. lanceolata.* The frequency of *Skdh-1a* and *Aat-2a* were much lower in *C. konishii* than in *C. lanceolata.* Treating *C. konishii* and *C. lanceolata* as one random mating population each, mean heterozygosity and percentage of polymorphic loci per individual of *C. konishii* was lower than that in *C. lanceolata* (Table 3). The effective number of alleles per locus was 1.57 for *C. konishii* and 1.79 for *C. lanceolata.*

Discussion

Environmental heterogeneity, such as lofty mountains and deep valleys, might potentially be expected to favor genetic differentiation in *C. konishii* in Taiwan. The central mountain range runs north to south, and consists of more than 100 peaks higher than 3000 m. Mountains are characterized by steep slopes (>45°), erosion, and heavy rainfall during the summer season, thus streams cut through forming deep valleys. *C. konishii* can be found growing erratically anywhere from the top of the mountains to the valley from elevations of 1300 m to 2800 m. Physical barriers are always possible between locations. Area 1 was separated from areas 2 and 3 by mountains over 3000 m, which decline gradually at the north end such that the areas were not absolutely isolated. The overall F_{ST} of 0.029 indicates the physical barrier does not restrict gene flow between areas. This is consistent with data from many other conifers, which indicates relatively little interpopulational differentiation (Hamrick et al. 1992). The lack of population substructuring could be the re-

Table 2. Allele frequencies and the expected and observed heterozygosities for the eight loci at the species level of *Cunninghamia konishii* and *C. lanceolata*

Locus		*C. konishii* (n = 120)	*C. lanceolata* (n = 160)
Idh-1	*a*	0.000	0.019
	b	0.000	0.009
	c	1.000	0.972
	H_o	0.000	0.055
	H_e	0.000	0.056
Pgm-2	*a*	0.017	0.000
	b	0.966	0.981
	c	0.017	0.019
	H_o	0.050	0.038
	H_e	0.066	0.037
Pgi-1	*a*	0.000	0.031
	b	0.104	0.183
	c	0.000	0.017
	d	0.896	0.752
	e	0.000	0.017
	H_o	0.125	0.372
	H_e	0.187	0.401
Skdh-1	*a*	0.075	0.531
	b	0.925	0.469
	H_o	0.117	0.512
	H_e	0.139	0.500
Skdh-2	*a*	0.108	0.213
	b	0.400	0.147
	c	0.492	0.622
	d	0.000	0.019
	H_o	0.550	0.500
	H_e	0.589	0.548
6Pgd-1	*a*	1.000	1.000
6Pgd-2	*a*	0.085	0.070
	b	0.440	0.325
	c	0.201	0.281
	d	0.274	0.325
	H_o	0.556	0.530
	H_e	0.687	0.708
Aat-2	*a*	0.213	0.561
	b	0.787	0.439
	H_o	0.308	0.433
	H_e	0.336	0.494
Avg.	H_o	0.213	0.305
	H_e	0.251	0.343

Table 3. Levels of allozyme variation within populations for several local gymnosperms

Species	N^a	P^b	H^c	$F_{is}{}^d$	$F_{it}{}^d$	$A_e{}^e$	Reference
Amentotaxus							
formosana	2	5	0.004	−0.099	0.047	1.00	Wang et al. 1996
Chamacyparis							
taiwanensis	2	22	0.052	0.036	0.039	1.06	Lin et al. 1994
formosensis	3	21	0.087	0.109	0.046	1.10	Lin et al. 1994
Taiwania							
cryptomerioides	4	52	0.145	−0.036	0.053	1.21	Lin et al. 1993
Cunninghamia							
konishii	5	62.3	0.219	0.107	0.029	1.48	This study
konishii[f]	5	75	0.251	—	—	1.57	This study
Cunninghamia							
lanceolata	16	88	0.394	—	0.057	>3	Yeh et al. 1994
lanceolata	2	100	0.299	—	—	>4.2	Muller-Stark and Liu 1989
lanceolata[f]	—	87.5	0.343	—	—	1.79	This study
Gymnosperms	8.9	53.4	0.151	—	0.073	1.20	Hamrick et al. 1992
Gymnosperms[f]	8.9	71.1	0.169	—	—	1.22	Hamrick et al. 1992

[a] Number of studied populations.

[b] Percentage polymorphic loci.

[c] Expected heterozygosity.

[d] Fixation indices.

[e] Number of effective alleles per locus.

[f] At species level.

sult of more or less continuous distribution of *C. konishii* (Liu 1966), and a high level of gene flow, that is, pollen and seed dispersal.

High genetic diversity was proven for *C. konishii* in this study even though a rather limited number of loci were used. The level of expected heterozygosity at the population level in *C. konishii* (0.219) is higher than the values reported for many other conifers (H_e = 0.151) (Hamrick et al. 1992). In terms of percentage of polymorphic loci, number of alleles per locus, and effective number of alleles per locus, *C. konishii* also has higher values than most other conifers. Genetic diversity of *C. konishii* based on analysis using random amplified polymorphic DNA markers is also quite high; 91% of polymorphic fragments was found (Wang WY, unpublished results). *Chamaecyparis, Taiwania,* and *Cunninghamia* have similar distribution ranges and growth habitats in Taiwan. *Chamaecyparis* and *Taiwania,* however, have low genetic diversity (Table 3) and are very limited in distribution in mainland China. The explanation as to why every parameter of genetic diversity of *C. konishii* is considerably higher than those of other local gymnosperms is probably related to the association between *C. konishii* and *C. lanceolata* in geological ages rather than the heterogeneity of environmental factors. *C. lanceolata* is a long-lived species originally inhabiting southern China, and is one of the coniferous species with the highest genetic diversity (Yeh et al. 1994). It was reported that during the late Pleistocene, *C. konishii* dominated in the Tali glacial stage, from about 50,000 to 10,000 B.P. when Taiwan was part of mainland China (Tsukada 1967). It is inferred that gene flow from *C. lanceolata* went freely into Taiwan without restriction. Treating *C. konishii* and *C. lanceolata* as separate taxa, the unbiased genetic distance between them was 0.070. This distance is slightly higher than that between areas of *C. konishii,* suggesting limited differentiation between these two taxa. However, the extent of genetic differentiation between these two species (F_{ST}) is 0.057. Thus about 94% of the genetic variation resides within taxa. This result indicates that *C. konishii* is probably a variety of *C. lanceolata* and still maintains a high level of genetic variation. Isolation between these two taxa has not resulted in allozyme differentiation in *C. konishii*; however, one site change in the *rbcL* gene was found between these two species based on RFLP analysis of six polymerase chain reaction-amplified chloroplast genes (Tsumura et al. 1995).

Genetic drift has occurred in *C. konishii* through long isolation from its supposed distribution center, resulting in a reduction in the number of alleles per locus and the loss of rare alleles (*Idh-1, Pgi-1,* and *Skdh-2*). Some alleles like *Skdh-1* and *Aat-2* are fixed in *C. konishii.* The observation of much higher expected heterozygosities and much higher measures of other genetic parameters (Table 3) of *C. lanceolata* than those of *C. konishii* indicates that genetic drift may still prevail.

From the Division of Silviculture, Taiwan Forestry Research Institute, 53 Nan-Hai Road, Taipei, Taiwan. Financial support provided by the Council of Agriculture (86-AST-1.5-FOD-03) is gratefully acknowledged. Contribution No. 99 of Taiwan Forestry Research Institute. Address correspondence to Dr. Lin at the address above or e-mail: tpl1222@ms3.hinet.net.

References

Cheliak WM and Pitel JA, 1984. Techniques for starch gel electrophoresis of enzymes from forest tree species. Information Report PI-X-42. Chalk River, Ontario: Petawawa National Forest Institute; 19–45.

Davis BJ, 1964. Disc electrophoresis II: method and application to human serum protein. Ann NY Acad Sci 121:404–427.

Feret PP, 1971. Isozyme variation in *Picea glauca* (Moench) Voss seedlings. Silvae Genet 20:46–50.

Hamrick JL, Godt MJW, and Sherman-Broyles SL, 1992. Factors influencing levels of genetic diversity in woody plant species. In: Population genetics of forest trees (Adams WT, Strauss SH, Copes DL, and Griffin AR, eds). Dordrecht, The Netherlands: Kluwer Academic; 95–124.

Lin TP, Lee TY, Yang LF, Chung YL, and Yang JC, 1994. Comparison of the allozyme diversity in several populations of *Chamaecyparis formosensis* and *Chamaecyparis taiwanensis.* Can J For Res 24:2128–2134.

Lin TP, Lu CS, Chung YL, and Yang JC, 1993. Allozyme variation in four populations of *Taiwania cryptomerioides* in Taiwan. Silvae Genet 42:278–284.

Liu T, 1966. Study on the phytogeography of the conifers and taxads of Taiwan (in Chinese). Bulletin no. 122. Taipei, Taiwan: Taiwan Forestry Research Institute.

Muller-Starck G and Liu YQ, 1989. Genetics of *Cunninghamia lanceolata* Hook. 2. Genetic variation within and between two provenances samples. Silvae Genet 38: 172–177.

Tsukada M, 1967. Vegetation in subtropical Formosa during the Pleistocene glaciations and the Holocene. Palaeogeog Palaeoclimat Palaeoecol 3:49–64.

Tsumura Y, Yoshimura K, Tomaru N, and Ohba K, 1995. Molecular phylogeny of conifers using RFLP analysis of PCR-amplified specific chloroplast genes. Theor Appl Genet 91:1222–1236.

Wang CT, Wang WY, Chiang CH, Wang YN, and Lin TP, 1996. Low genetic variation in *Amentotaxus formosana* Li revealed by isozyme analysis and random amplified polymorphic DNA markers. Heredity 77:388–395.

Yeh FC, Shi J, Yang R, Hong J, and Ye Z, 1994. Genetic diversity and multilocus associations in *Cunninghamia lanceolata* (Lamb.) Hook from the People's Republic of China. Theor Appl Genet 88:465–471.

Yeh FC and Boyle T, 1996. POPGENE version 1.11, Microsoft Windows-based software for population genetic analysis.

Received May 27, 1997
Accepted December 10, 1997

Corresponding Editor: James L. Hamrick